Sedimentární záznam v rekonstrukci fosilních ekosystémů II.

Geobiologie magisterská, LS

fyzická stratigrafie, chemostratigrafie, geochemie paleoenvironmentální

Karel Martínek
ÚGP (Ústav geologie a paleontologie)

syllabus přednášky

- fyzická stratigrafie, genetická stratigrafie, sekvenční stratigrafie, cyklostratigrafie, chemostratigrafie
- geochemie paleoenvironmentální
- cykličnost v sedimentárním záznamu
- případové studie

Stratigrafie

- biostratigrafie
- fyzická stratigrafie
  - litostratigrafie
  - genetická stratigrafie (alostratigrafie – uvažuje alogenní řídící mechanismy, extrapánevní, opak autogenních procesů, např. autocykličnost fluviálních nebo deltových sedimentů)
    - např. sekvenční stratigrafie
- chemostratigrafie

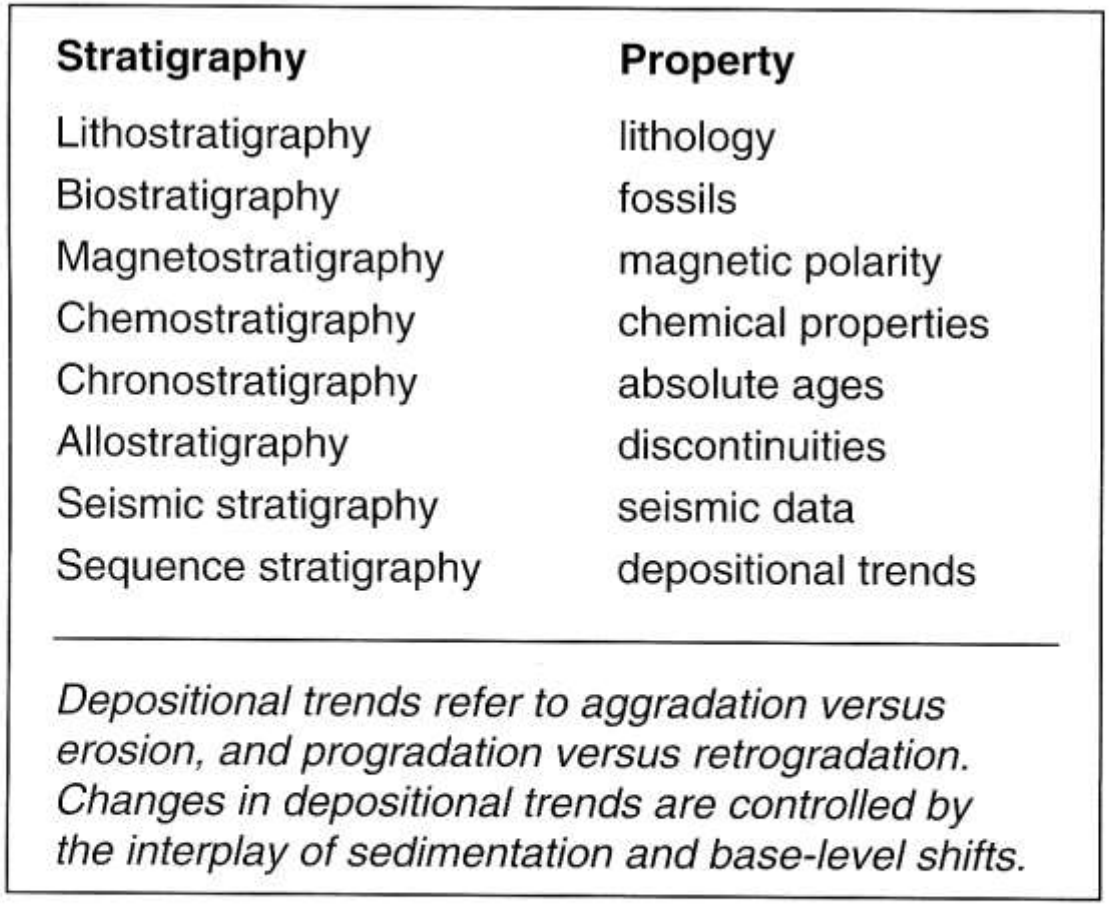

Stratigraphy	Property
Lithostratigraphy	lithology
Biostratigraphy	fossils
Magnetostratigraphy	magnetic polarity
Chemostratigraphy	chemical properties
Chronostratigraphy	absolute ages
Allostratigraphy	discontinuities
Seismic stratigraphy	seismic data
Sequence stratigraphy	depositional trends

Depositional trends refer to aggradation versus erosion, and progradation versus retrogradation. Changes in depositional trends are controlled by the interplay of sedimentation and base-level shifts.

FIGURE 1.3 Types of stratigraphy, defined on the basis of the property they analyze. The interplay of sedimentation and shifting base level at the shoreline generates changes in depositional trends in the rock record, and it is the analysis and/or correlation of these changes that defines the primary objectives of sequence stratigraphy.

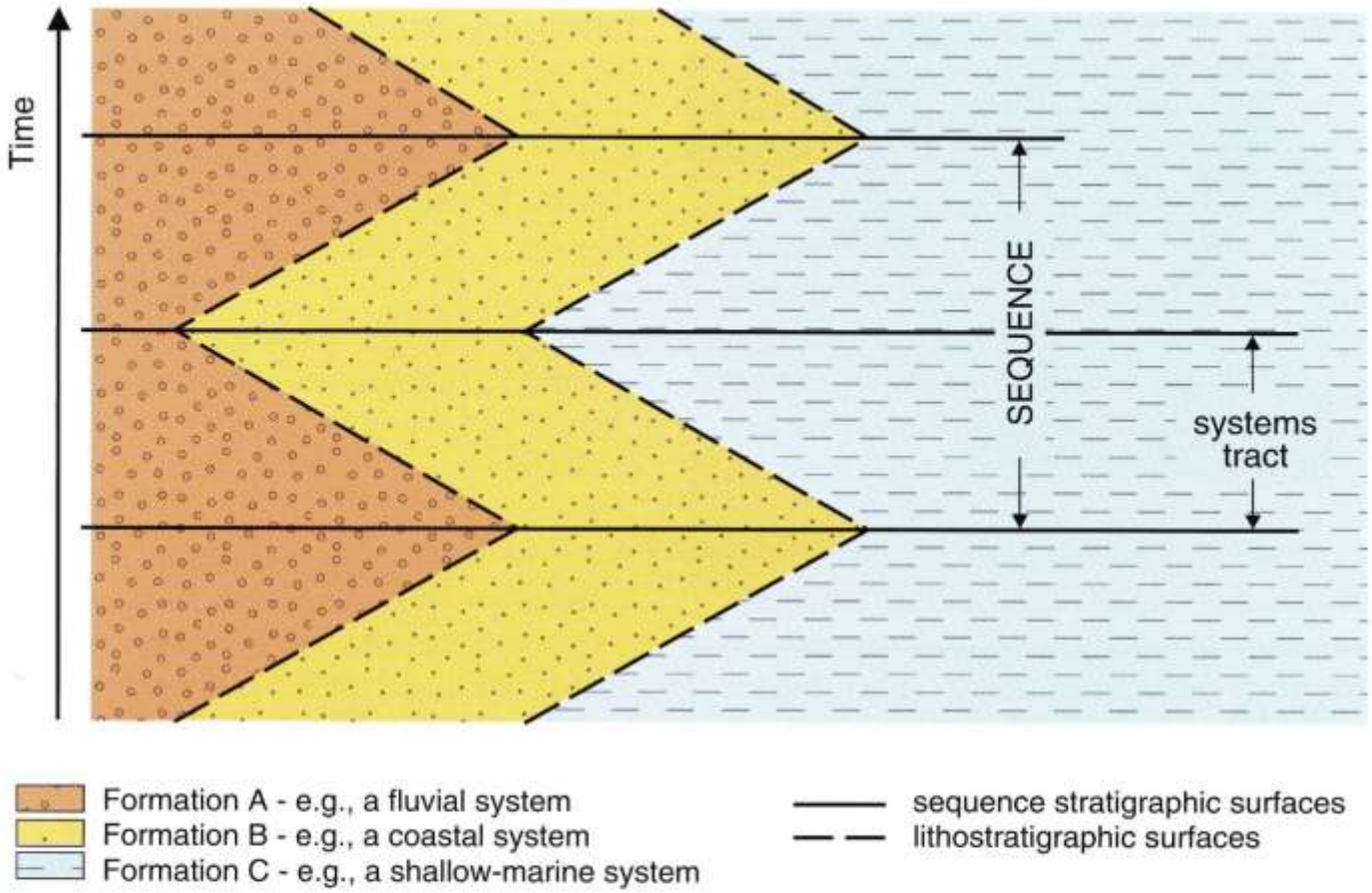

FIGURE 1.12 Conceptual contrast between lithostratigraphy and sequence stratigraphy. Sequence stratigraphic surfaces are event-significant, and mark changes in depositional trends. In this case, their timing is controlled by the turnaround points between transgressions and regressions. Lithostratigraphic surfaces are highly diachronous facies contacts. Note that the system tract and sequence boundaries cross the formation boundaries. Each systems tract is composed of three depositional systems in this example, and is defined by a particular depositional trend, i.e., progradational or retrogradational. A sequence corresponds to a full cycle of changes in depositional trends. This example implies continuous aggradation, hence no breaks in the rock record, with the cyclicity controlled by a shifting balance between the rates of base-level rise and the sedimentation rates.

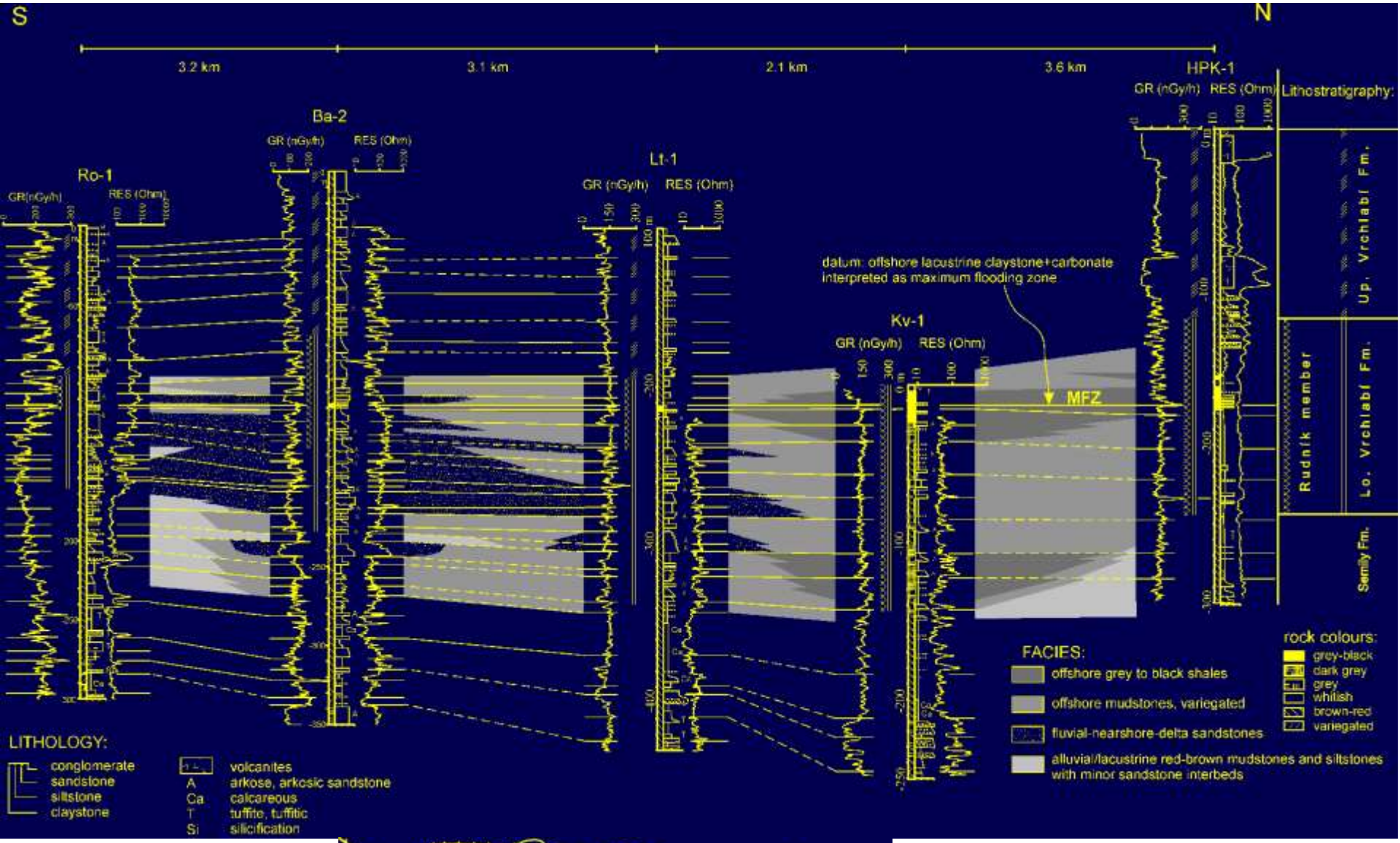
S
N
3.2 km
3.1 km
2.1 km
3.6 km
Ro-1
Ba-2
Lt-1
Kv-1
HPK-1
GR (nGy/h)
RES (Ohm)
Lithostratigraphy:
Up. Vrchlabí Fm.
Rudník member
Lo. Vrchlabí Fm.
Semily Fm.
datum: offshore lacustrine claystone+carbonate interpreted as maximum flooding zone
MFZ
FACIES:
offshore grey to black shales
offshore mudstones, variegated
fluvial-nearshore-delta sandstones
alluvial/lacustrine red-brown mudstones and siltstones with minor sandstone interbeds
rock colours:
grey-black
dark grey
grey
whitish
brown-red
variegated
LITHOLOGY:
conglomerate
sandstone
siltstone
claystone
volcanites
A arkose, arkosic sandstone
Ca calcareous
T tuffite, tuffitic
Si silicification


Vrchlabí
Kunratice
Lt-1
Kv-1
Trutnov
Nová Paka

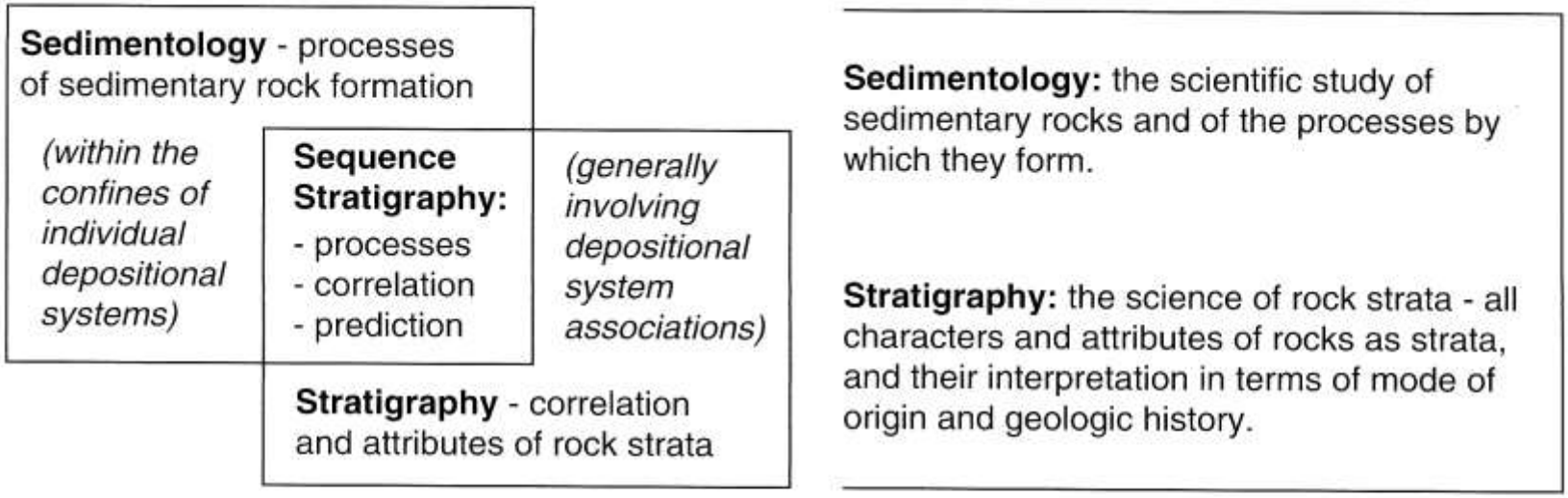

FIGURE 1.2 Sequence stratigraphy and its overlap with the conventional disciplines of sedimentology and stratigraphy (definitions modified from Bates and Jackson, 1987). When applied to a specific depositional system, sequence stratigraphy helps to understand processes of facies formation, facies relationships, and facies cyclicity in response to base-level changes. At larger scales, the lateral correlation of coeval depositional systems becomes a more significant issue, which also brings in a component of facies predictability based on the principle of common causality related to the basin-wide nature of the allogenic controls on sedimentation.

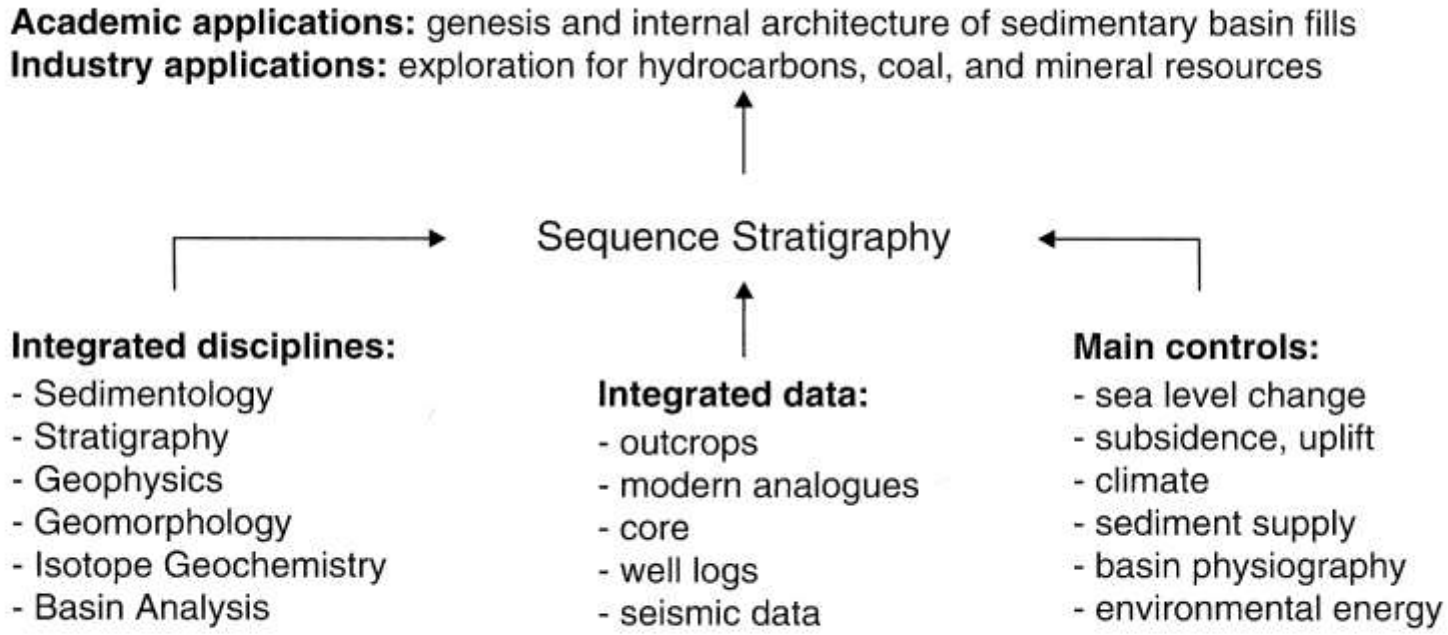

FIGURE 1.1 Sequence stratigraphy in the context of interdisciplinary research—main controls, integrated data sets and subject areas, and applications.

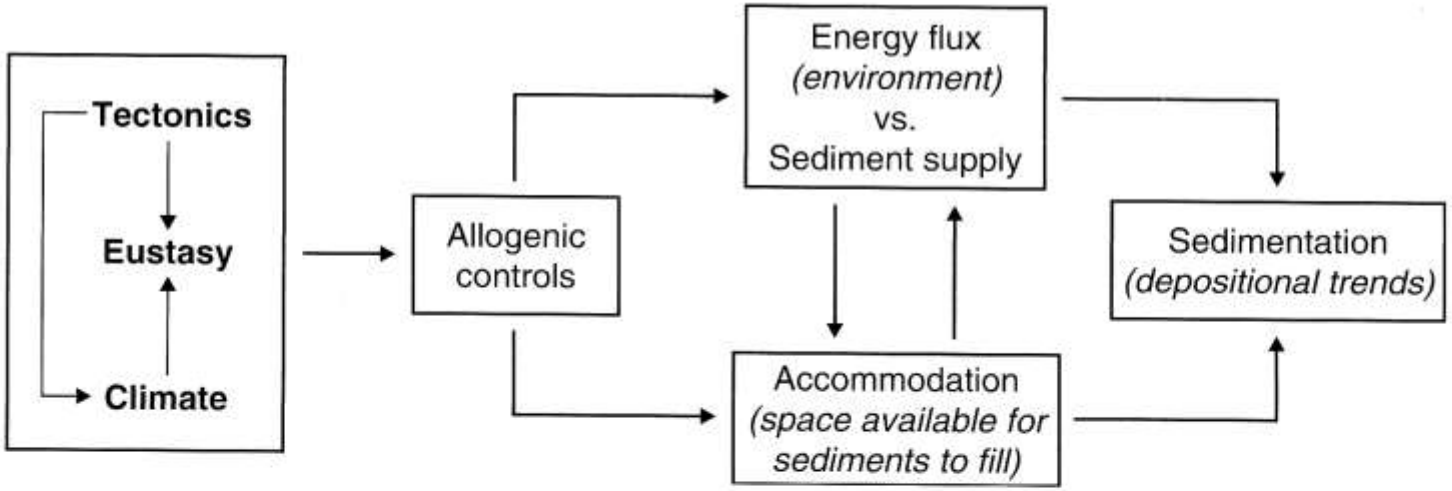

FIGURE 3.1 Allogenic controls on sedimentation, and their relationship to environmental energy flux, sediment supply, accommodation, and depositional trends (modified from Catuneanu, 2003). In any depositional environment, the balance between energy flux and sediment supply is key to the manifestation of processes of sediment accumulation or reworking. Besides tectonics, additional processes such as thermal subsidence (crustal cooling), sediment compaction, water-depth changes, isostatic, and flexural loading, also contribute to the total subsidence or uplift in the basin. Accommodation is affected by the balance between energy flux and sediment supply (i.e., increased energy 'erodes' accommodation; increased sediment supply adds to the amount of available accommodation), but it is also independently controlled by external factors such as eustasy and tectonism. At the same time, changes in accommodation controlled directly by external factors may alter the balance between energy flux and sediment supply at any location within the basin (e.g., deepening of the water as a result of sea-level rise lowers the energy flux at the seafloor). The interplay of all allogenic controls on sedimentation, as reflected by changes in accommodation and energy flux/sediment supply, ultimately determines the types of depositional trends established within the basin.

Hierarchical order	Duration (My)	Cause
First order	200-400	Formation and breakup of supercontinents
Second order	10-100	Volume changes in mid-oceanic spreading centers
Third order	1-10	Regional plate kinematics
Fourth and fifth order	0.01-1	Orbital forcing

FIGURE 3.2 Tectonic and orbital controls on eustatic fluctuations (modified from Vail *et al.*, 1977, and Miall, 2000). Local or basin-scale tectonism is superimposed and independent of these global sea-level cycles, often with higher rates and magnitudes, and with a wide range of time scales.

SEKVENČNÍ STRATIGRAFIE

Diagrams from
Coe, A. et al. 2003. The Sedimentary Record of Sea Level Change. Cambridge University Press
Nichols, G. 1999. Sedimentology and Stratigraphy. Blackwells
Plint, A.G. and Uličný, D. 1999. Notes for a short course in Sequence Stratigraphy

www.strata.geol.sc.edu/log-stacking.html

Stratigrafie – studuje stáří a chronologické vztahy horninových těles

SEKVENČNÍ STRATIGRAFIE

– studuje chronologické vztahy těles sedimentárních hornin, které vykazují určitou cyklicitu a jsou spojovány do geneticky provázaných celků - **sekvencí**

Sekvenčněstratigrafický vývoj je dán vztahem mezi

akomodací a přínosem sedimentu

akomodační prostor – prostor pro potenciální akumulaci sedimentu

relativní změny hladiny – projev změn akomodačního prostoru; hrají významnou roli v prostředích citlivých na hloubku vody (šelfy, jezera,...)

fluviální prostředí - akomodační prostor kontrolován **spádovou křivkou** řeky

eolická prostředí - akomodace ovlivňována geomorfologií, směrem větru, přínosem sedimentu a hladinou podzemní vody

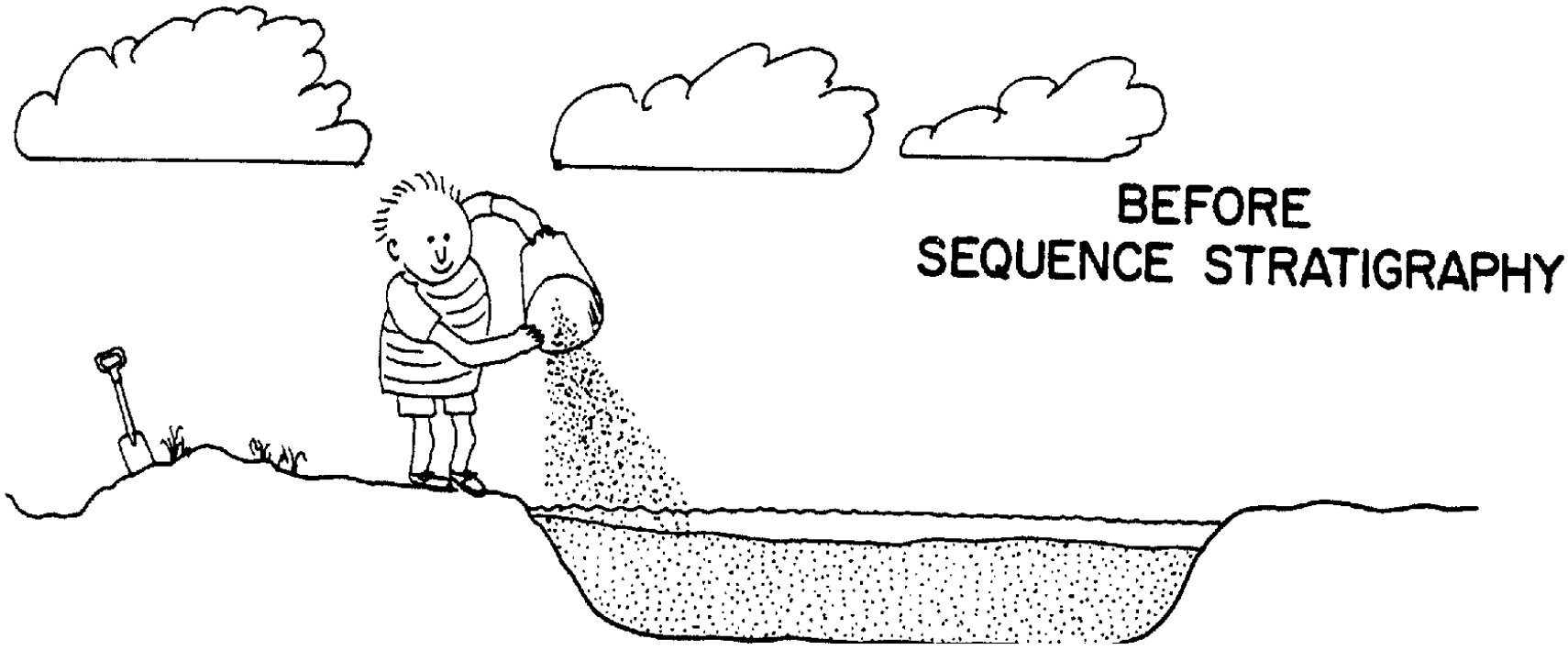
BEFORE
SEQUENCE STRATIGRAPHY

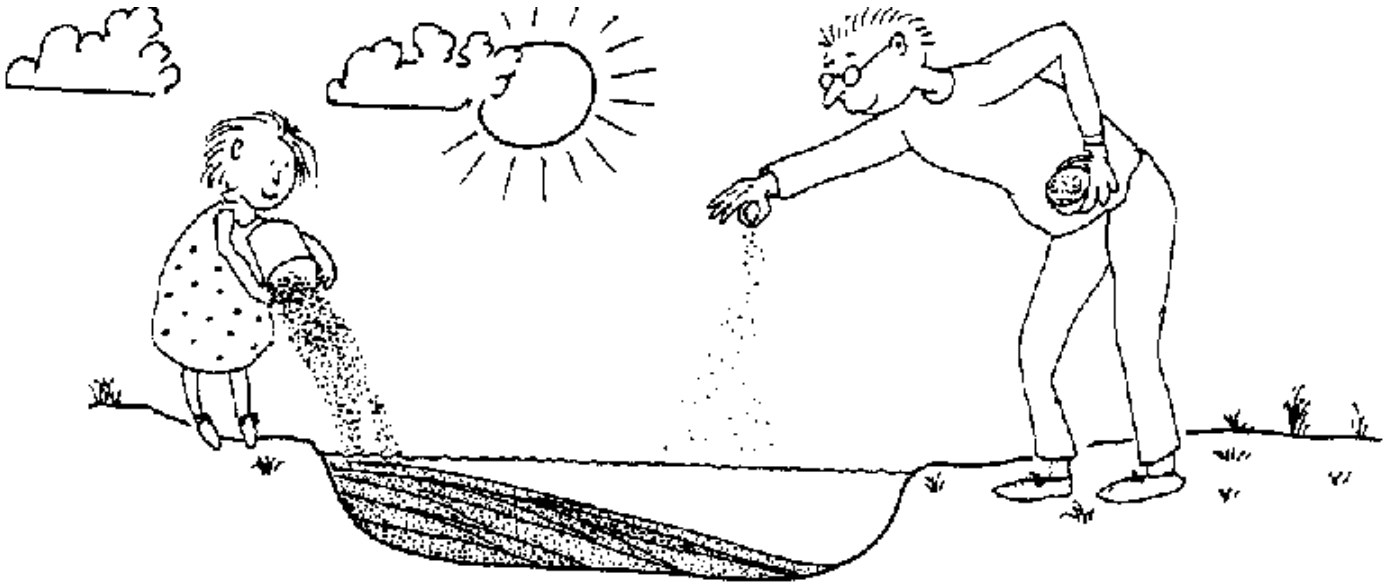

AFTER SEQUENCE STRATIGRAPHY

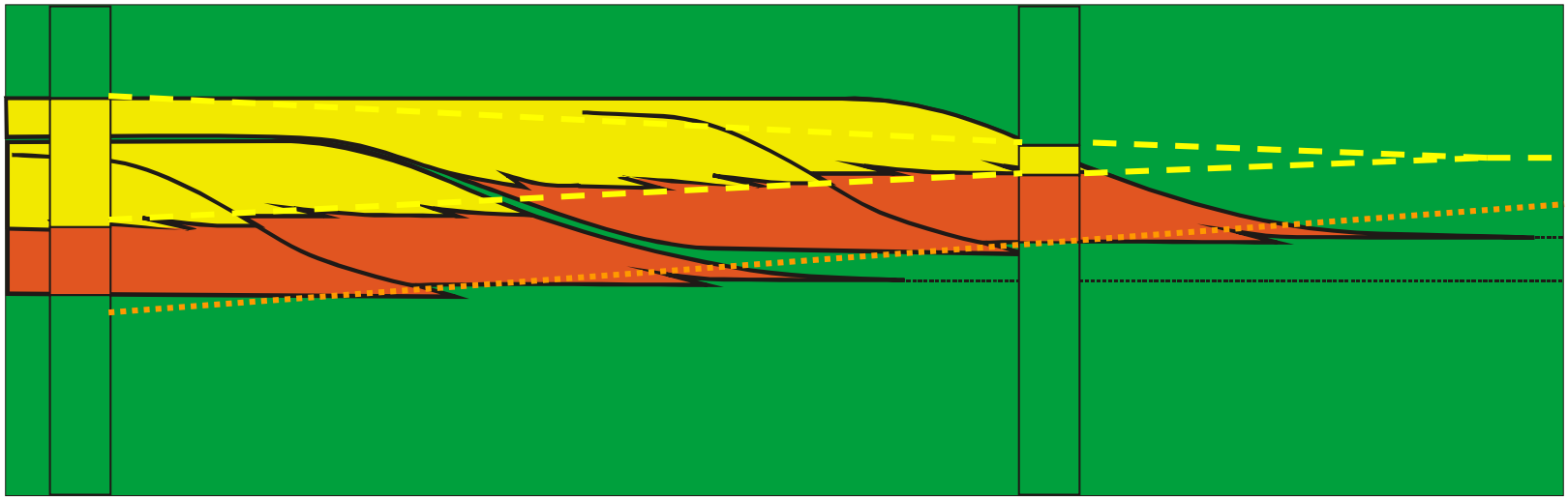

ZÁKLADNÍ REAKCE SEDIMENTÁRNÍCH SYSTÉMŮ NA RELATIVNÍ ZMĚNY HLADINY

Depositional Sequences: clastic shelf

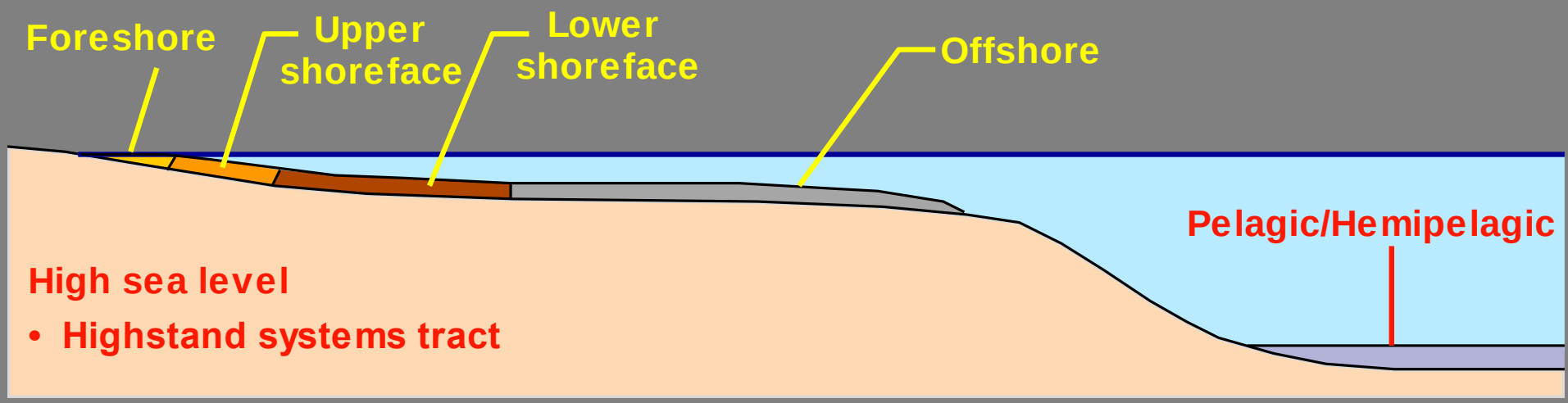

VÝVOJ KLASTICKÉHO ŠELFU V ZÁVISLOSTI NA ZMĚNÁCH HLADINY

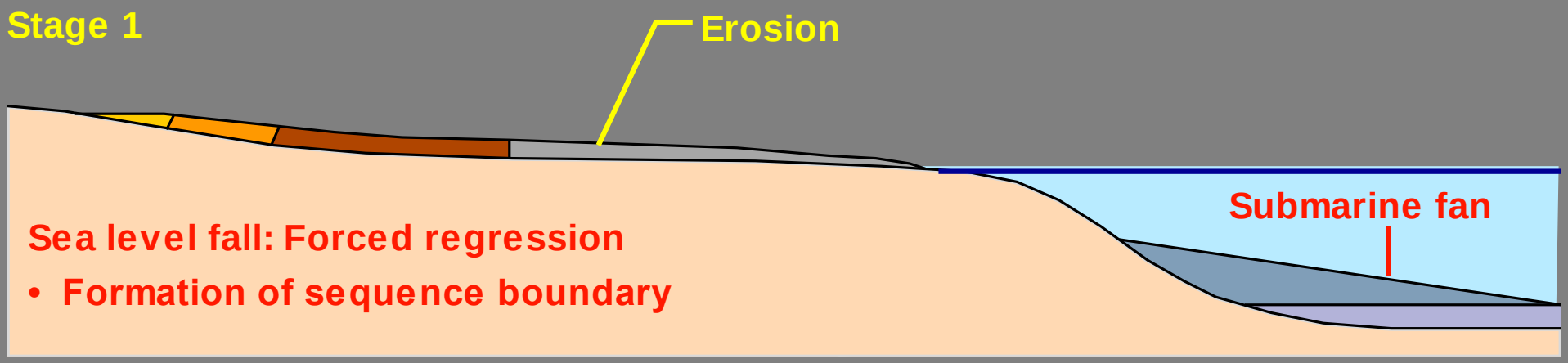

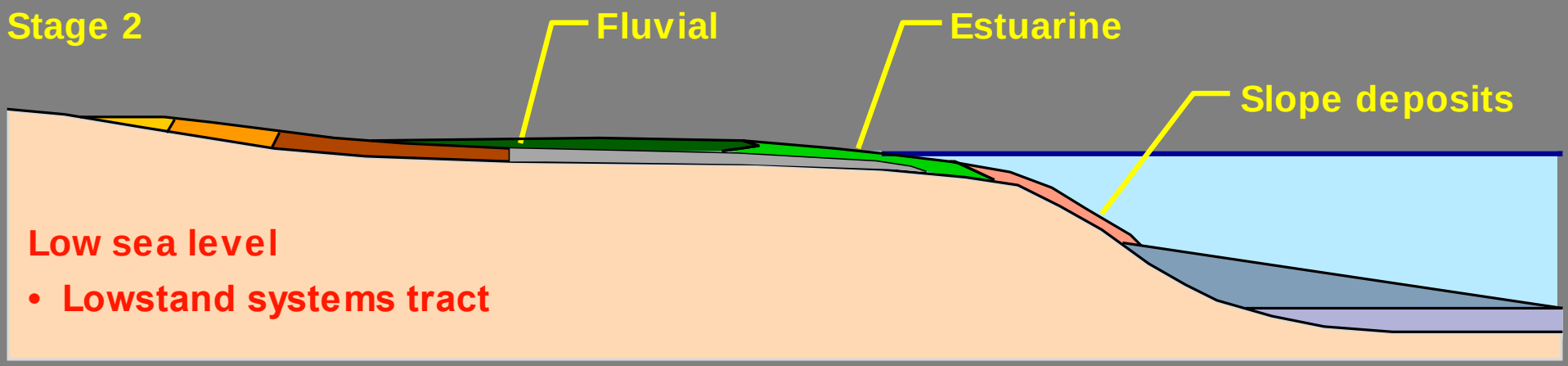
Stage 2
Fluvial
Estuarine
Slope deposits
Low sea level
• Lowstand systems tract

Stage 3

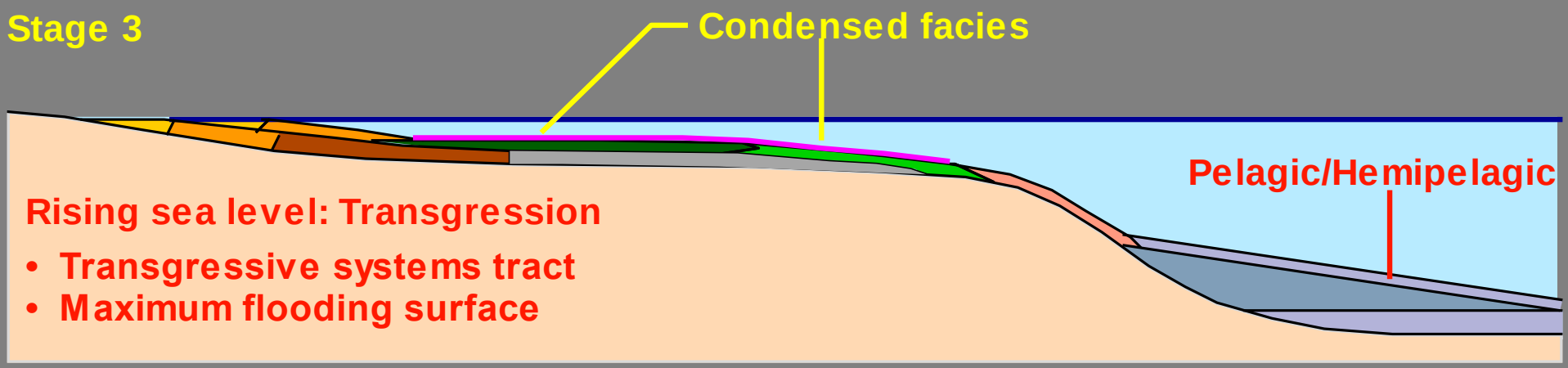

Rising sea level: Transgression

- Transgressive systems tract
- Maximum flooding surface

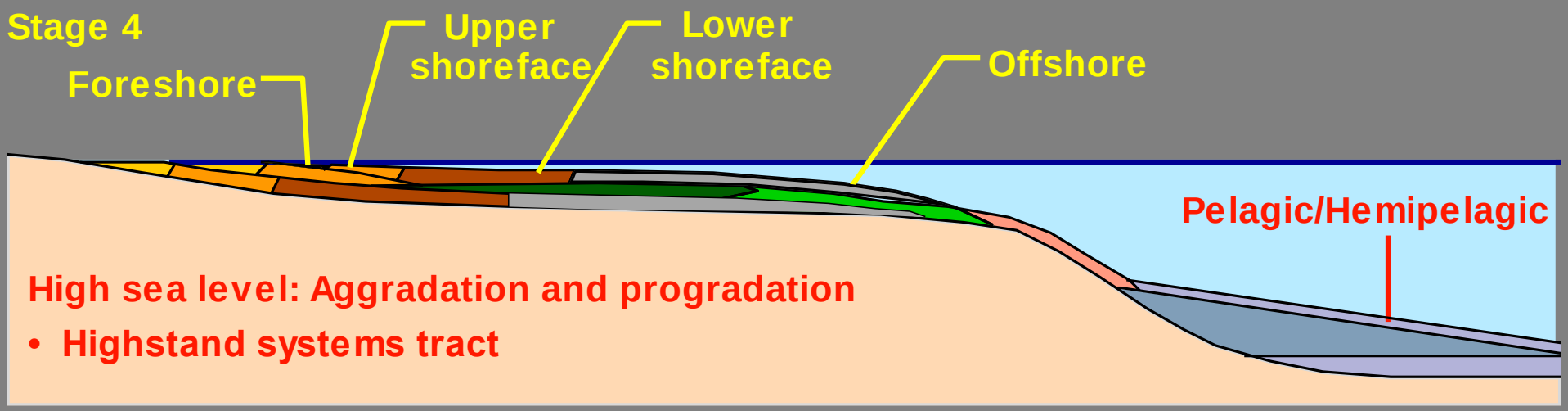

High sea level: Aggradation and progradation

- **Highstand systems tract**

SEDIMENTÁRNÍ SEKVENCE

- stratigrafická jednotka, vymezena na bázi i na vrchu výraznými plochami diskordance nebo jejich korelačními ekvivalenty

- reprezentuje období sedimentace určitého sedimentárního systému mezi dvěma epizodami **výrazného poklesu hladiny**

⇒ **sekvenční stratigrafie umožňuje rekonstruovat vývoj hladiny**

Sekvenční hranice – plocha představující povrch vzniklý během výrazného poklesu hladiny, často erozivní

SEDIMENTÁRNÍ SEKVENCE V KLASTICKÉM ŠELFU

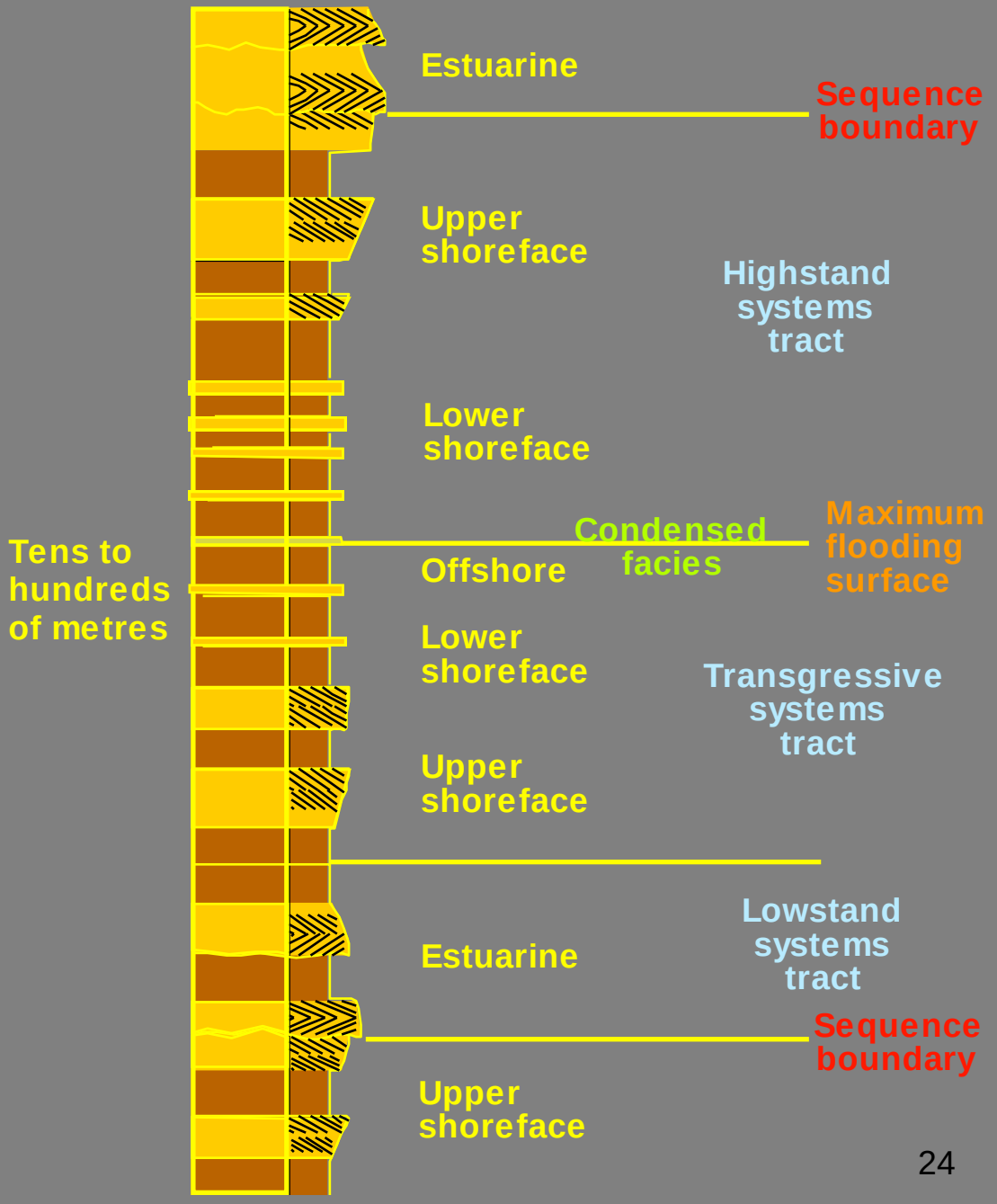

TRAKTY SEDIMENTÁRNÍCH SEKVENCÍ

trakty (*systems tracts*)

části sekvence odpvídající jednotlivým etapám vývoje hladiny

- **Trakt vysoké hladiny (HST)**
- **Trakt klesající hladiny (FSST)**
- **Trakt nízké hladiny (LST)**
- **Trakt rostoucí hladiny (TST)**

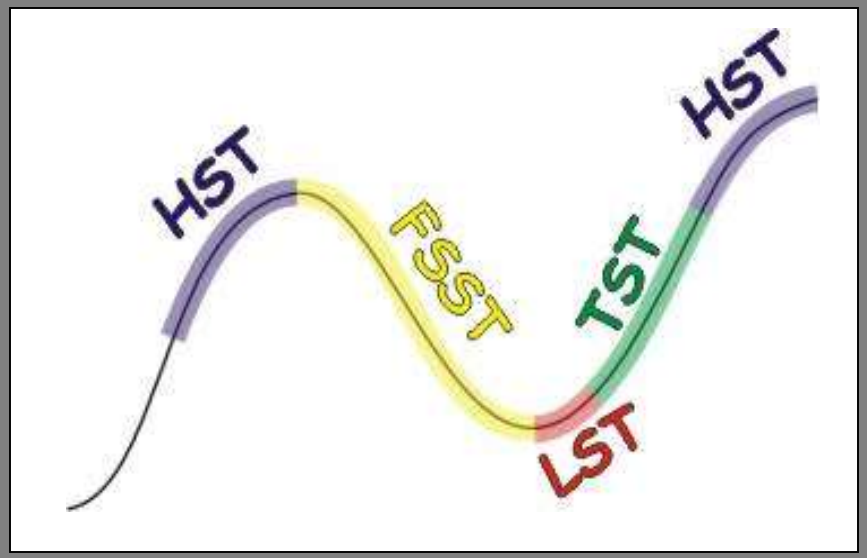

Types of shelf margin

Shelf break margin

Steep slope at shelf edge

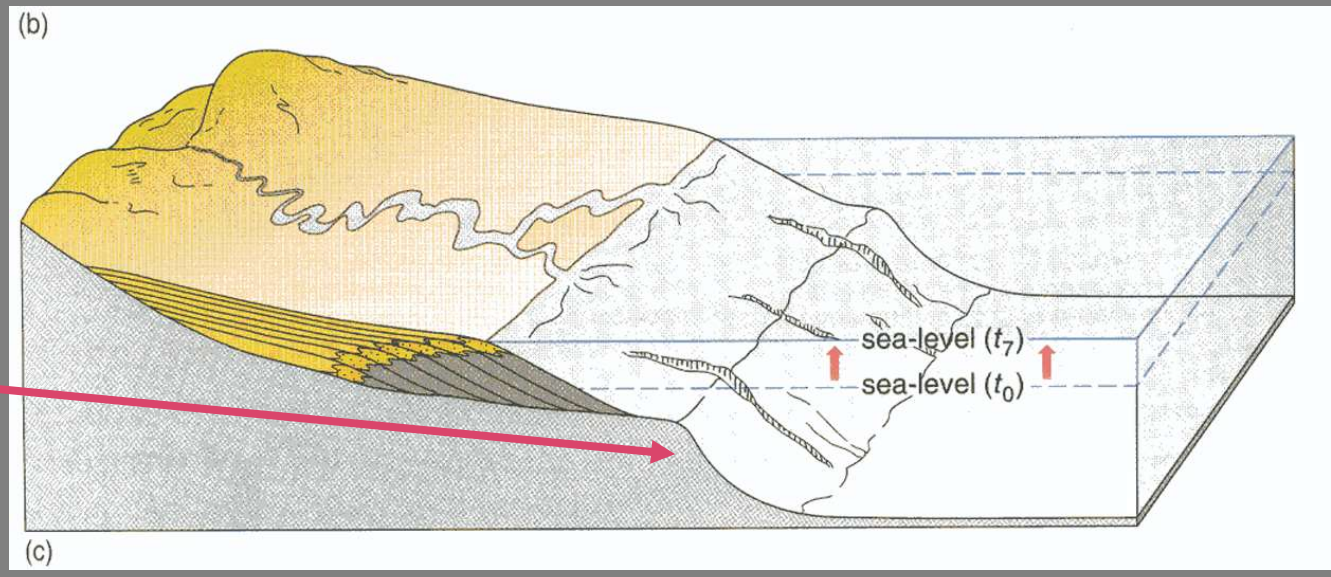

Ramp margin

No distinct shelf edge

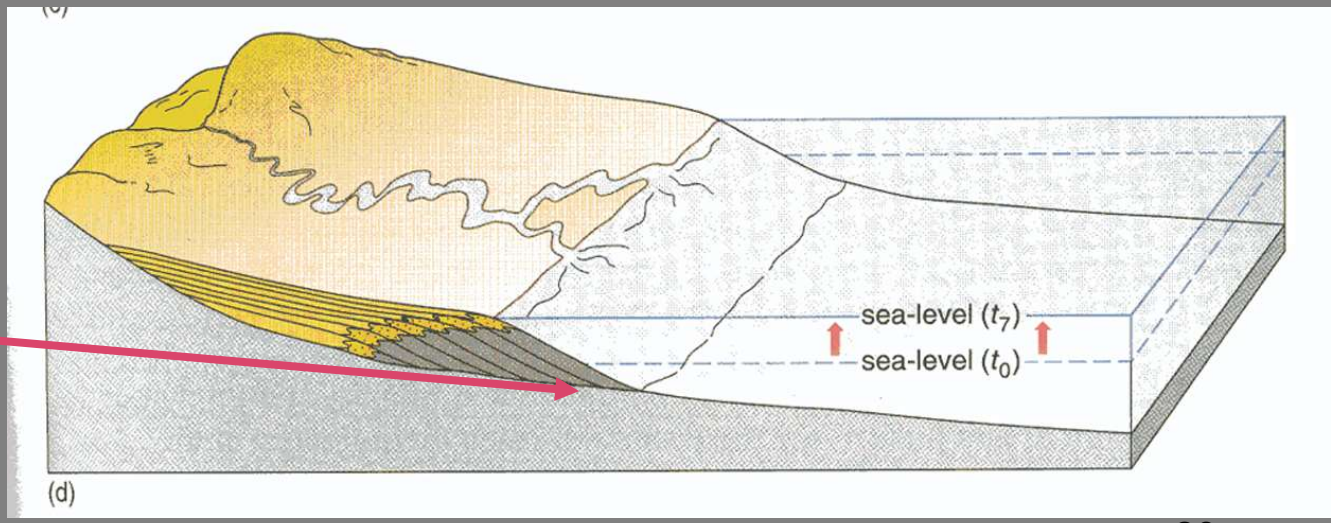

TRAKT VYSOKÉ HLADINY (HST)

- zpomalování transgrese

  ⇒ sedimentace vyrovnává nárůst akomodace

  ⇒ agradace, agradace+progradace
- oddělení HST od TST – **plocha maximální záplavy (MFS)**
- ve vertikálním profilu jako přechod mezi retrogradačním a agradačně-progradačním stylem

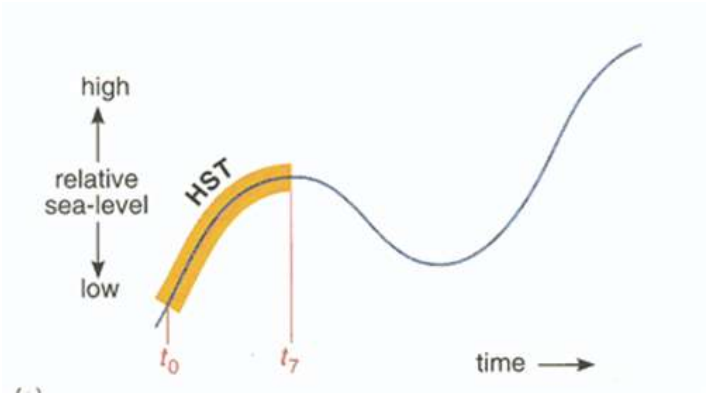

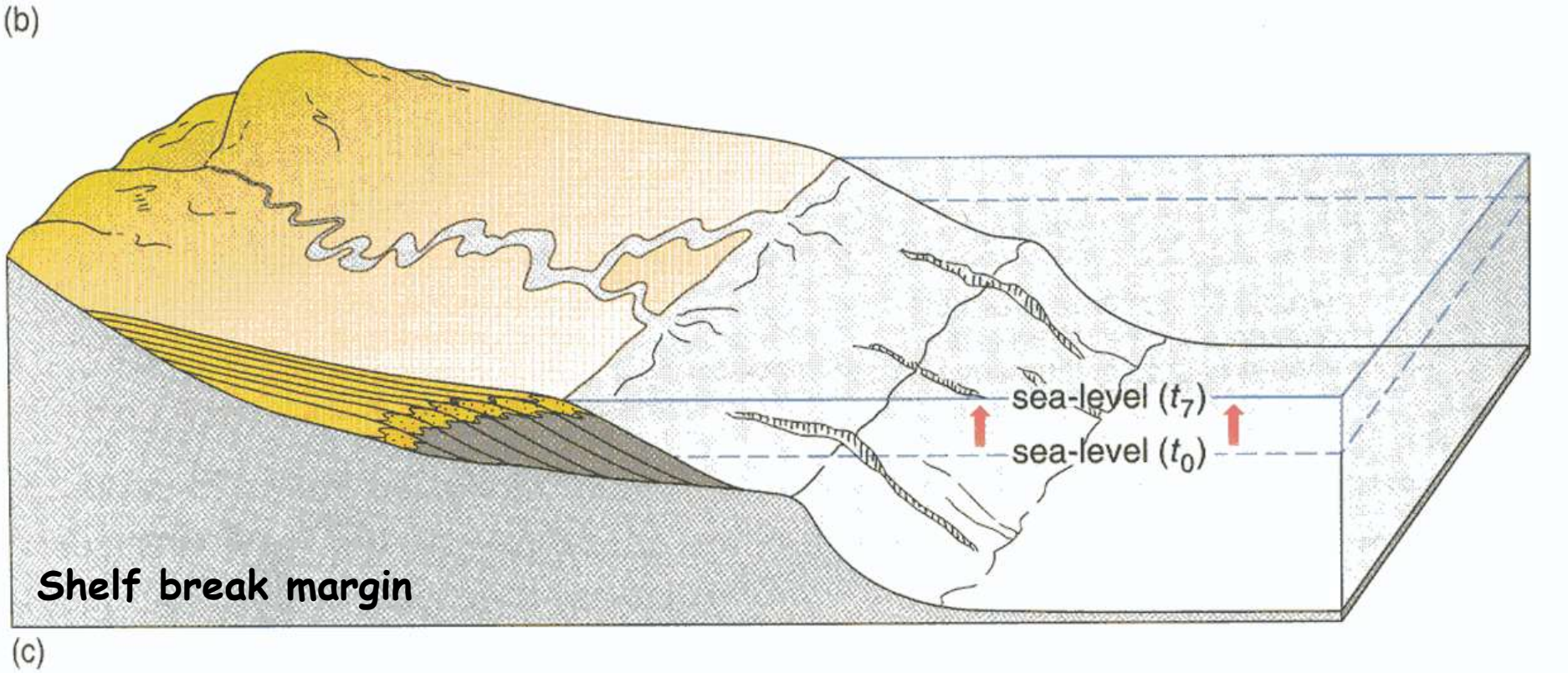

TRAKT KLESAJÍCÍ HLADINY (FSST)

- vzniká během poklesu hladiny (nucené regrese);
  není vždy vyvinut
- uspořádání parasekvencí – offlap
- FST je svchu vymezen sekvenční hranicí a na spodu
  RSME (regressive surface of marine erosion)

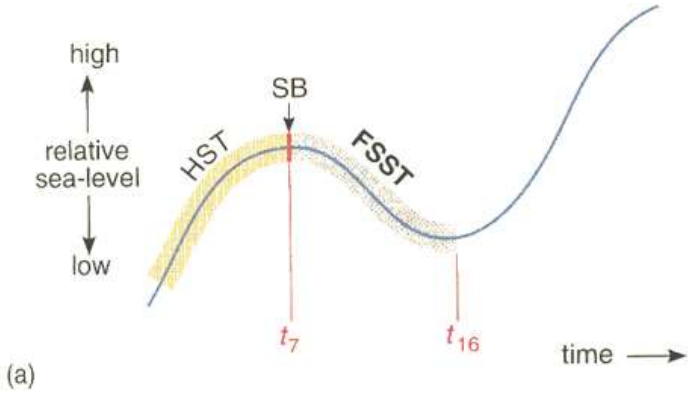

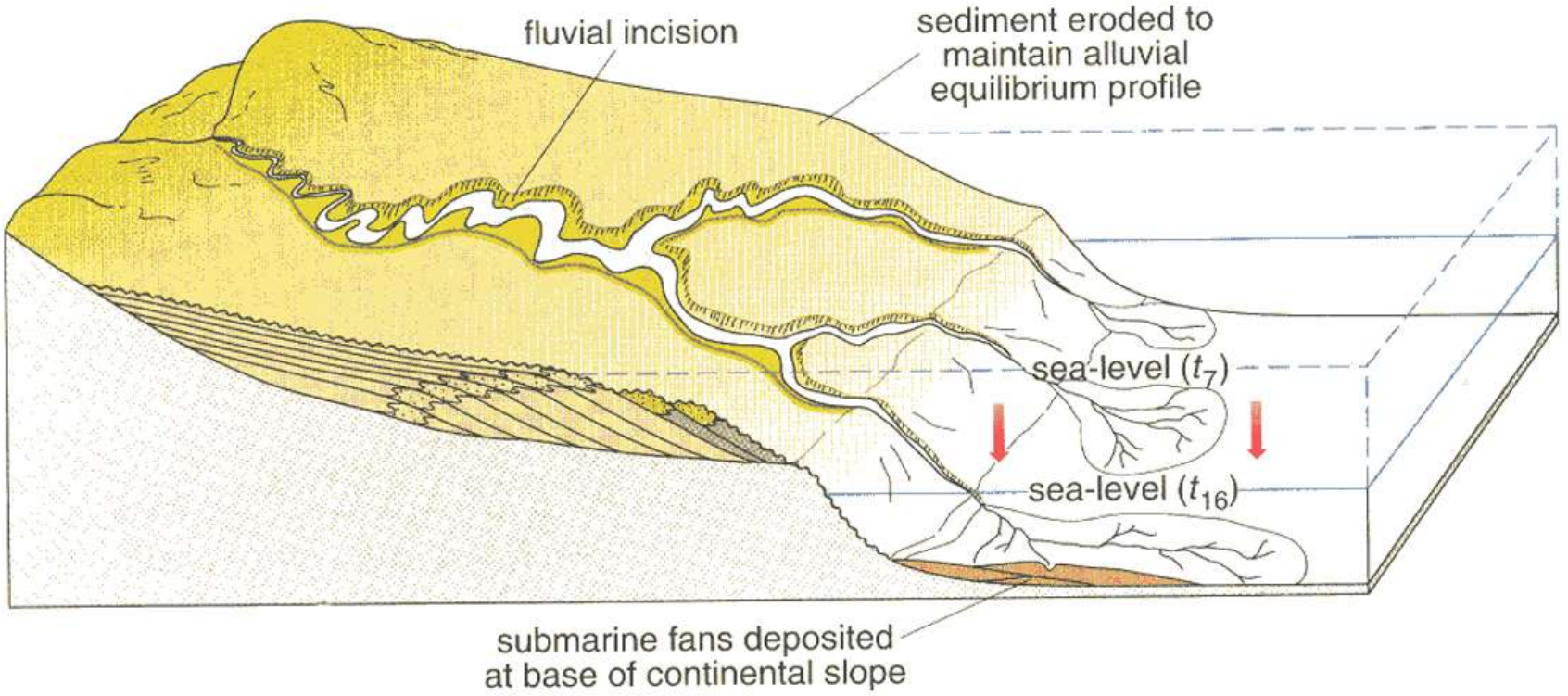

TRAKT NÍZKÉ HLADINY (LST)

• sedimentace během nízkého stavu hladiny

– období zlomu mezi regresí a transgresí

⇒ progradace, progradace +agradace

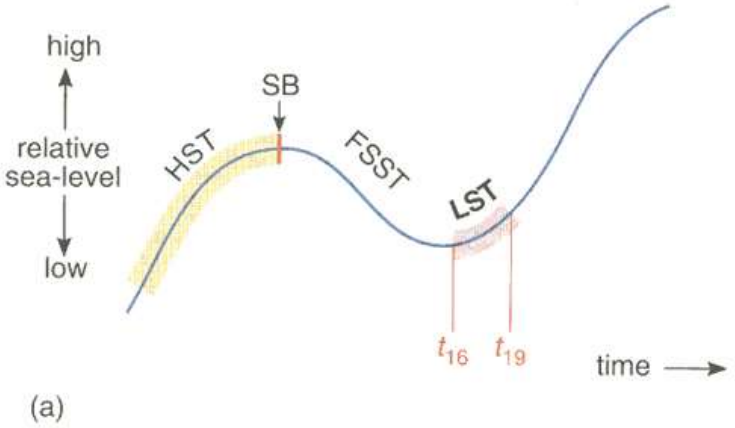

• sekvenční hranice je na bázi LST

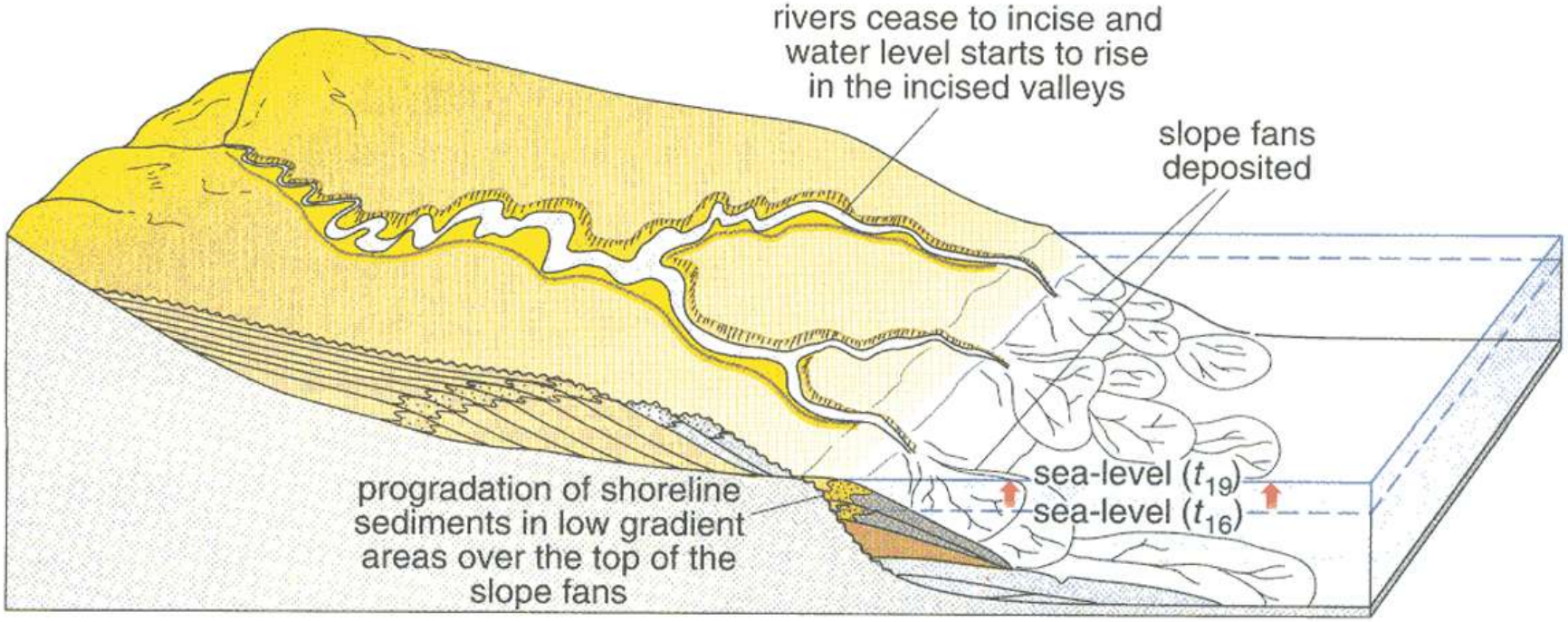

TRANSGRESNÍ POVRCH (TS)

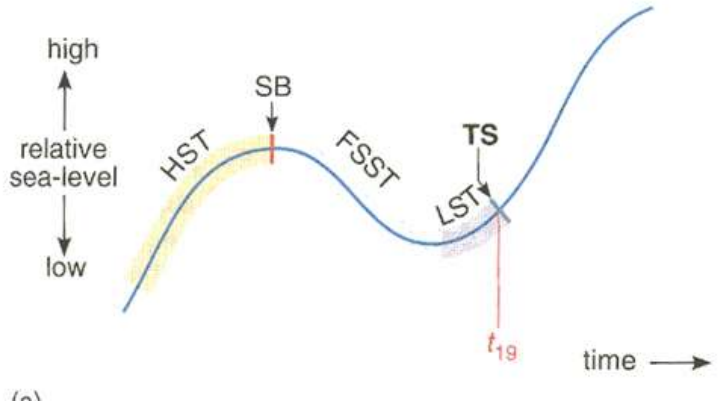

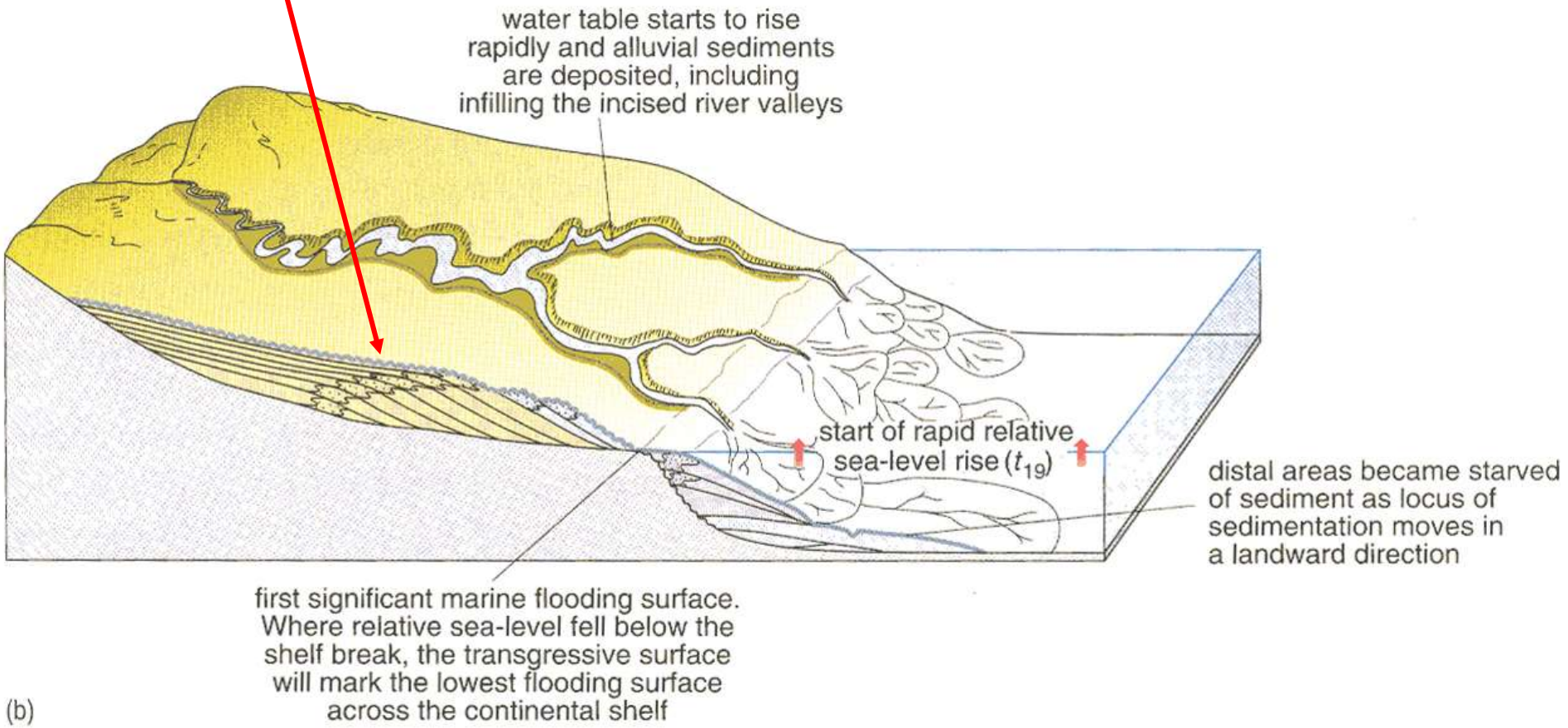

TRANSGRESNÍ TRAKT (TST)

• vzniká během period rychlého růstu hladiny ⇒ transgrese

• retrogradace sedimentárního systému

⇒ mělkovodní facie jsou překryty hlubokovodními

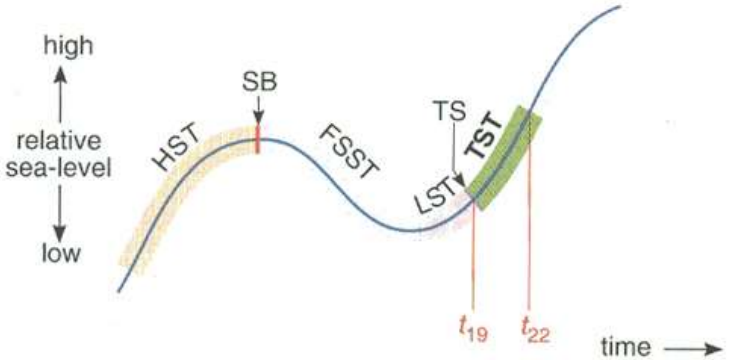

“ravinment surface“

erozivní povrch vznikající účinkem postupující báze vlnění během transgrese ⇒ často přetiskuje účinek subaerické eroze za nízkého stavu hladiny

(a)

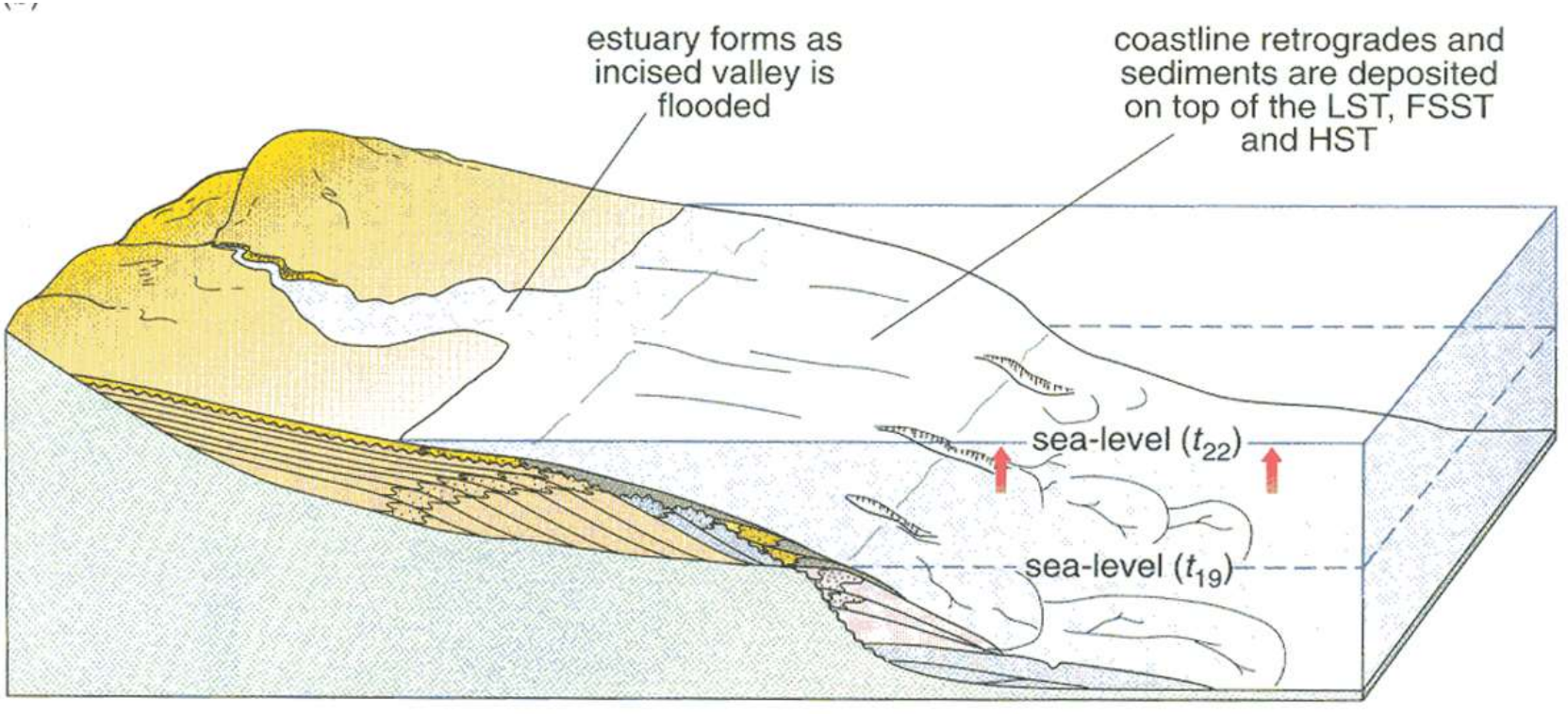

PLOCHA MAXIMÁLNÍ ZÁPLAVY (MFS)

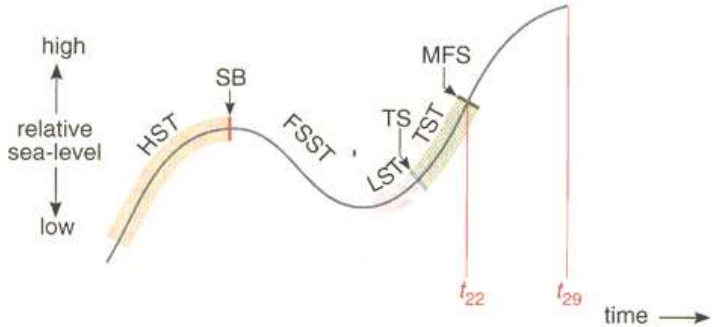

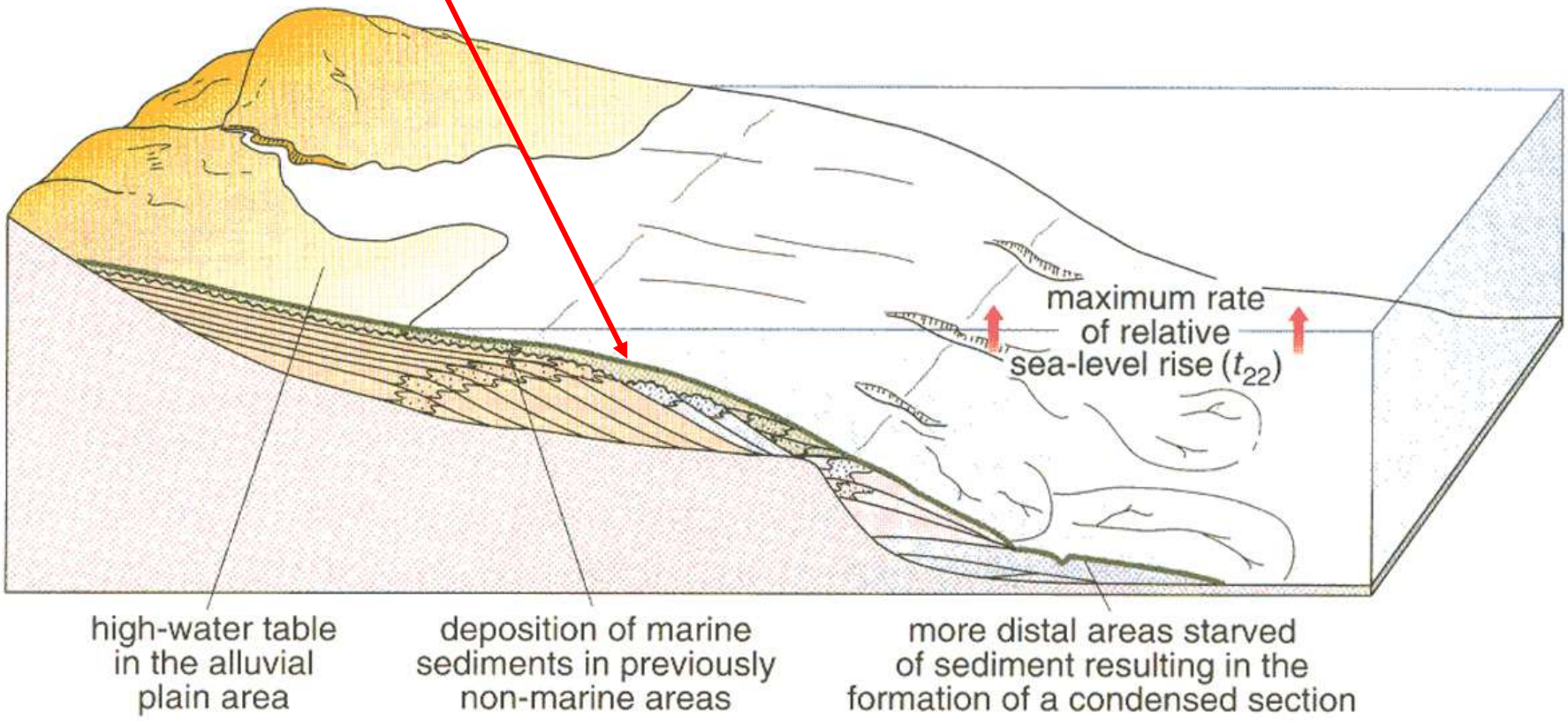

TRAKT VYSOKÉ HLADINY (HST)

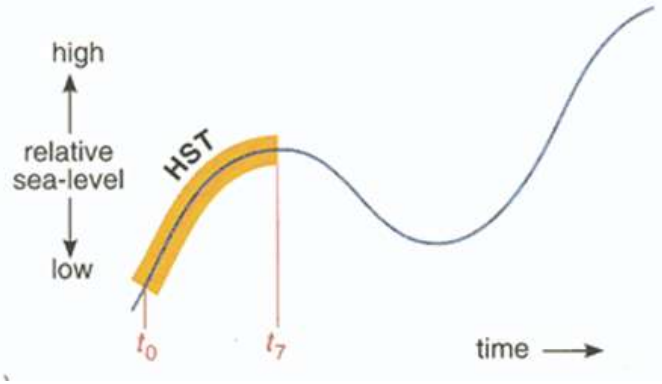

(b)

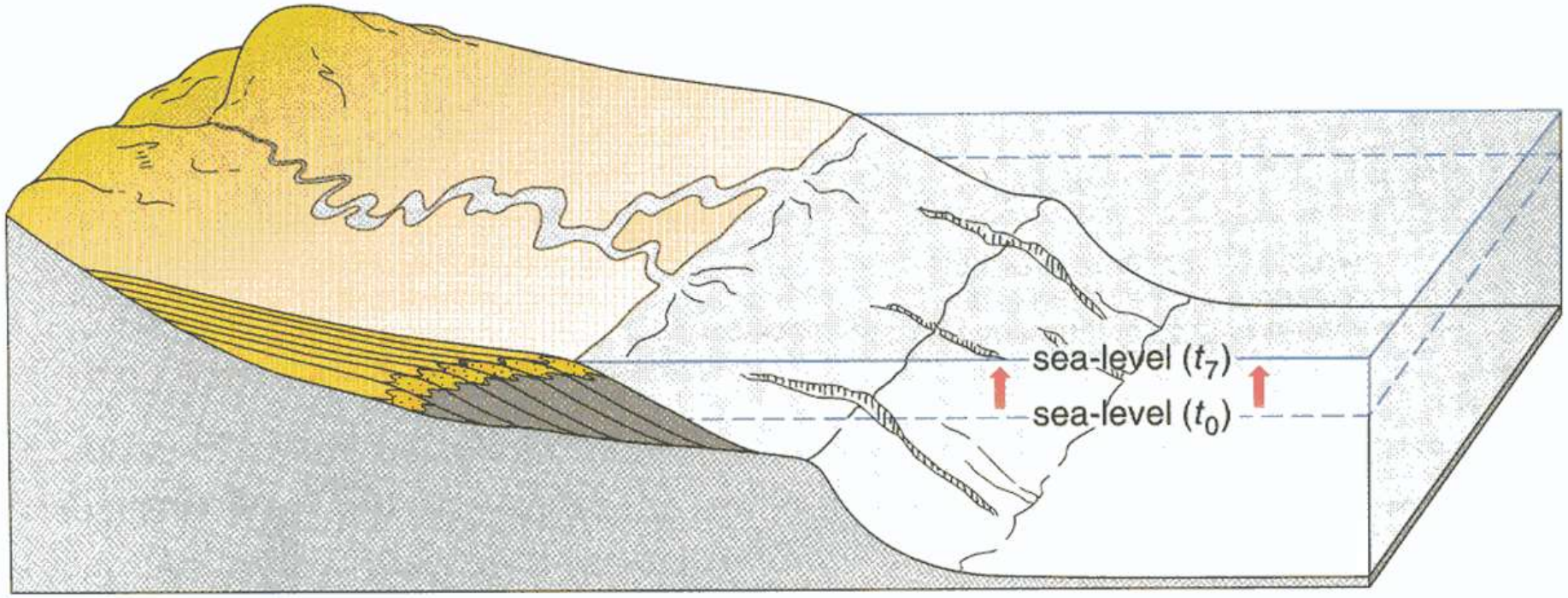

(c)

Types of shelf margin

Shelf break margin

Steep slope at shelf edge

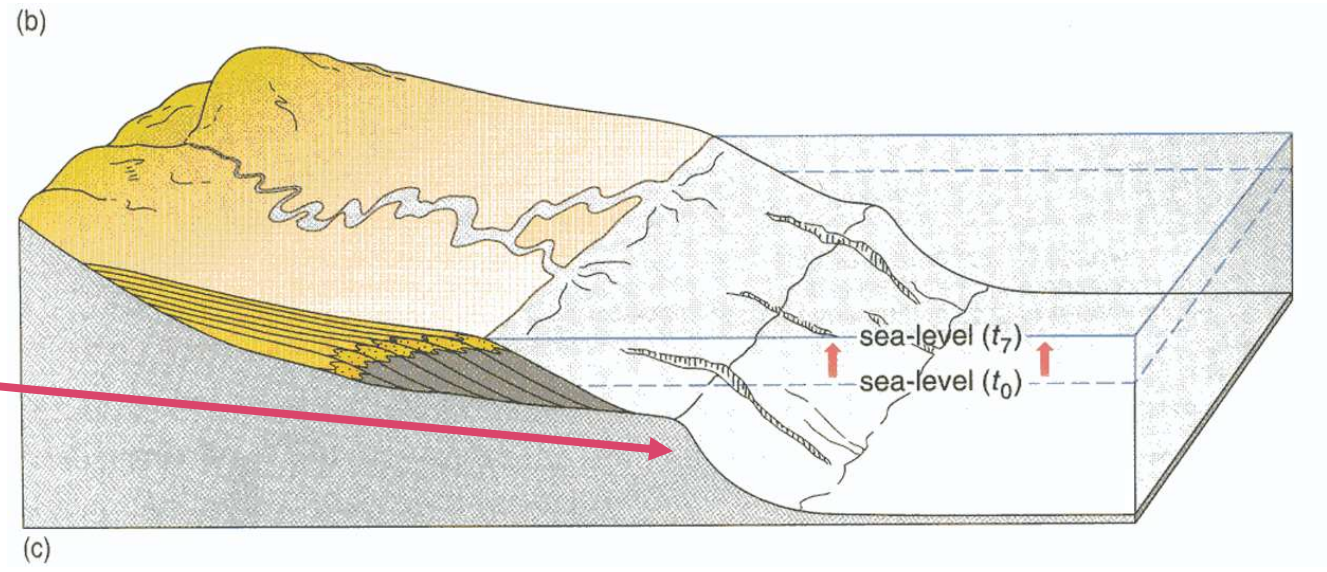

Ramp margin

No distinct shelf edge

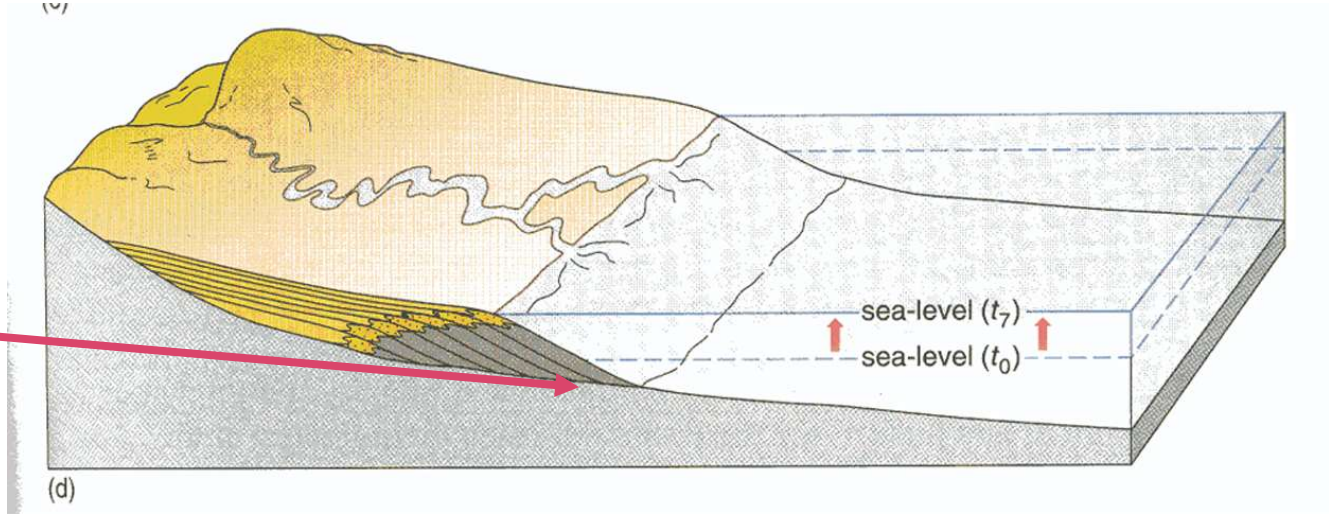

PARASEKVENCE

parasekvence – sukcese geneticky spjatých sedimentárních těles;
vymezena záplavovými plochami
- směrem do nadloží vykazuje změlčující trend
(v malém měřítku)

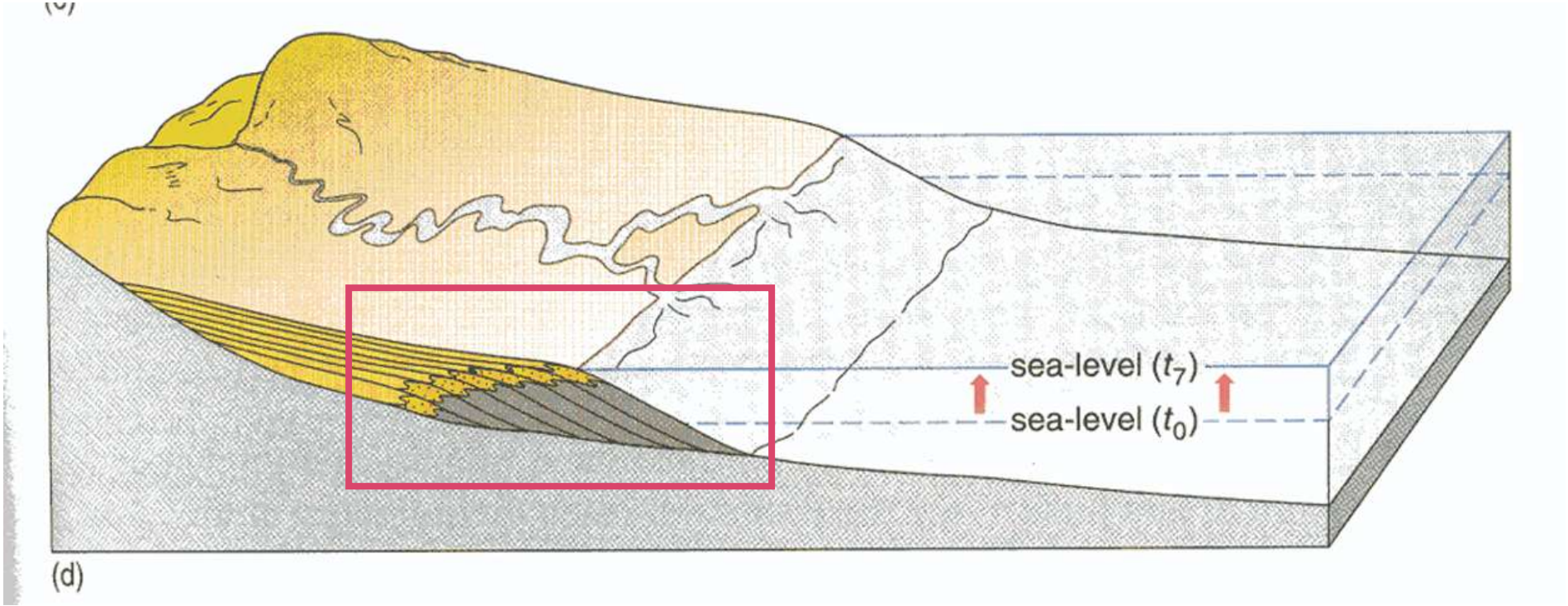

SEDIMENTÁRNÍ SEKVENCE

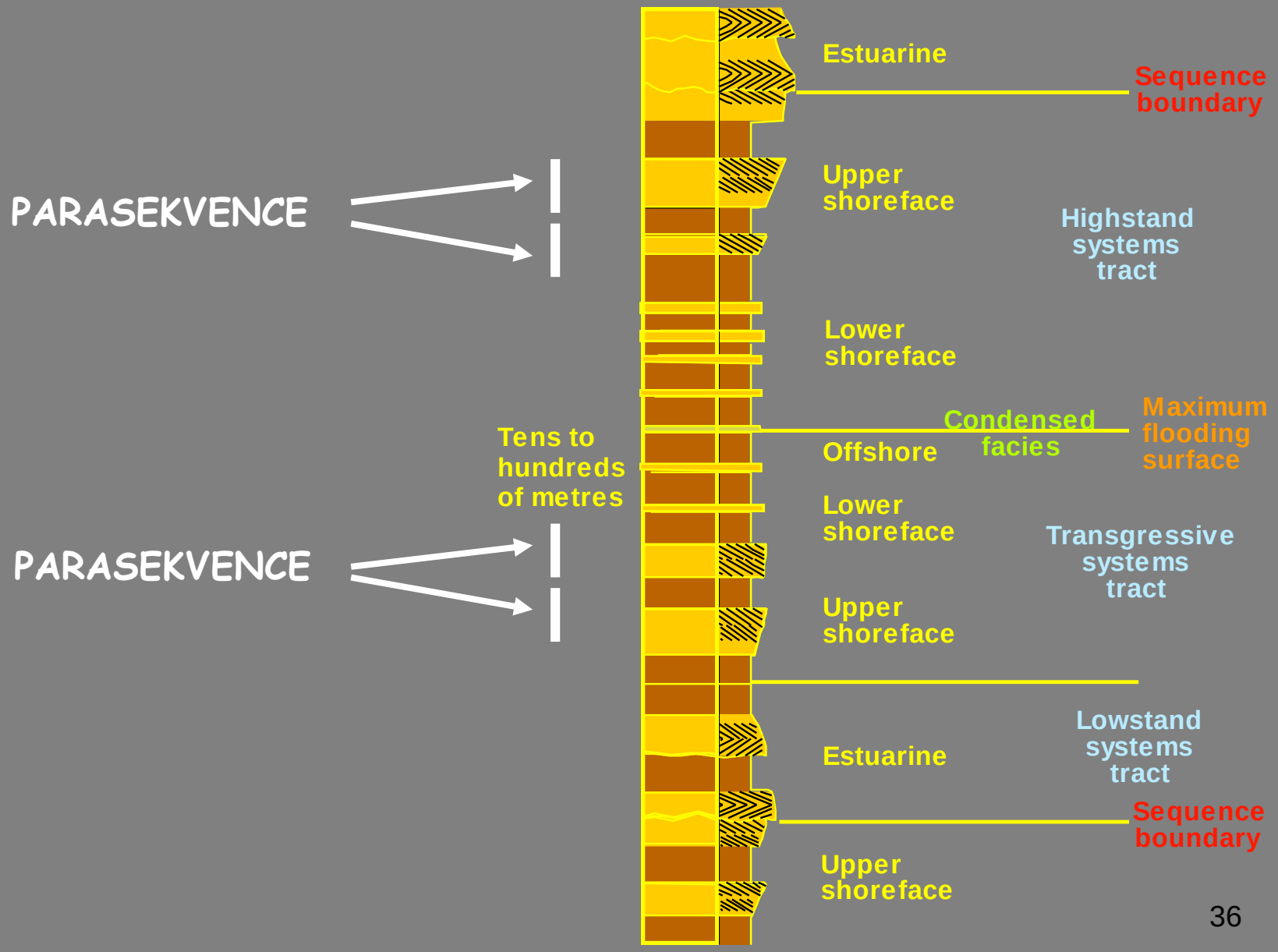

Parasequence stacking pattern

Ratio rate of deposition / Rate of accommodation >1

Ratio rate of deposition / Rate of accommodation <1

Ratio rate of deposition / Rate of accommodation =1

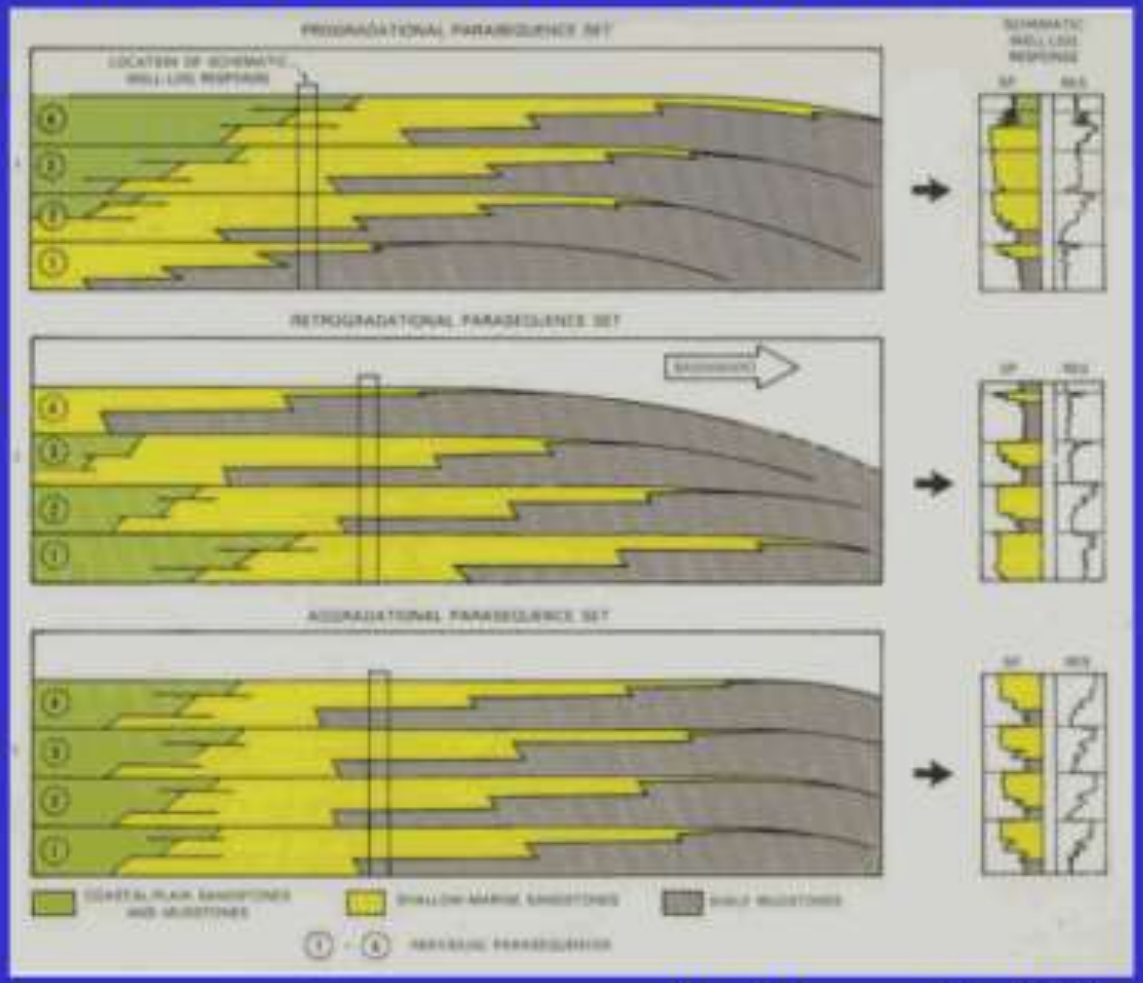

Van Wagoner et al. (1987)

KŘIVKA RELATIVNÍCH ZMĚN HLADINY

PŘEDPOKLAD: křivka má tvar sinusoidy

Křivka krátkodobých změn

Křivka dlohodobých změn

Kombinovaná křivka

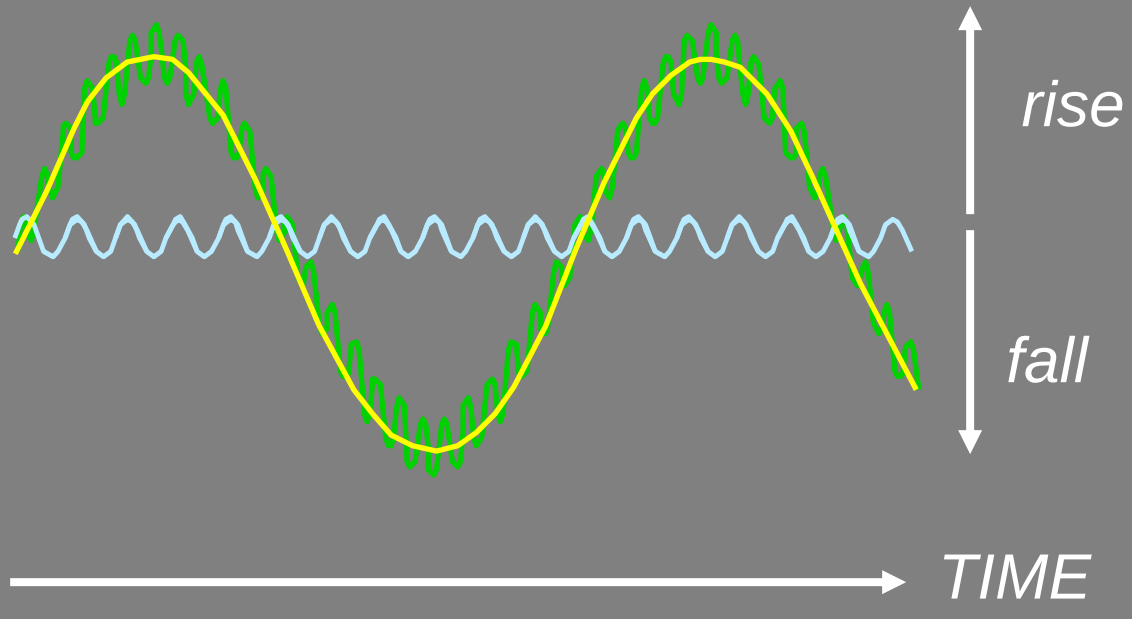

Sea level curve

Subsidence

Combined sea level curve

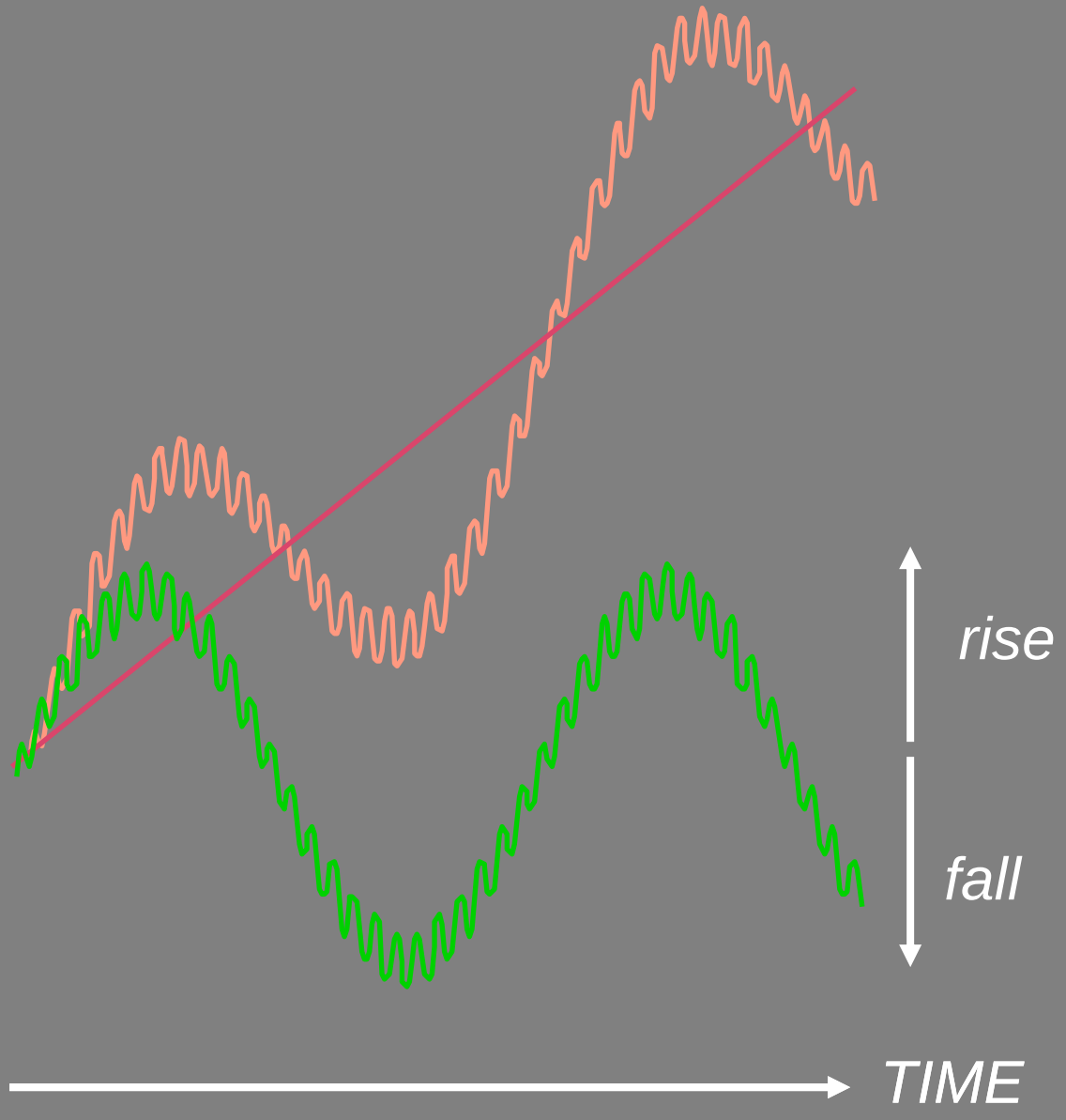

Falling Stage Systems Tract
Progradational parasequence
stacking patterns

Sea level curve

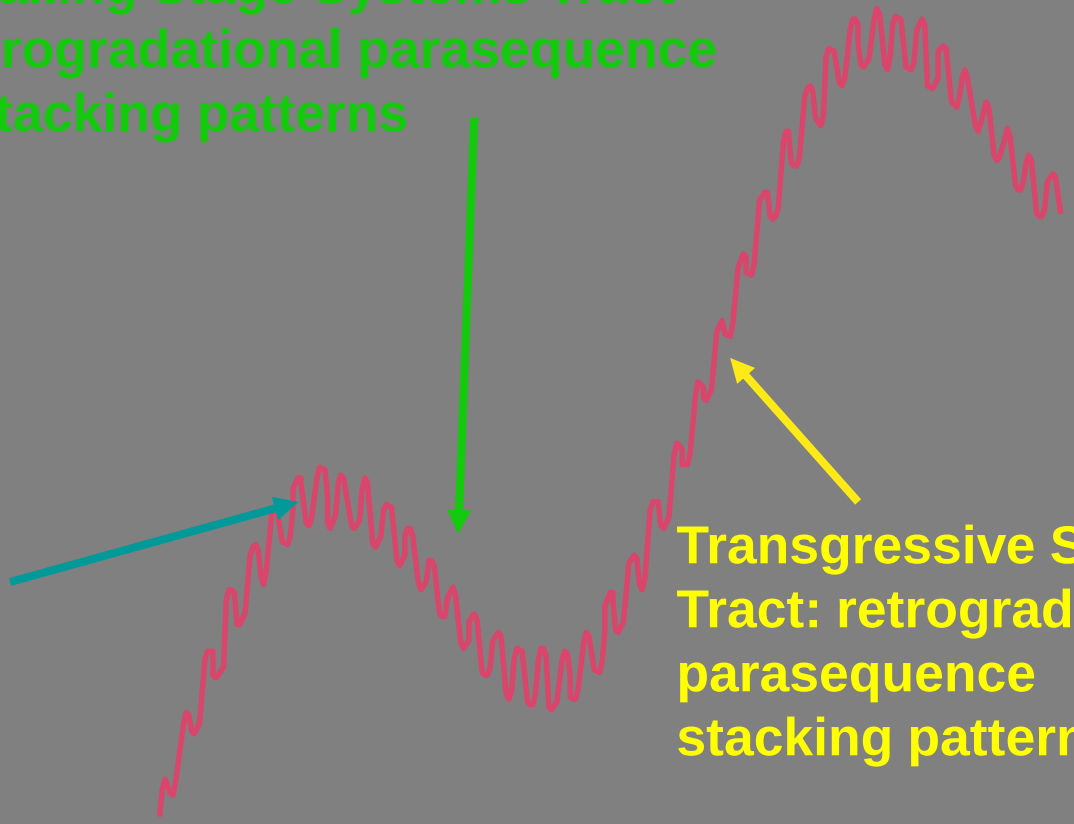

Highstand Systems
Tract: aggradational
parasequence
stacking patterns

Transgressive Systems
Tract: retrogradational
parasequence
stacking patterns

Fluvial environments

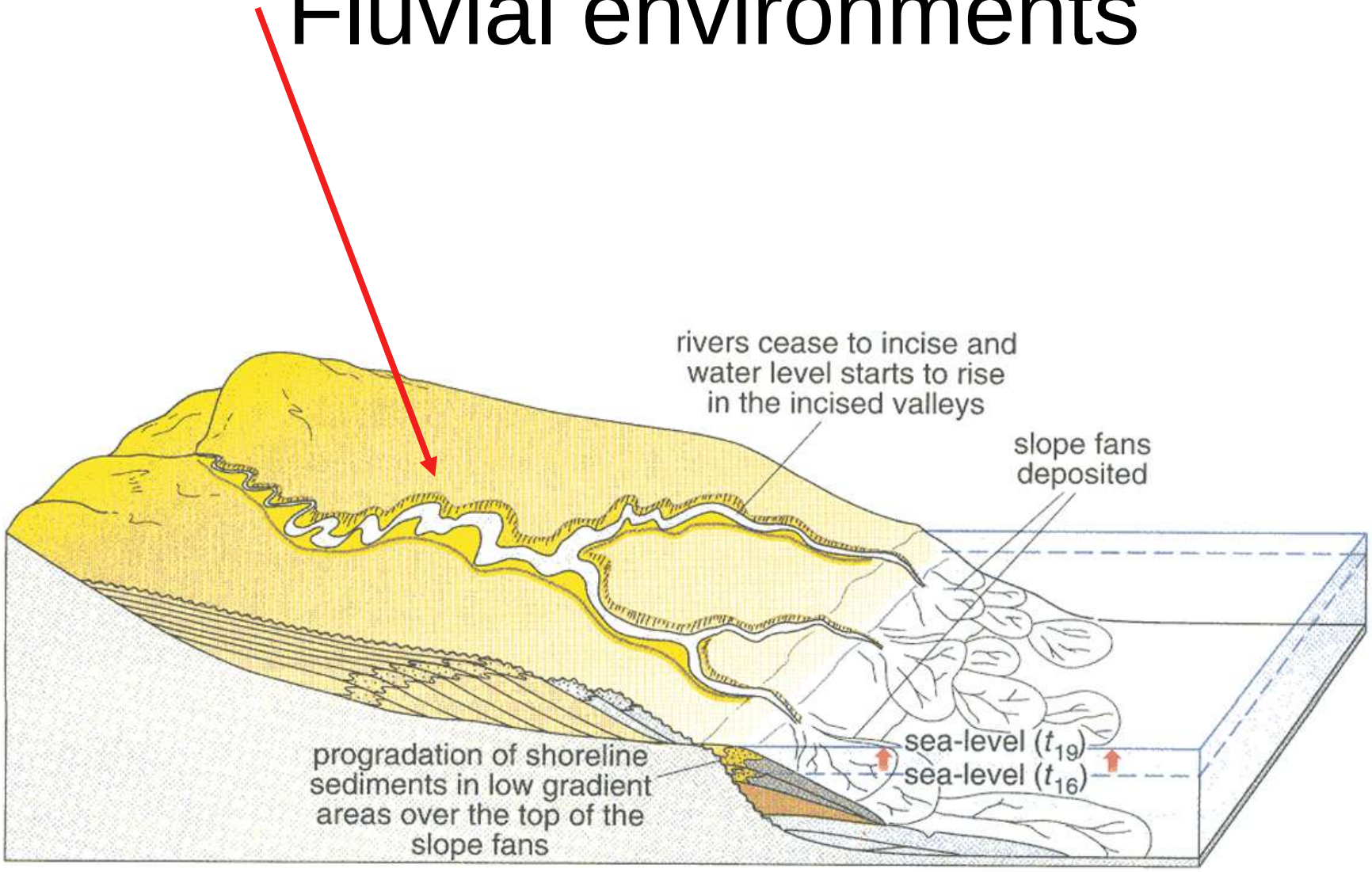

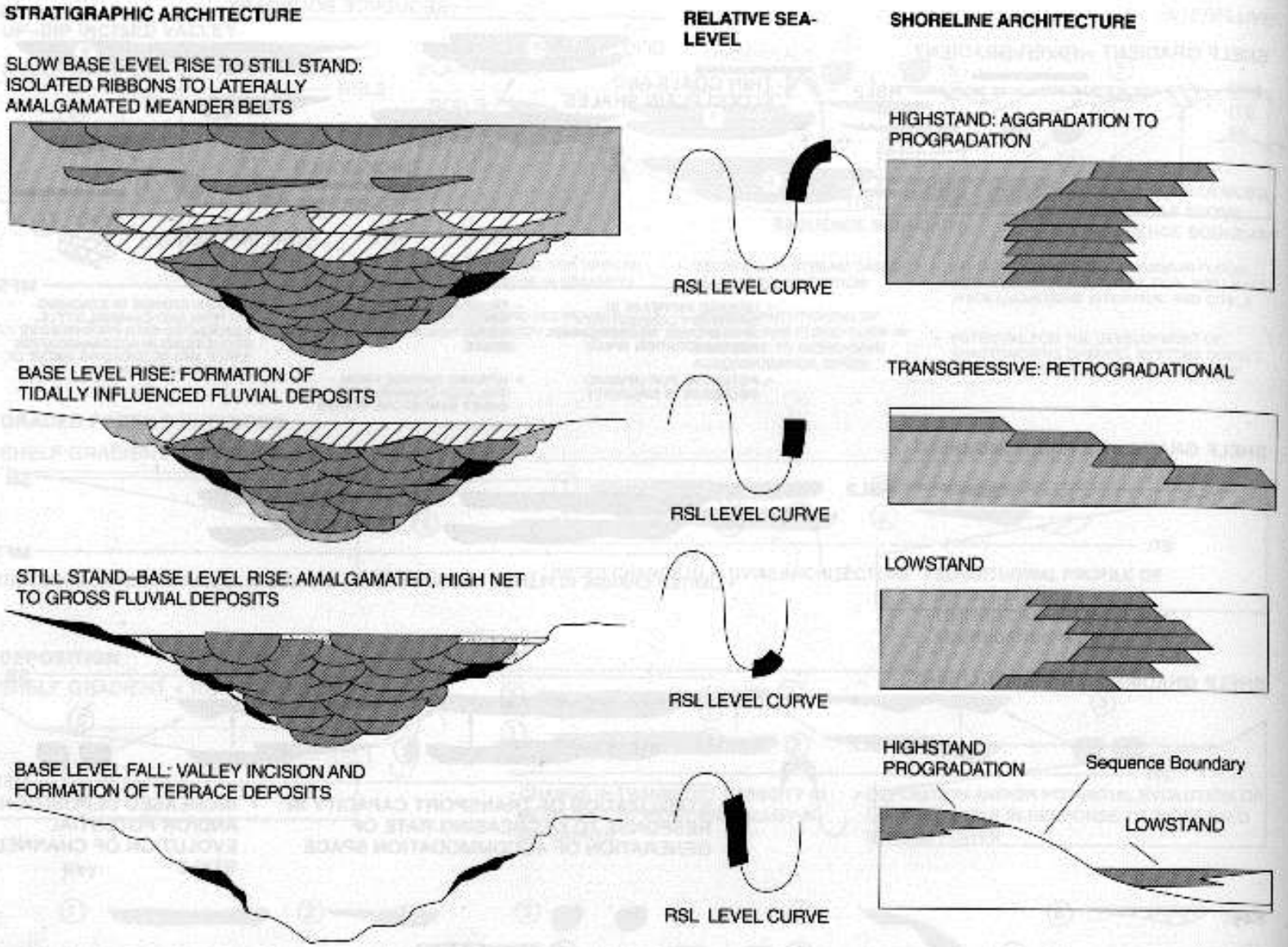

Fig. 7.11 Summary diagram illustrating the relationship between shoreface and fluvial architecture as a function of base level change (after Shanley and McCabe, 1993). Detailed correlations suggest the timing of the incised-valley fill occurred after the initial transgressive surface. For this reason Shanley and McCabe (1993) regard the valley-fill as 'alluvial-transgressive' deposits

Legarreta & Uliana 1998

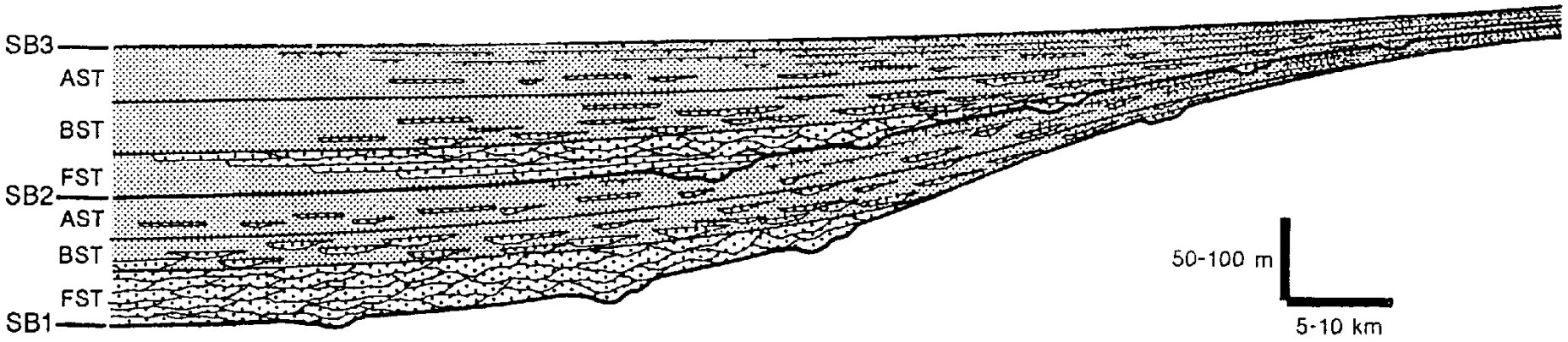

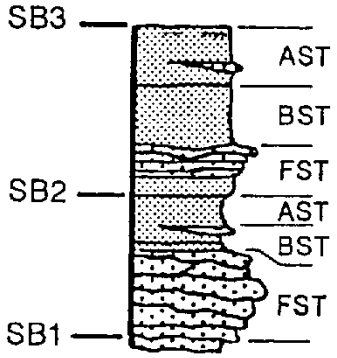

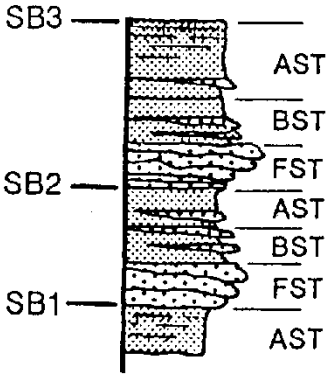

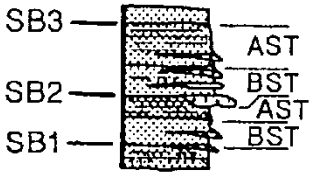

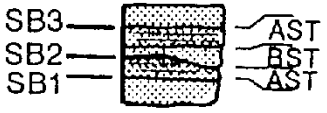

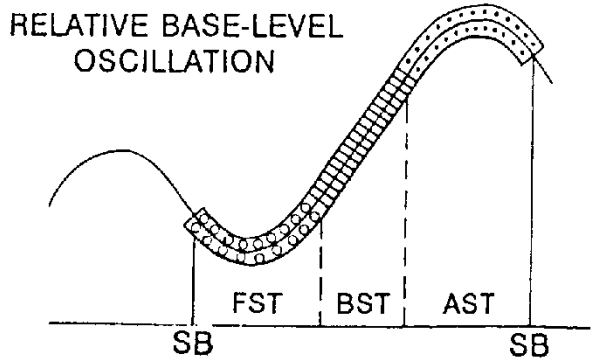

Martinsen et al. 1999

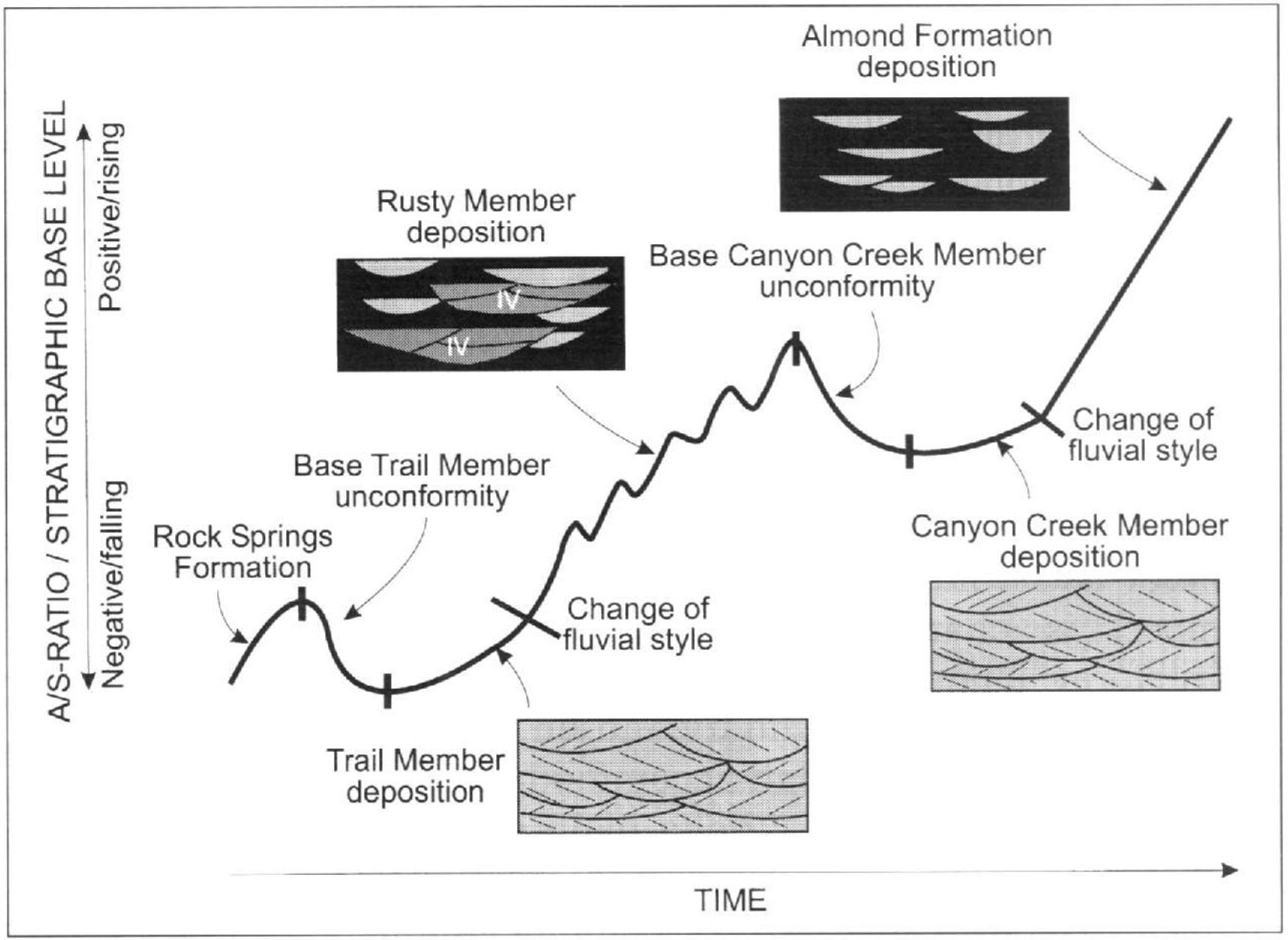

Fluvial environments

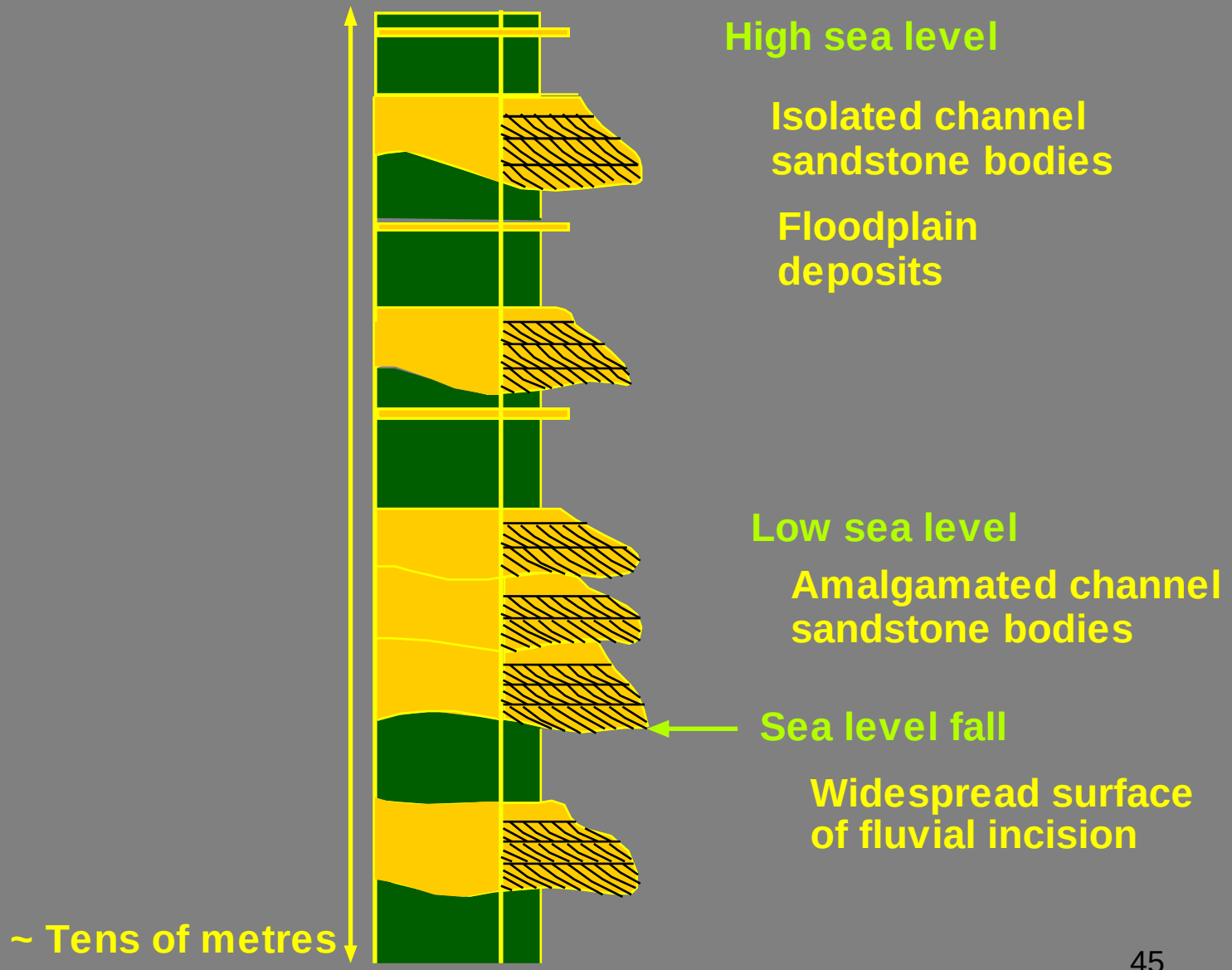

Deep marine environments

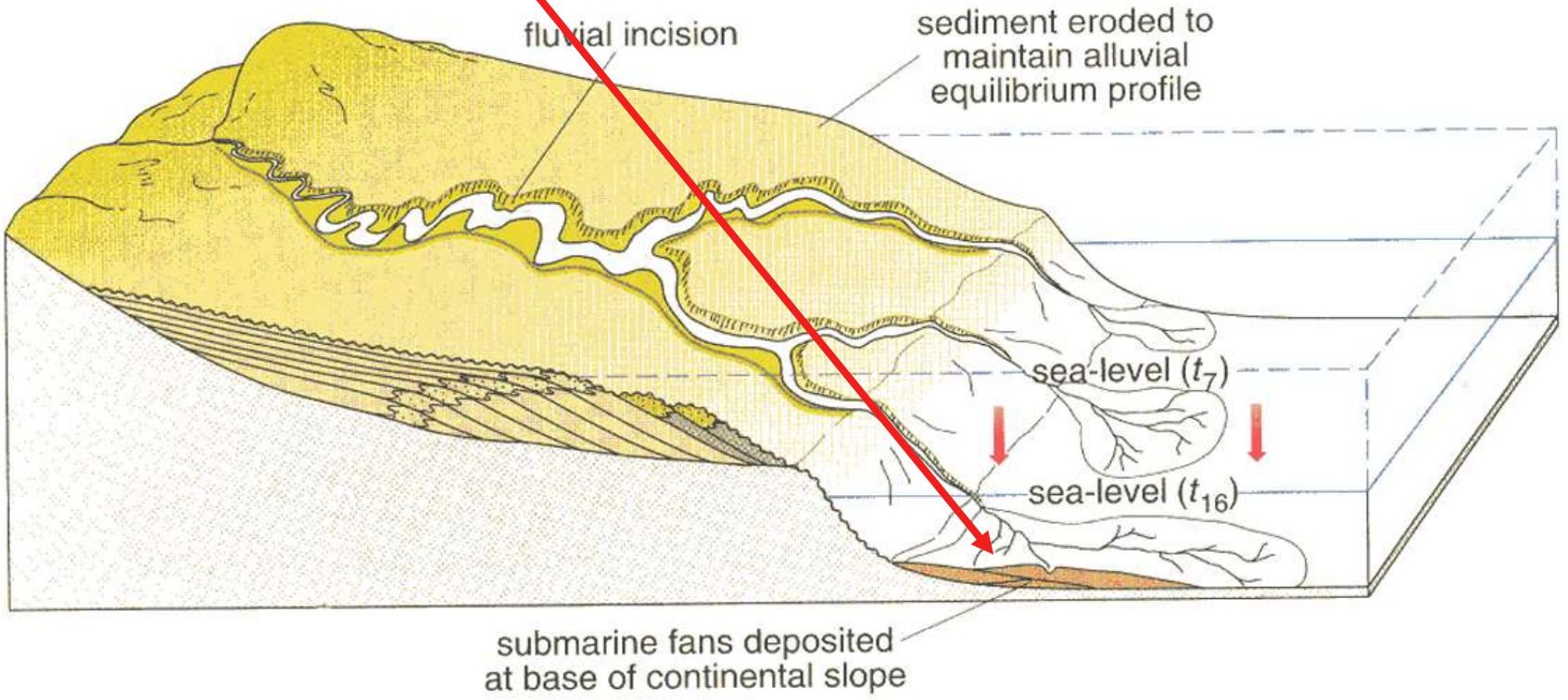

Deep marine environments

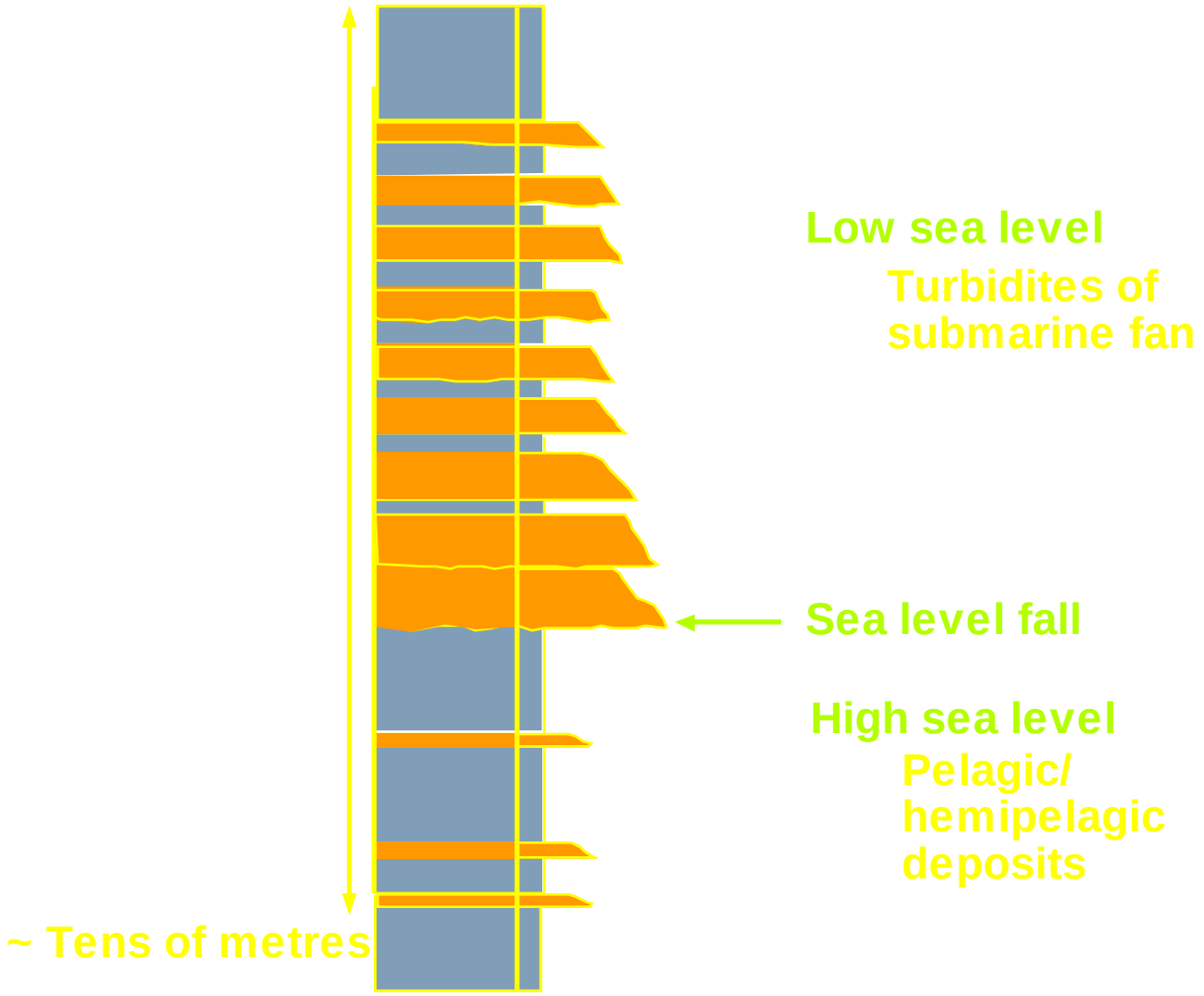

AKOMODAČNÍ PROSTOR, PŘÍČINY ZMĚN HLADINY A CYKLOSTRATIGRAFIE

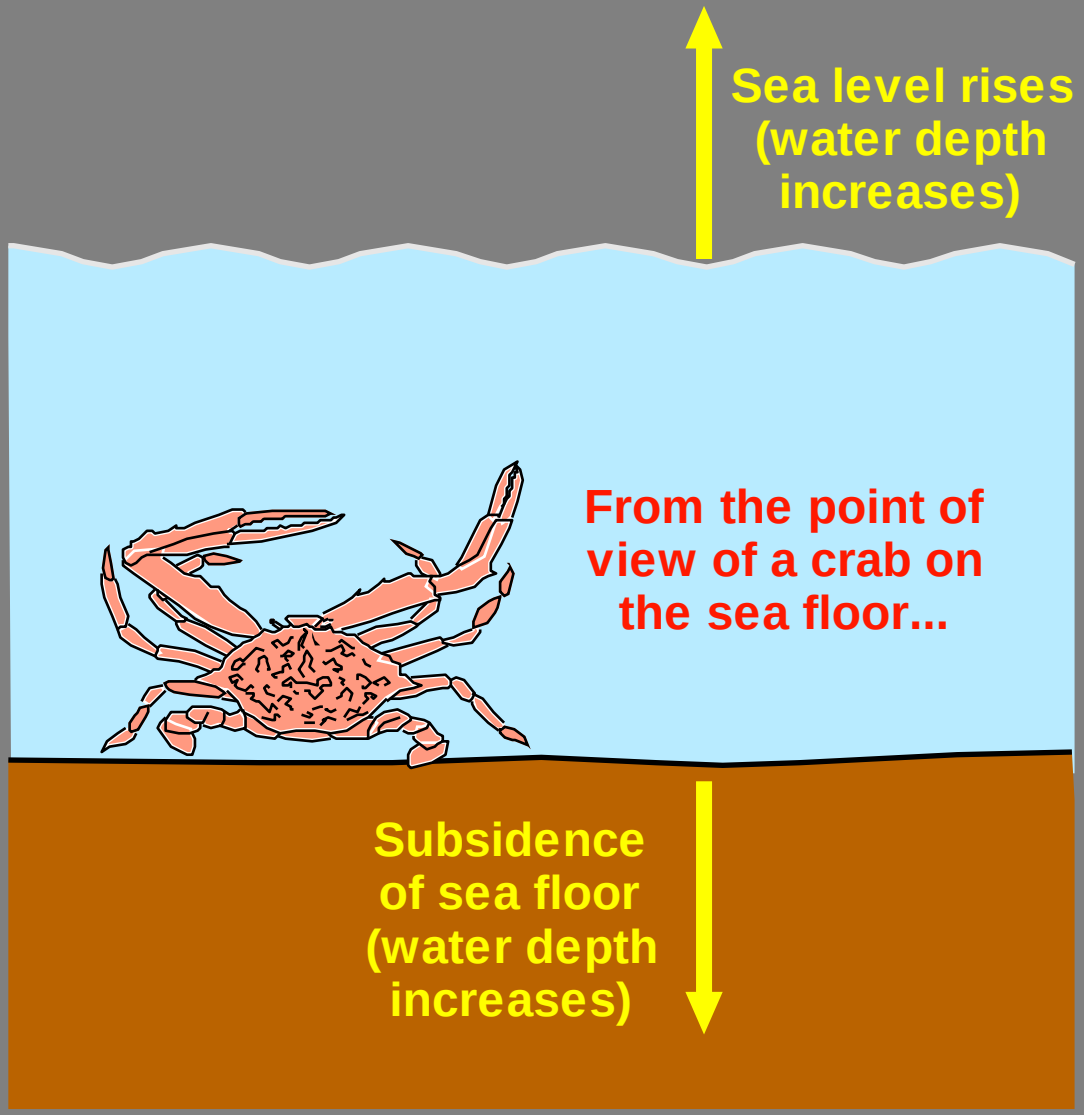

Sea level curve

Subsidence

Combined sea level curve

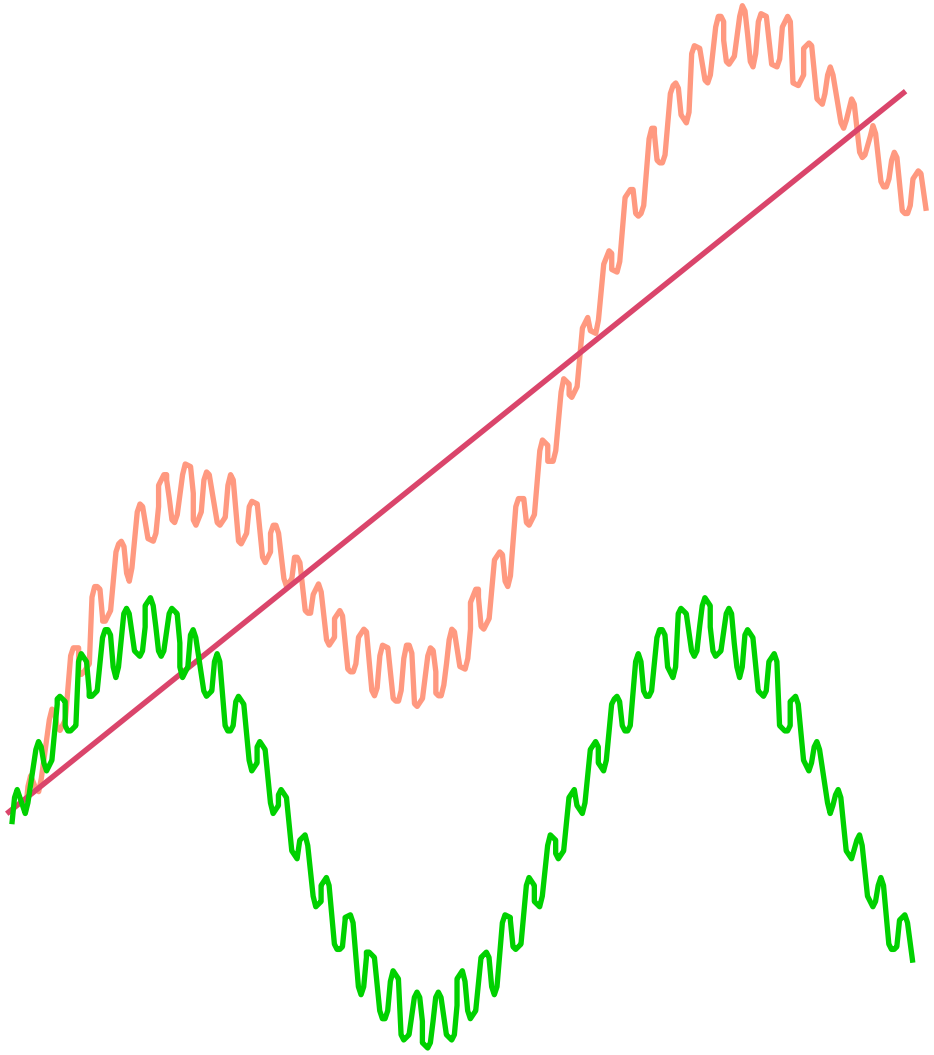

Local tectonics
e.g.

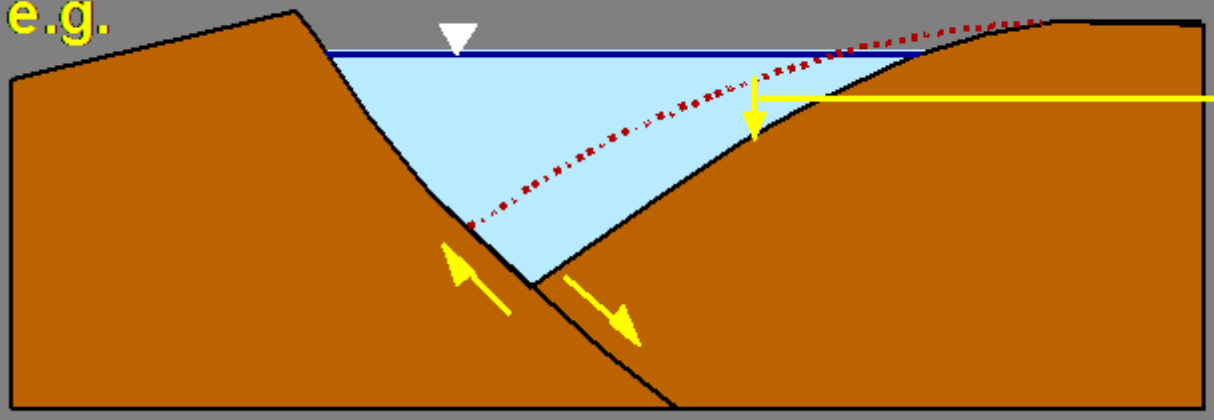

Relative sea level rise

Very variable rates and magnitudes of relative sea level changes

Sea water temperature

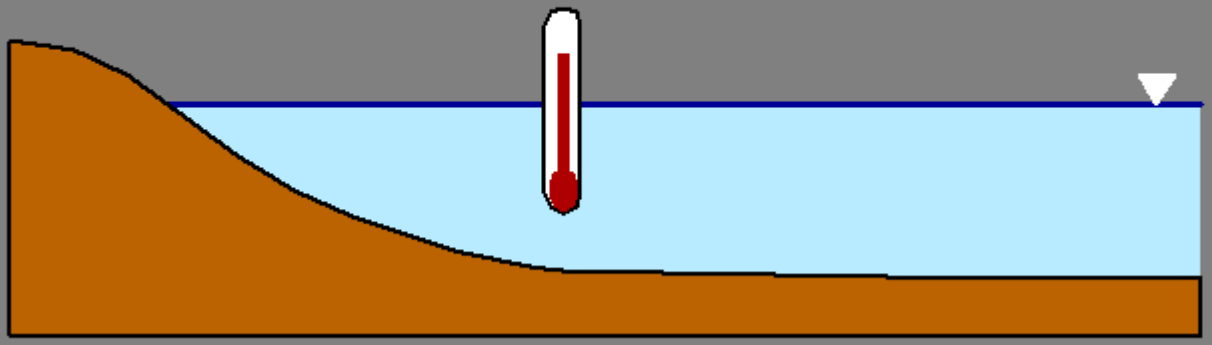

- Changes in sea water temperature cause thermal expansion/contraction

  Centimetres to a few metres change over hundreds to thousands of years

Exchange with water on continents

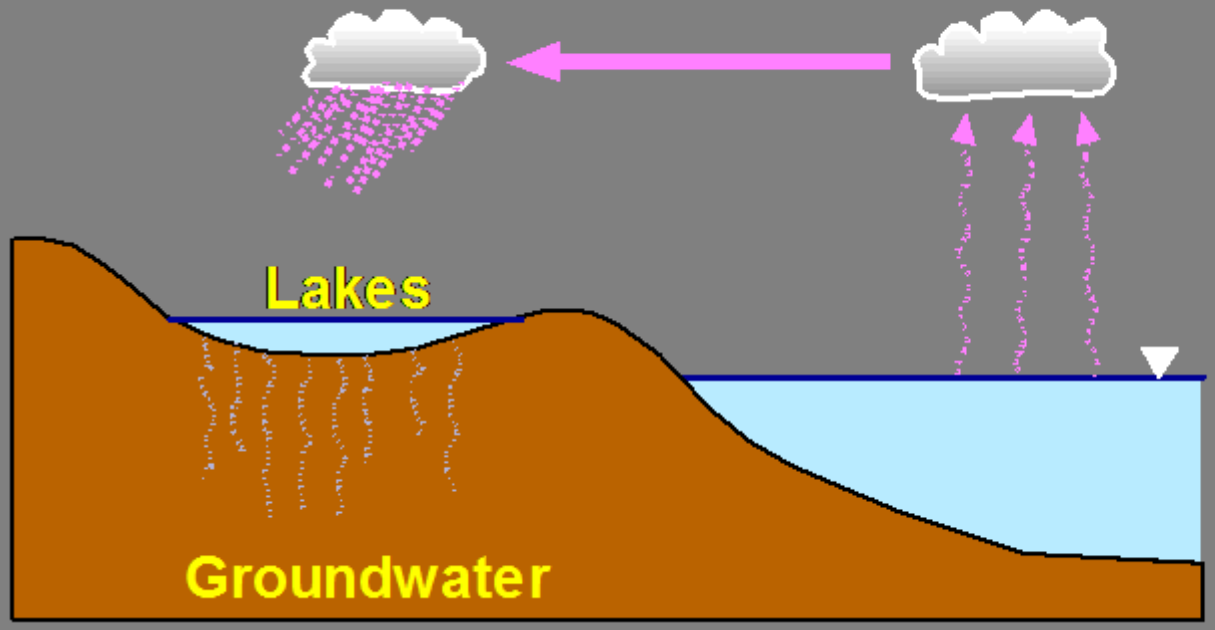

Centimetres to metres change over hundreds to thousands of years

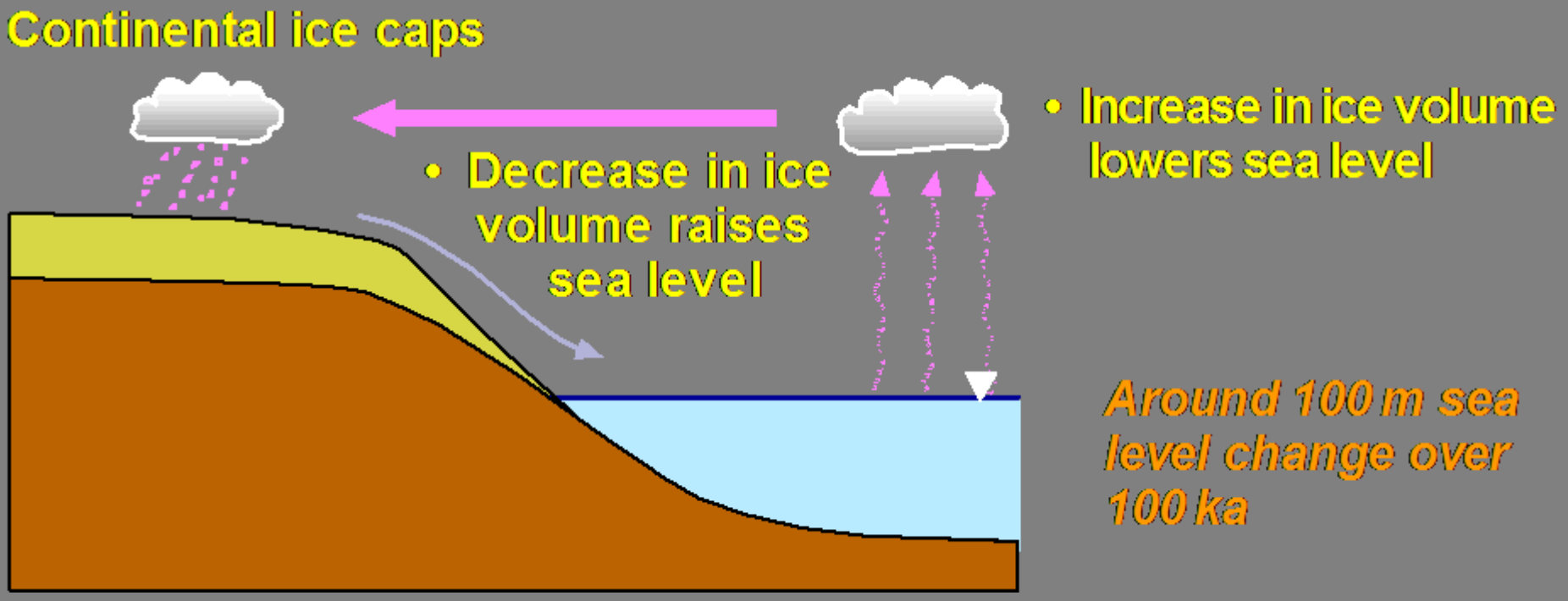
Continental ice caps
• Decrease in ice volume raises sea level
• Increase in ice volume lowers sea level
Around 100 m sea level change over 100 ka

Global scale thermo-tectonic

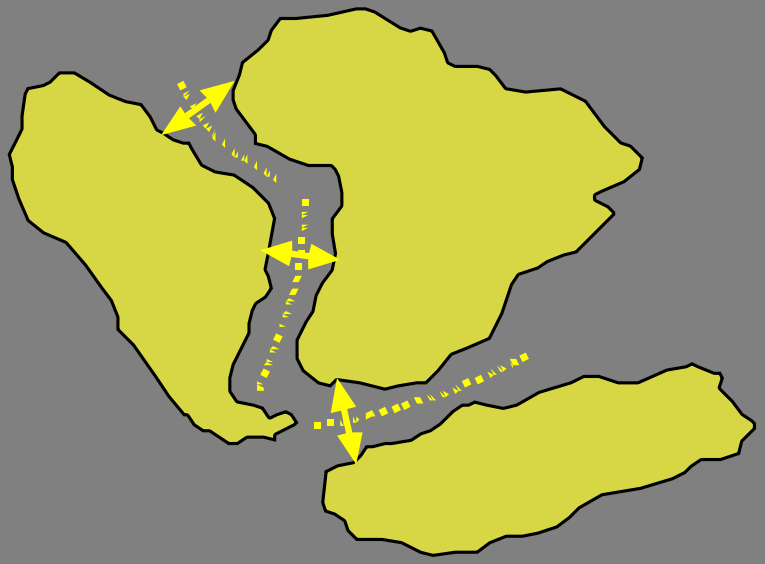

- Formation and breakup of supercontinents
- Changes in rates of formation of ocean crust

10–100 m sea level change over 10–100 Ma

Slow mid-ocean ridge spreading

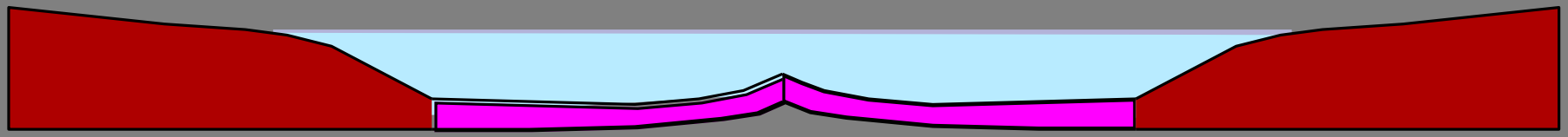

Oceanic crust cools and contracts

Fast mid-ocean ridge spreading

Sea water displaced onto continental shelves

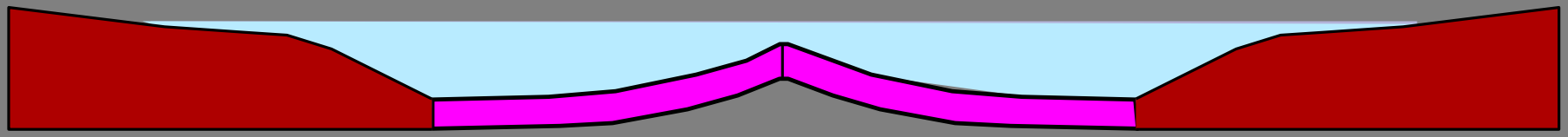

More hot, buoyant oceanic crust occupies more space in the ocean basin

Milankovitch Cycles

Changes in the eccentricity of the Earth's orbit around the Sun

100 ka cycle

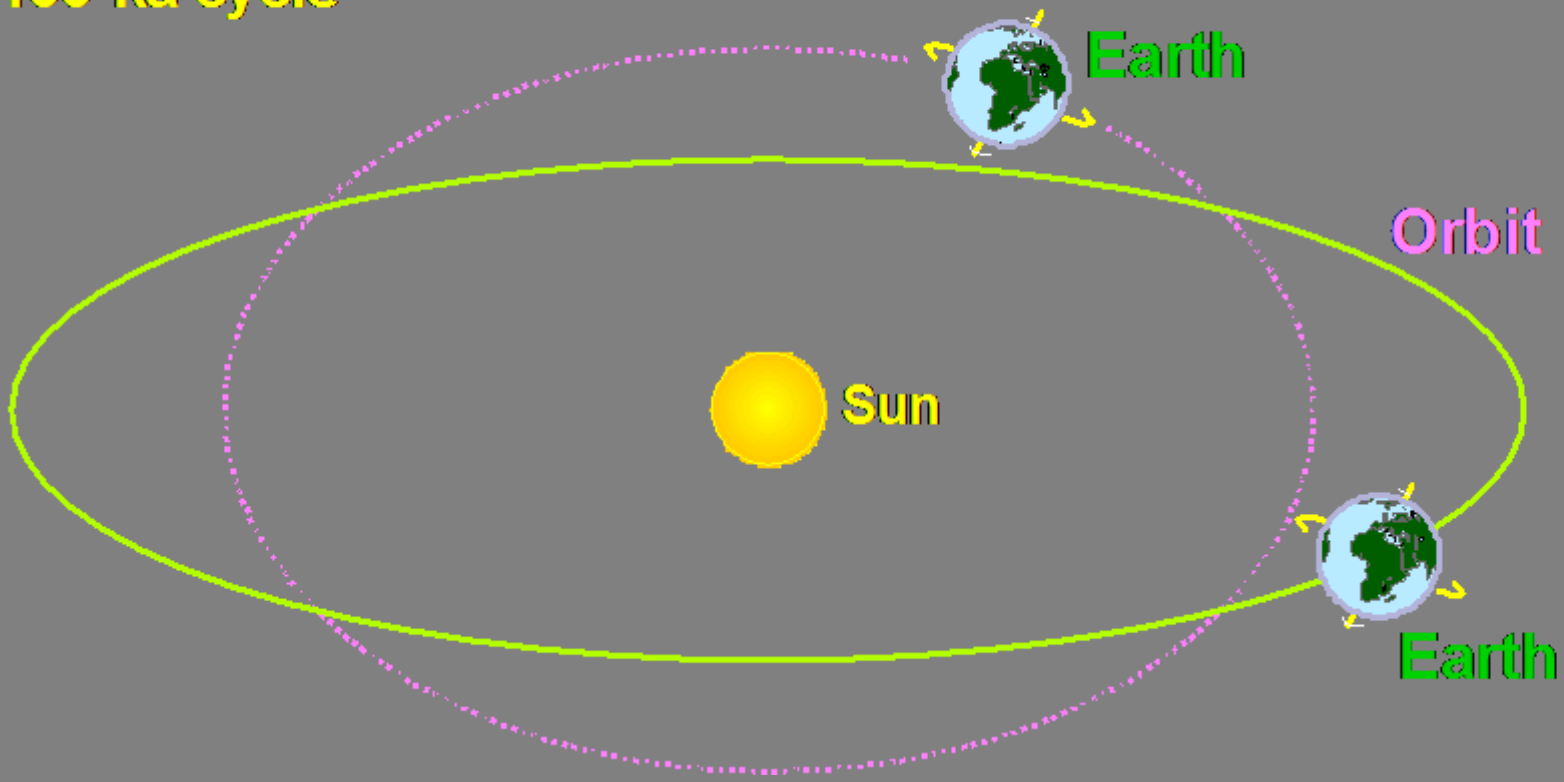

Changes in the obliquity (tilt) of the Earth's axis of rotation

41 ka cycle

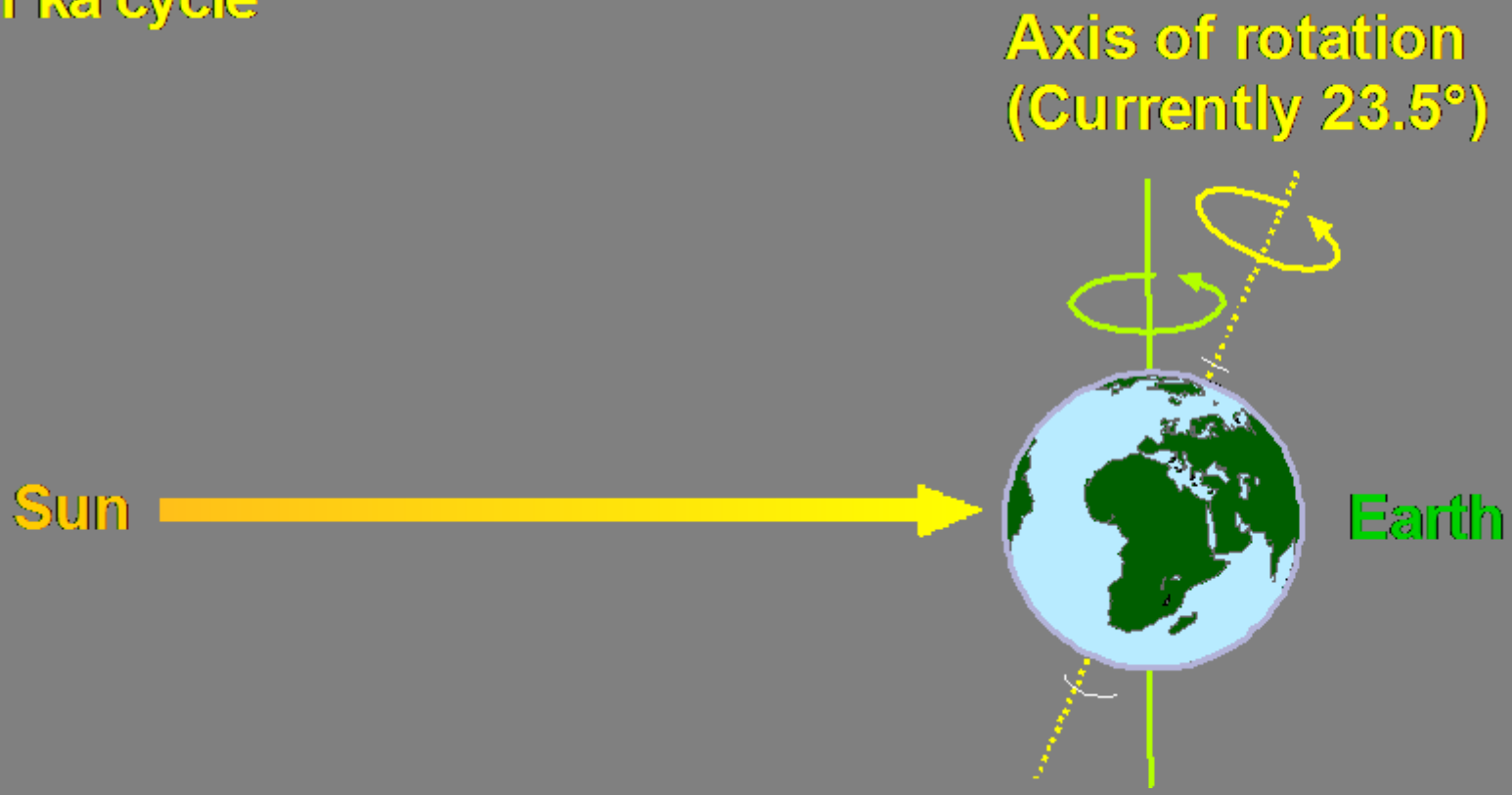

Milankovitch Cycles

Precession of the axis of rotation

22 ka cycle

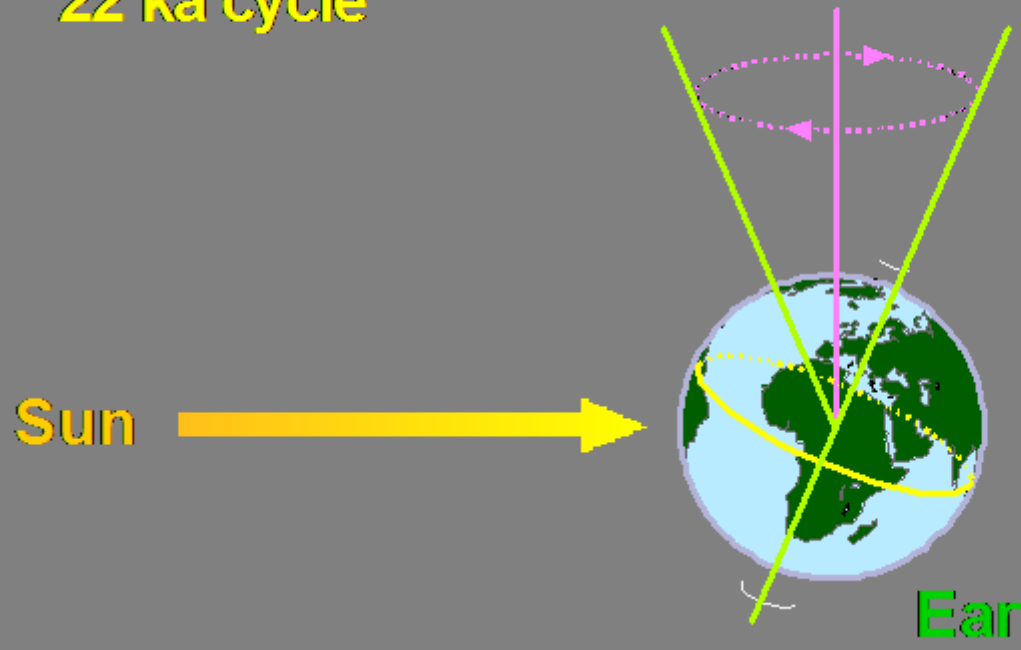

Tilt of the axis changes from being inclined towards the Sun to being inclined away from the Sun

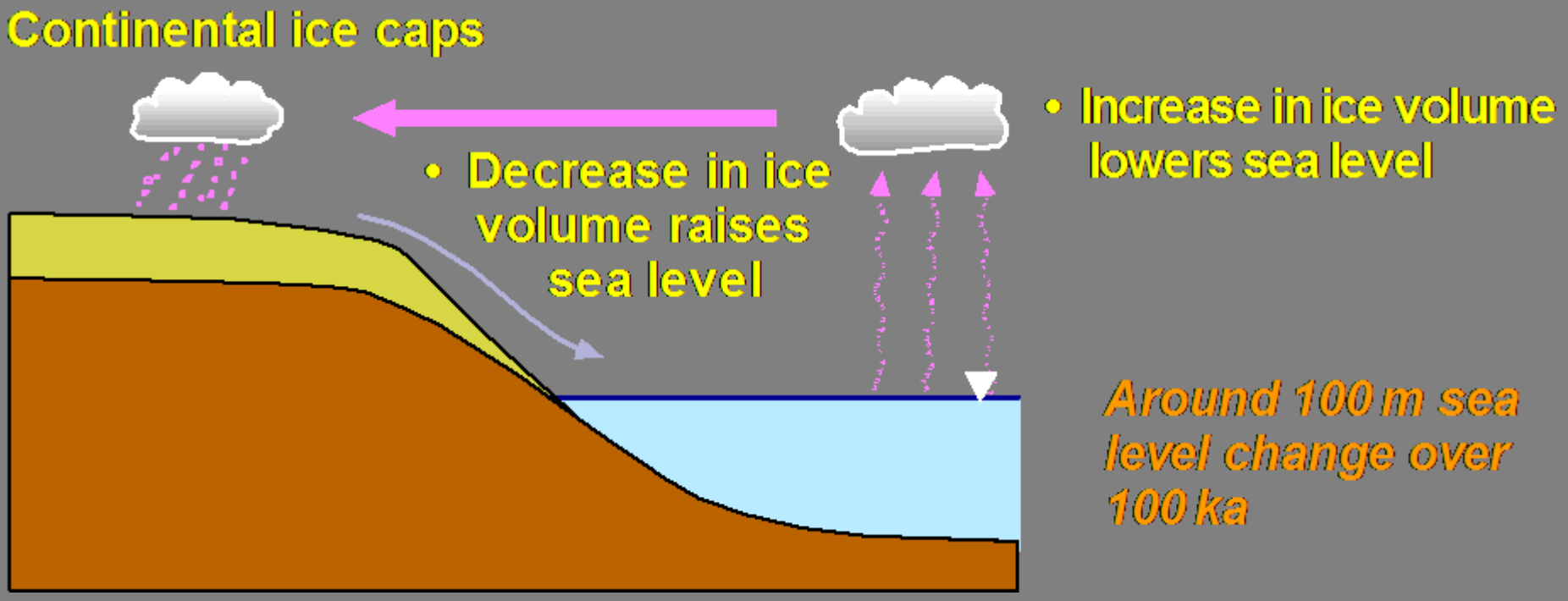
Continental ice caps
• Decrease in ice volume raises sea level
• Increase in ice volume lowers sea level
Around 100 m sea level change over 100 ka

KŘIVKA RELATIVNÍCH ZMĚN HLADINY

Křivka krátkodobých změn

Křivka dlohodobých změn

Kombinovaná křivka

Subsidence

Křivka relativních změn hladiny

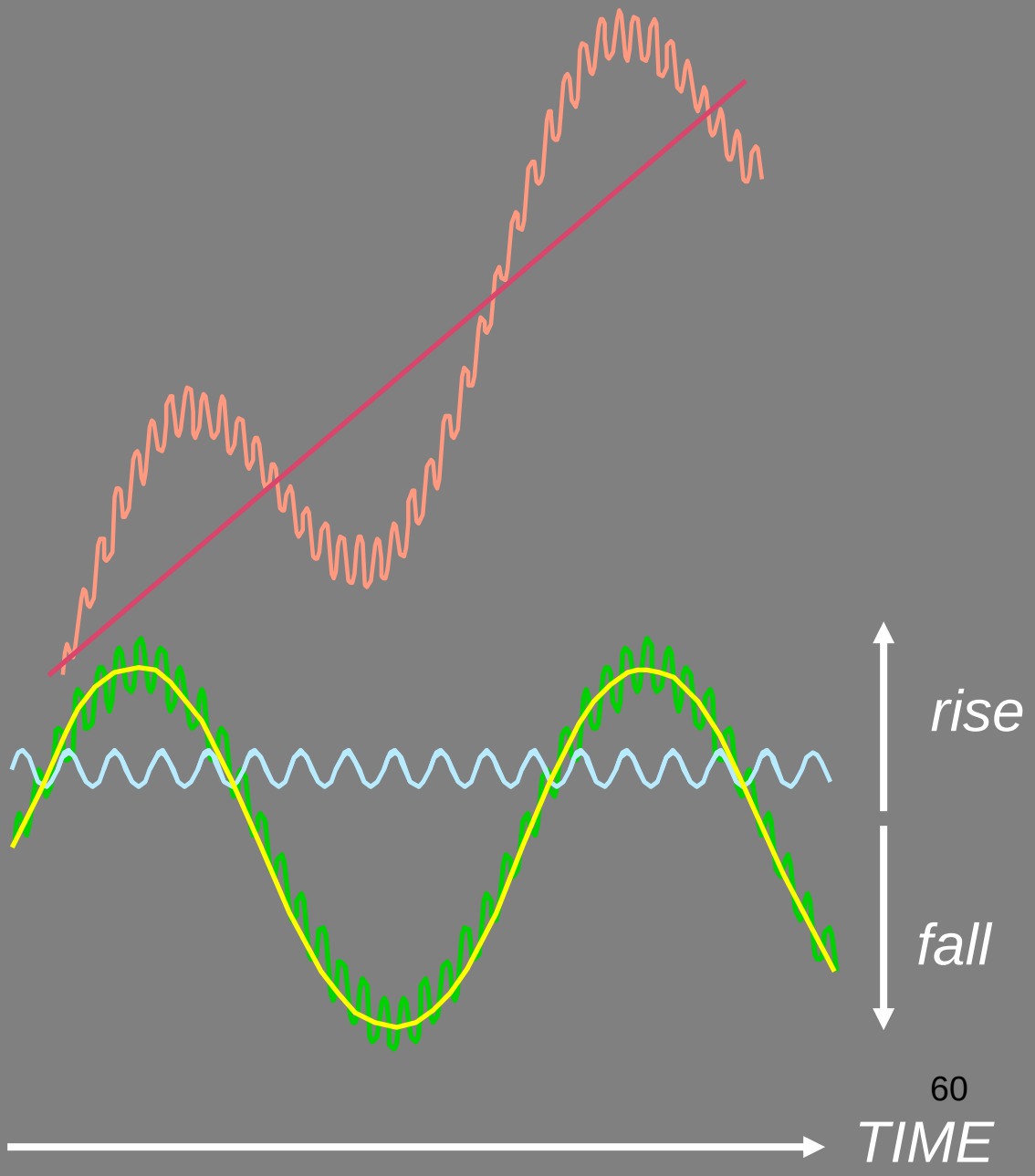

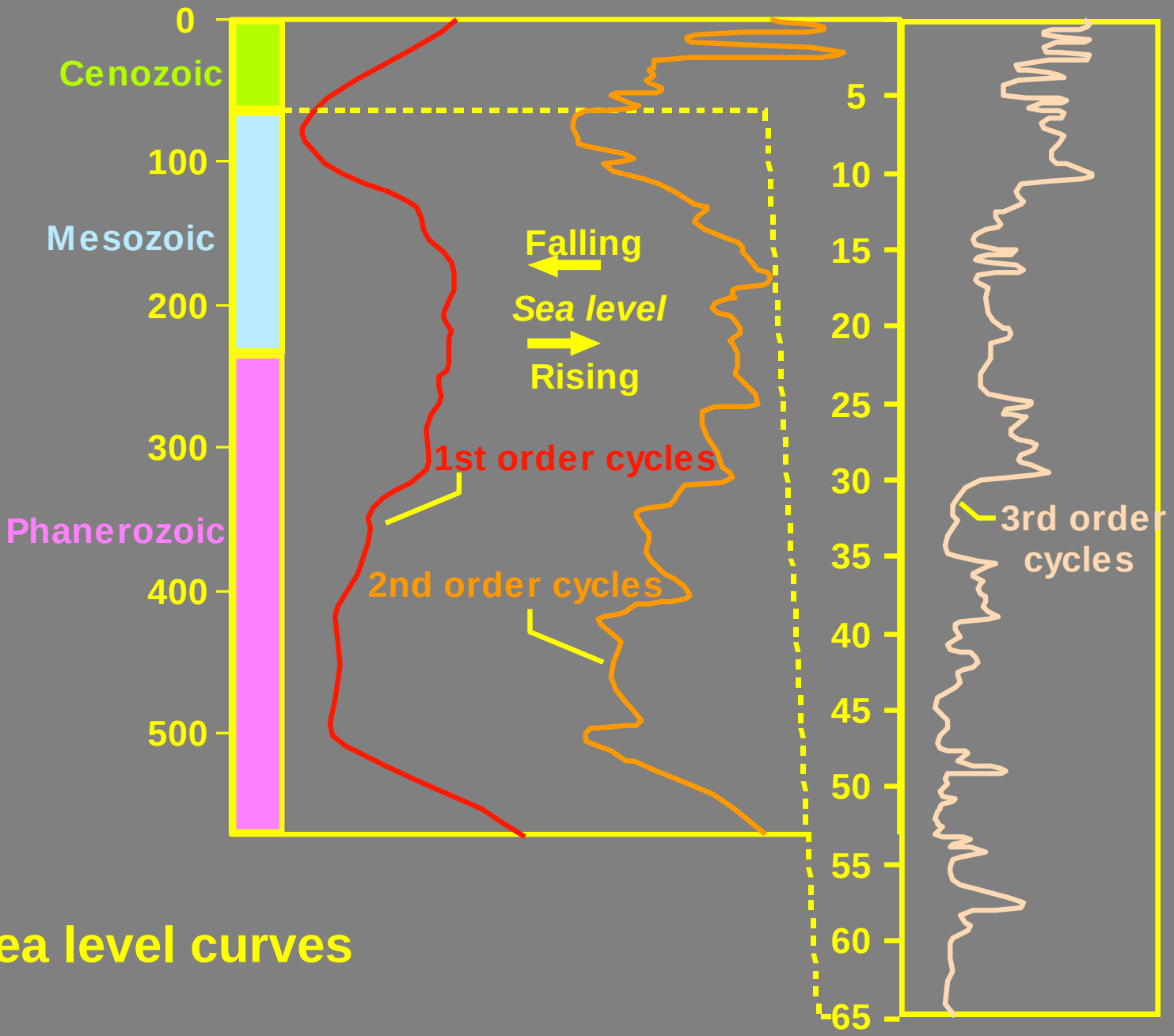

Global Sea level curves

Geochemie sedimentárních hornin, katodová luminiscence

stabilní izotopy

$\delta^{18}O$ [‰] = (($^{18}O/^{16}O_{vz}$ -$^{18}O/^{18}O_{SMOW}$)/ $^{18}O/^{18}O_{SMOW}$)*1000

vz – vzorek

$\delta^{13}C$ [‰] = (($^{13}C/^{12}C_{vz}$ -$^{13}C/^{12}C_{PDB}$)/ $^{13}C/^{12}C_{PDB}$)*1000

SMOW, PDB – standardy

procesy izot.frakcionace v hydrosféře - změny izot.složení vody s nadm.výškou, se zem. šířkou, →stratigrafie ledu

uhlíkový cyklus

karbonátové systémy, stratigrafie pelagických karbonátů, záznam teplotních, klimatických změn

$\delta^{13}C$ organické hmoty - typy metabolismu akvatických a terestrických rostlin

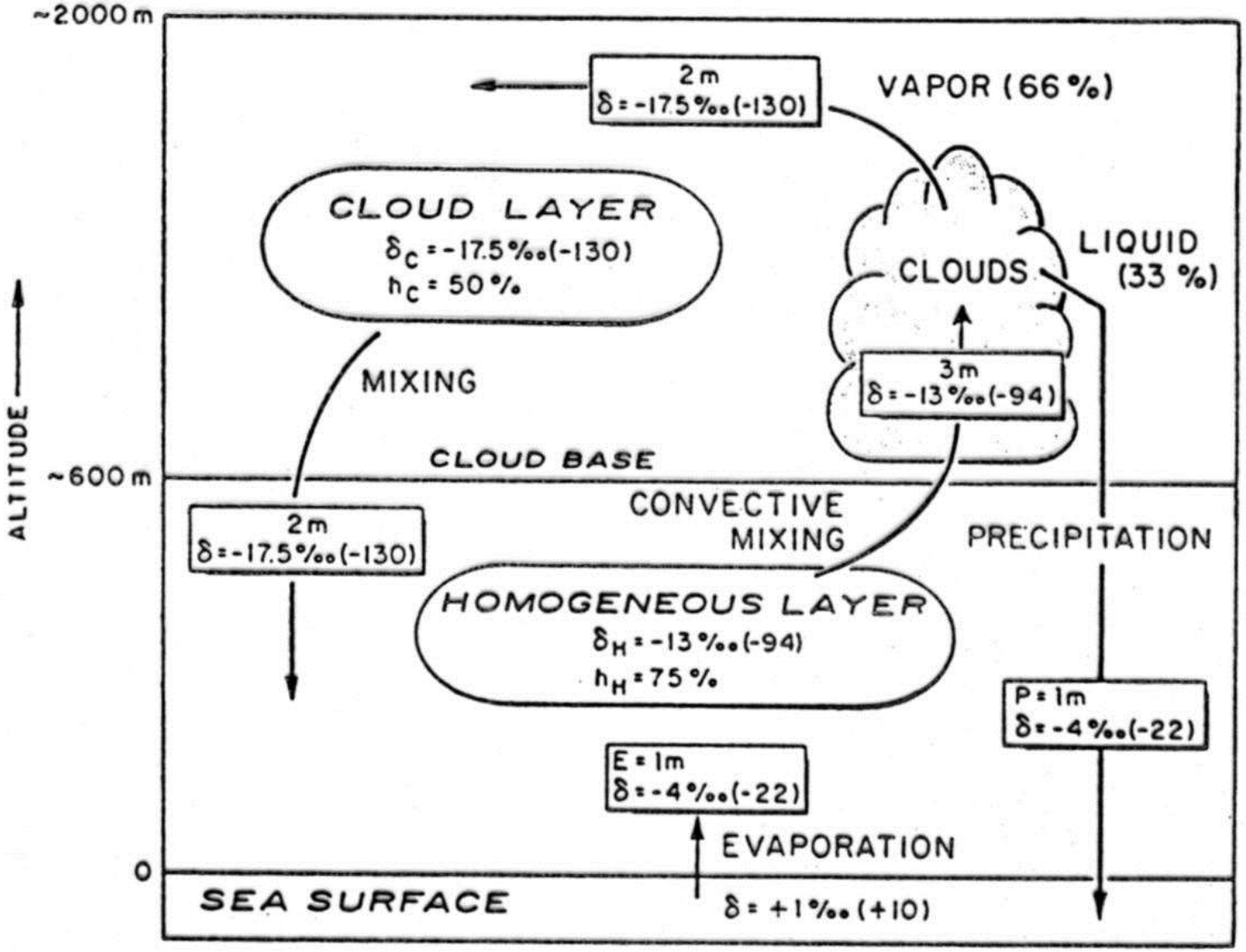

Fig. 1-9. Stable isotope composition of the marine atmosphere (from Craig and Gordon, 1965). δ-values are given for ^{18}O and, in parentheses, for deuterium.

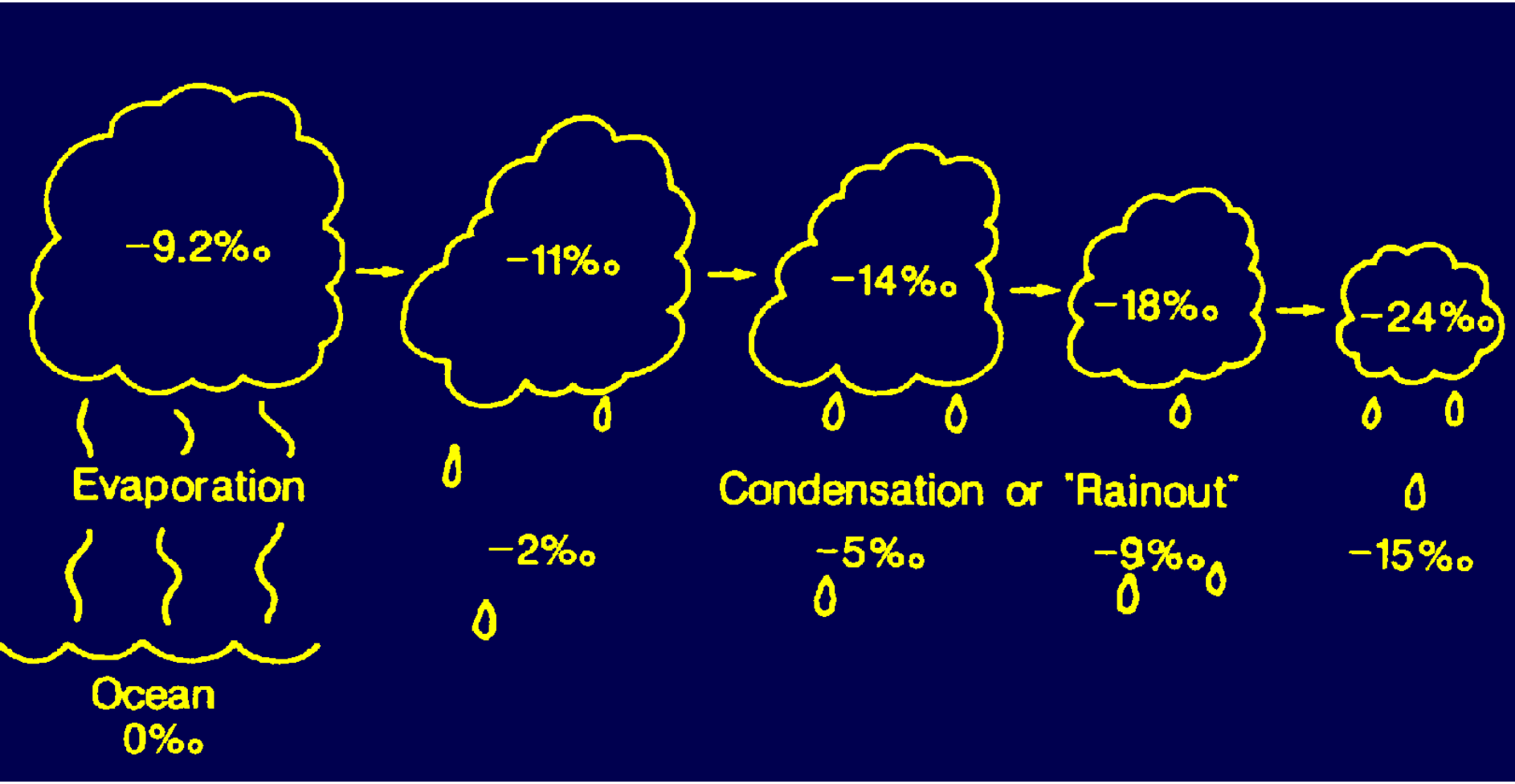

effect of distance

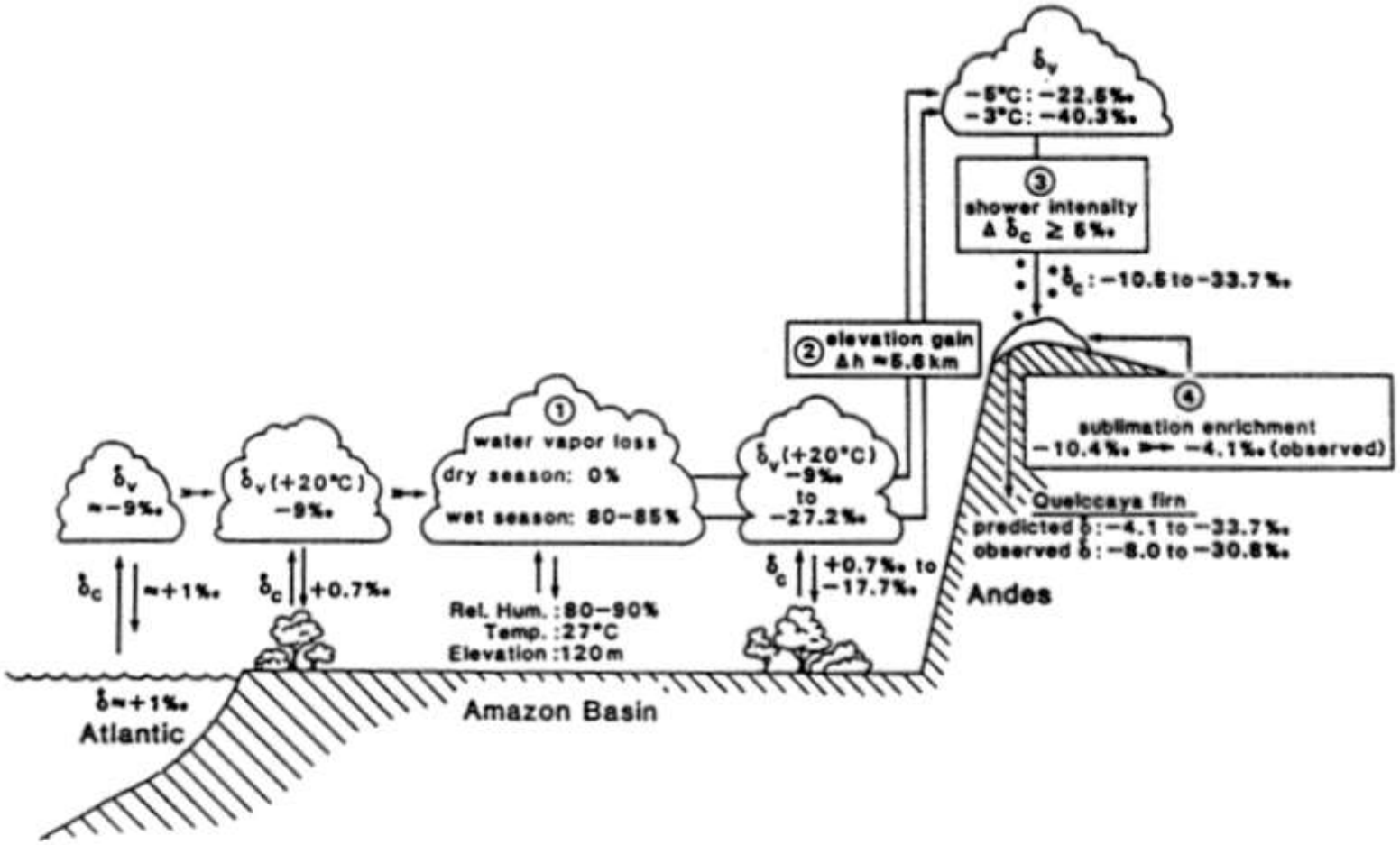

Fig. 1. Oxygen isotopic composition of atmospheric water vapor and precipitation from the tropical Atlantic Ocean across the Amazon Basin to Quelccaya. The ^{18}O depletion accompanying net water vapor loss from the air is calculated in three steps using a Rayleigh condensation equation, while 4) considers post-depositional isotope enrichment [Grootes et al., 1989]. Step 1), Water vapor depletion over the Amazon Basin varies from 0 % (dry season) to 85 % (wet season), resulting in a seasonal $\delta^{18}O$ change in precipitation of up to 18.4‰ ; Step 2), a 5.6 km increase in surface elevation from the Amazon Basin to Quelccaya results in a $\delta^{18}O$ decrease in precipitation of about 11‰; Step 3), strong convection in summer showers can increase the range of the seasonal $\delta^{18}O$ cycle by at least 5‰ (-10.5 to -33.7‰). Enrichment of $\delta^{18}O$ at the surface during the dry season may produce snow with $\delta^{18}O$ = -4.1‰. The observed range of $\delta^{18}O$ values in snow pits (-8.0 to -30.8‰) and its phase agree with the predicted range of -4.1 to -33.7‰.

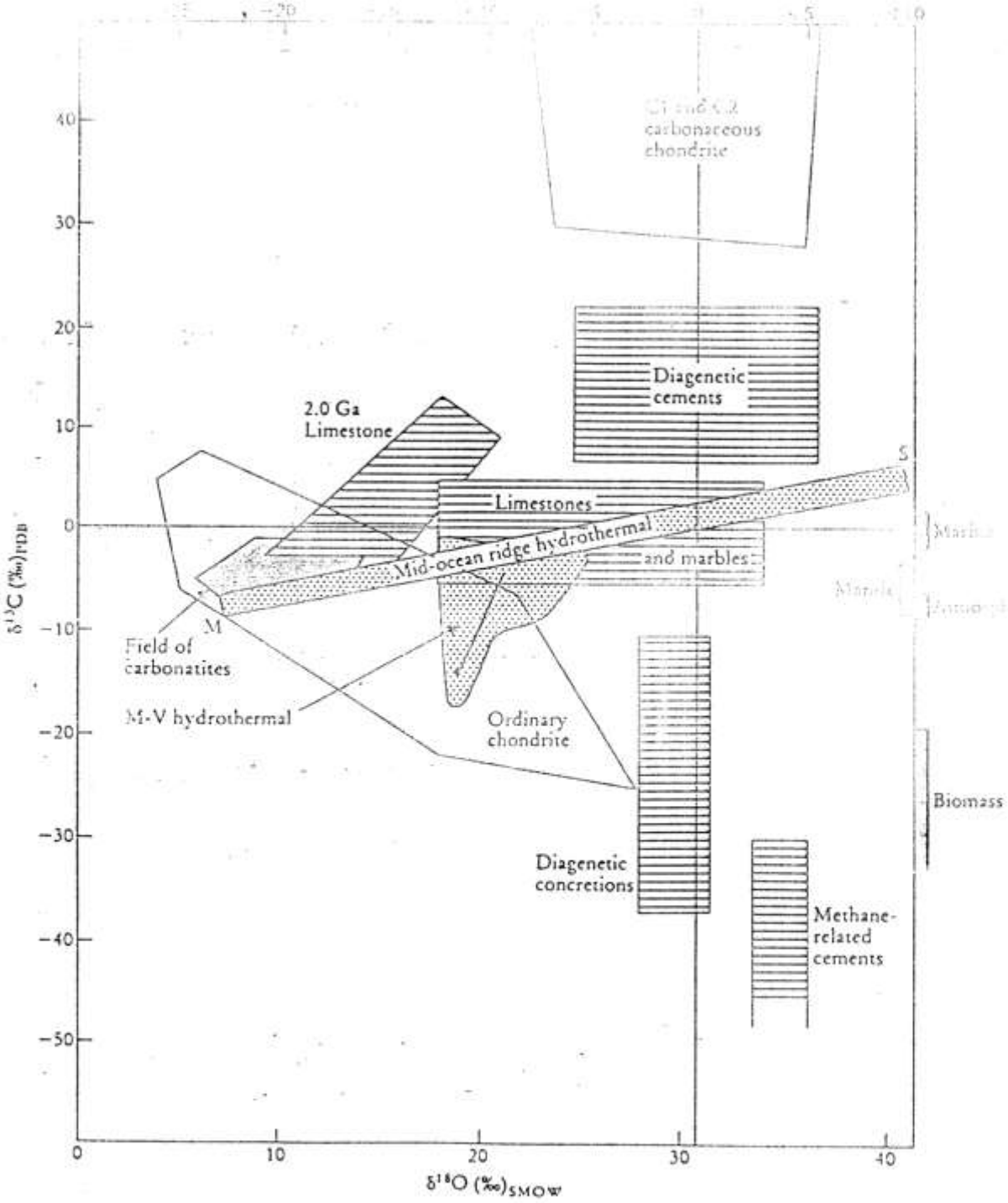
C1 and C2 carbonaceous chondrite
Diagenetic cements
2.0 Ga Limestone
Limestones and marbles
Mid-ocean ridge hydrothermal
S
M
Field of carbonatites
M-V hydrothermal
Ordinary chondrite
Diagenetic concretions
Methane-related cements
Biomass
Marine
Mantle
40
30
20
10
0
−10
−20
−30
−40
−50
0
10
20
30
40
$\delta^{13}C$ (‰)$_{PDB}$
$\delta^{18}O$ (‰)$_{SMOW}$

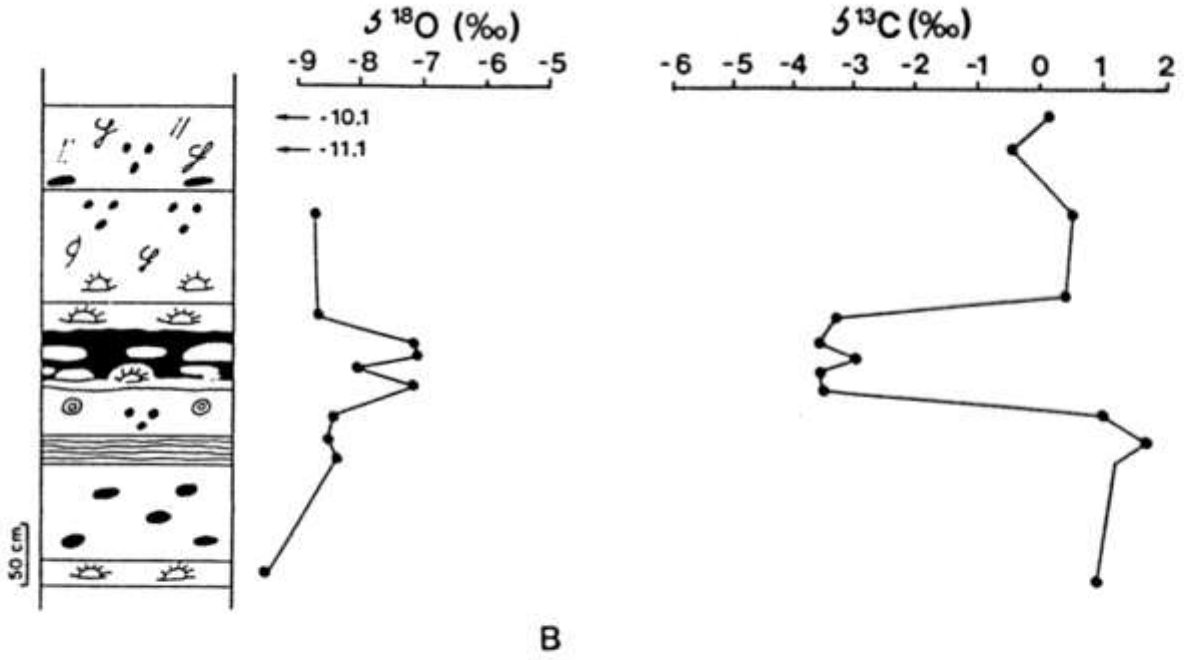

Fig. 3. Carbon and oxygen isotopic composition of peritidal limestones and paleosols in the lower Viséan in the Flémalle-Haute (A) and Walhorn (B) quarries. The investigated paleosols occur at the top of the Terwagne Formation.

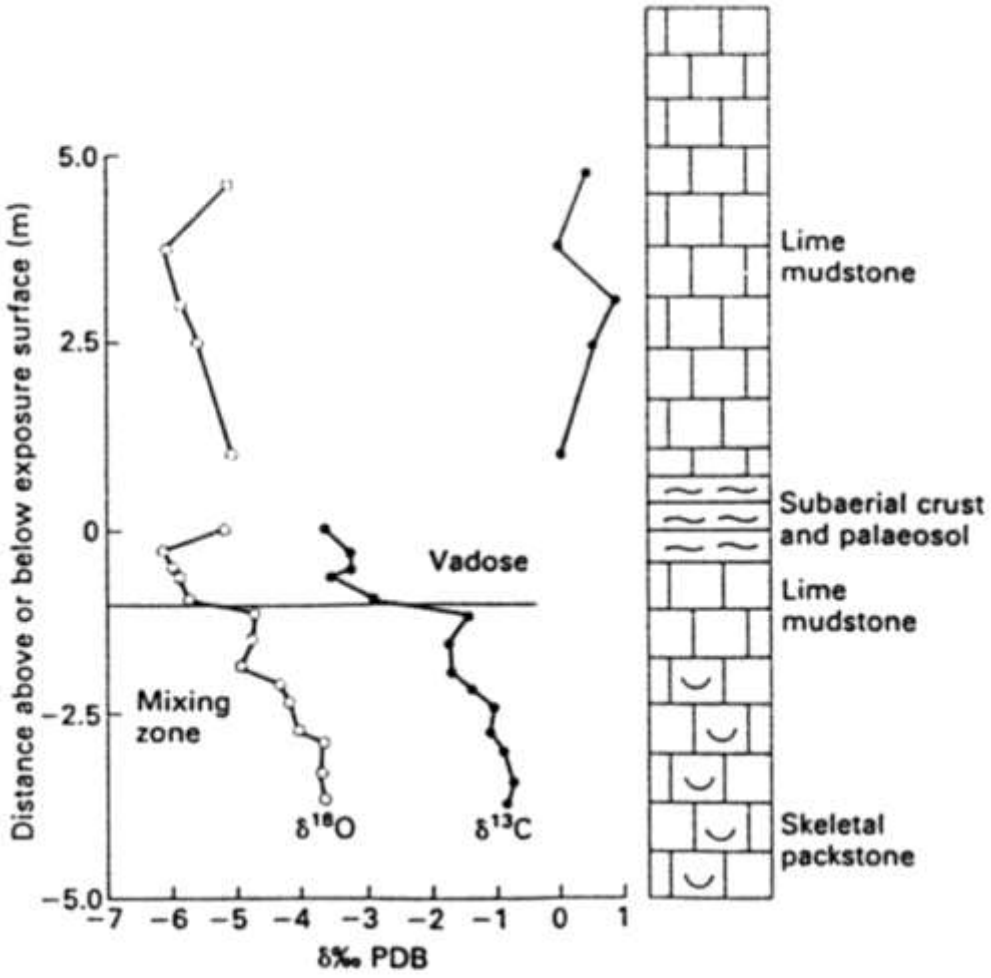

Fig. 9.31. Isotope profiles across a Mississippian emersion surface (Newman Limestone, Kentucky). Top five samples below exposure surface are depleted in ^{18}O and ^{13}C. Deeper samples show covariant increase in $\delta^{13}C$ and $\delta^{18}O$ thought to indicate diagenesis in marine-meteoric mixing zone. After Allan & Matthews (1982).

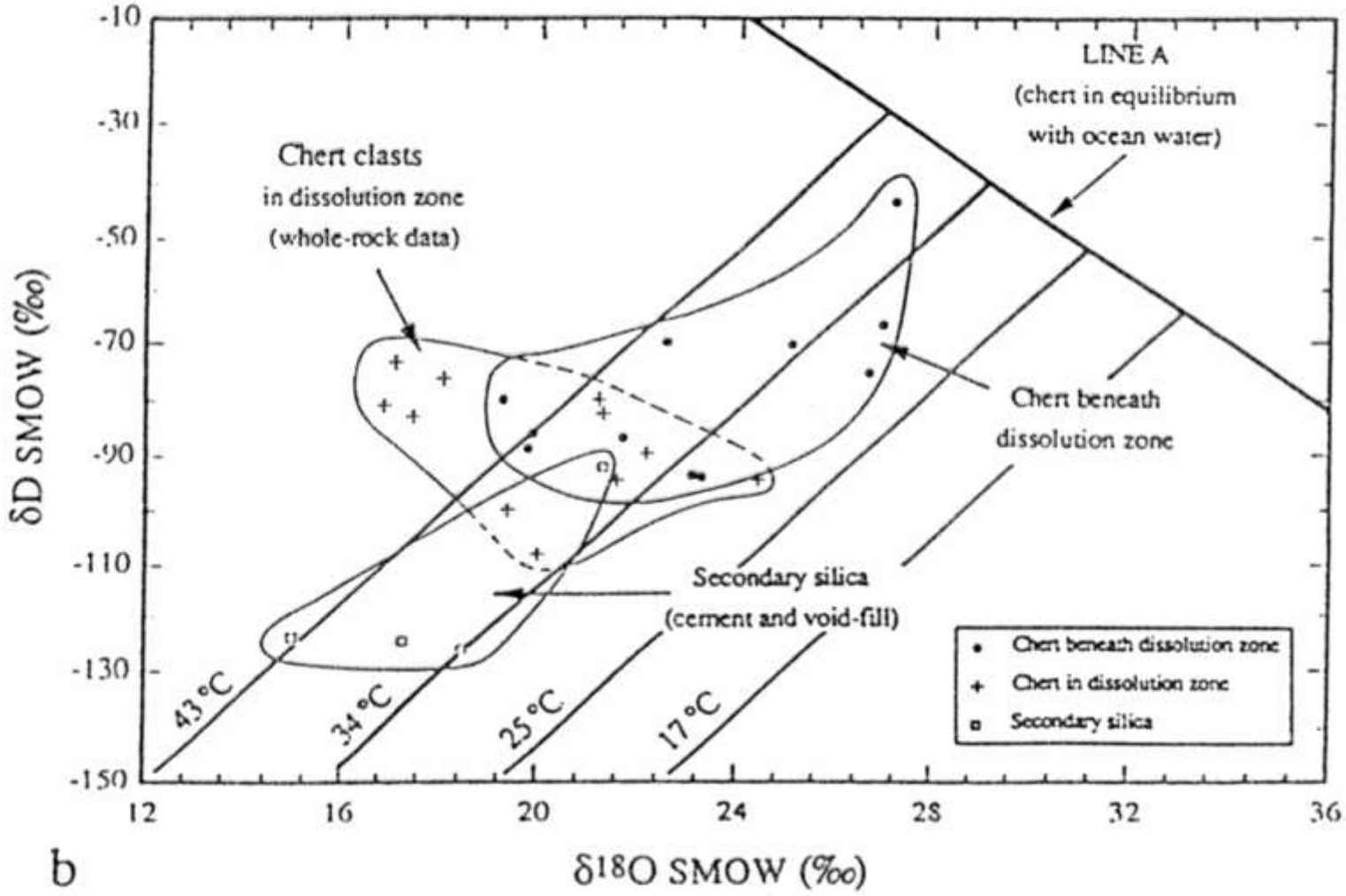

Figure 2. Isotopic composition of (a) Mescal and (b) Beck Spring cherts. Line A represents cherts in equilibrium with Standard Mean Ocean Water (SMOW), from Knauth and Epstein (1976). Temperatures of chert crystallization are from Knauth and Epstein (1976). Domains are strongly elongated in direction roughly parallel to meteoric water line. Early coastal chert δ values plot closest to line A; secondary silica values plot farthest away. Whole-rock samples include both early diagenetic and secondary chert.

TDC – total dissolved carbon

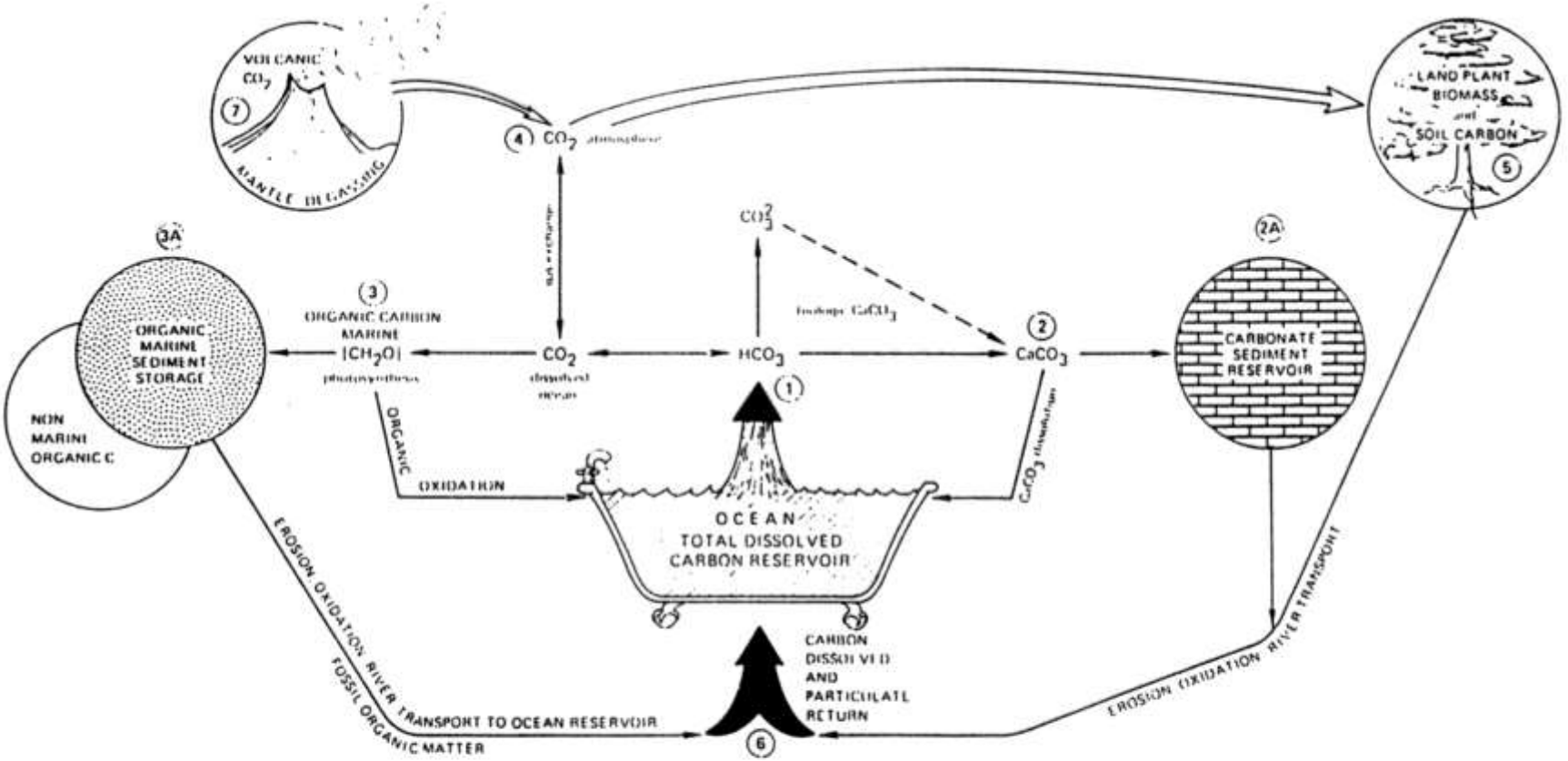

THE TERRESTRIAL CARBON SYSTEM, MAJOR RESERVOIRS AND FLUXES

Figure 1-30. Representation of major reservoirs and reservoir transfers in the carbon cycle (after Scholle and Arthur, 1980). See Table 1-4 for estimated masses, fluxes, and $\delta^{13}C$ values.

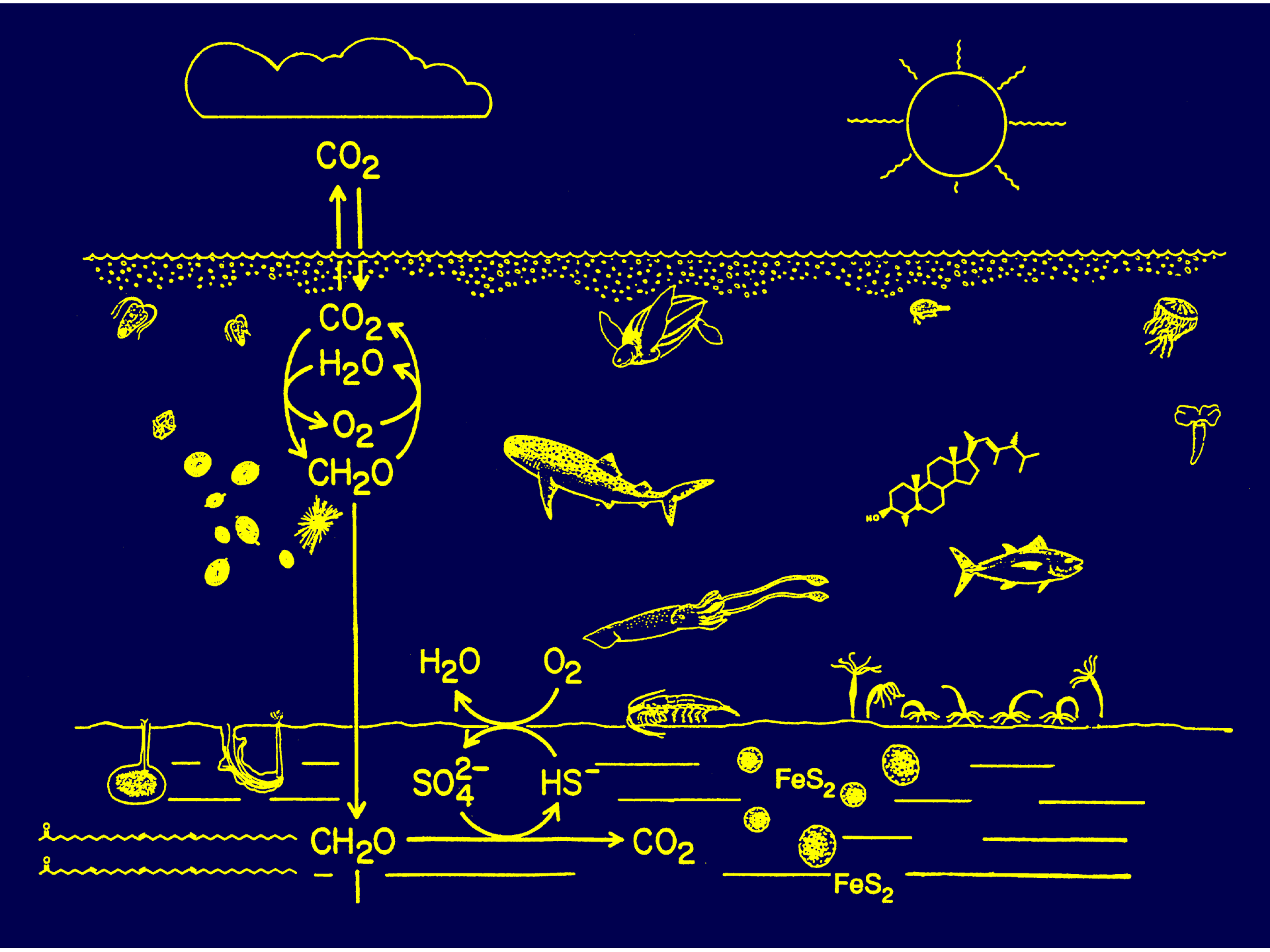
CO_2
CO_2
H_2O
O_2
CH_2O
HO
H_2O
O_2
SO_4^{2-}
HS^-
FeS_2
CH_2O
CO_2
FeS_2

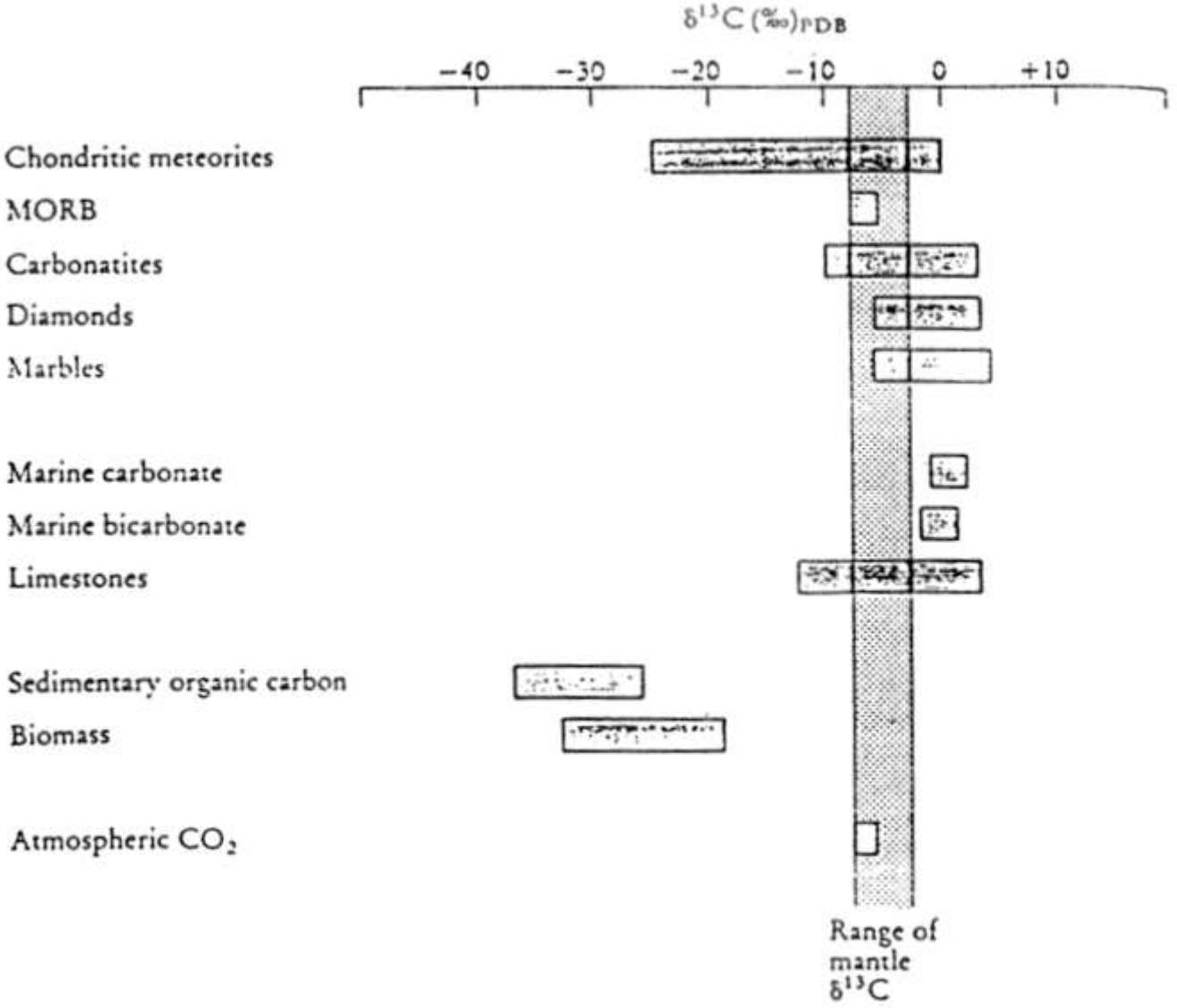

Natural $\delta^{13}C$ reservoirs. The ranges of $\delta^{13}C$ values in natural, carbon-bearing samples. Data from Kerridge (1985), Exley *et al.* (1986), Field and Fifarek (1986), Hoefs (1987) and Schidlowski (1987).

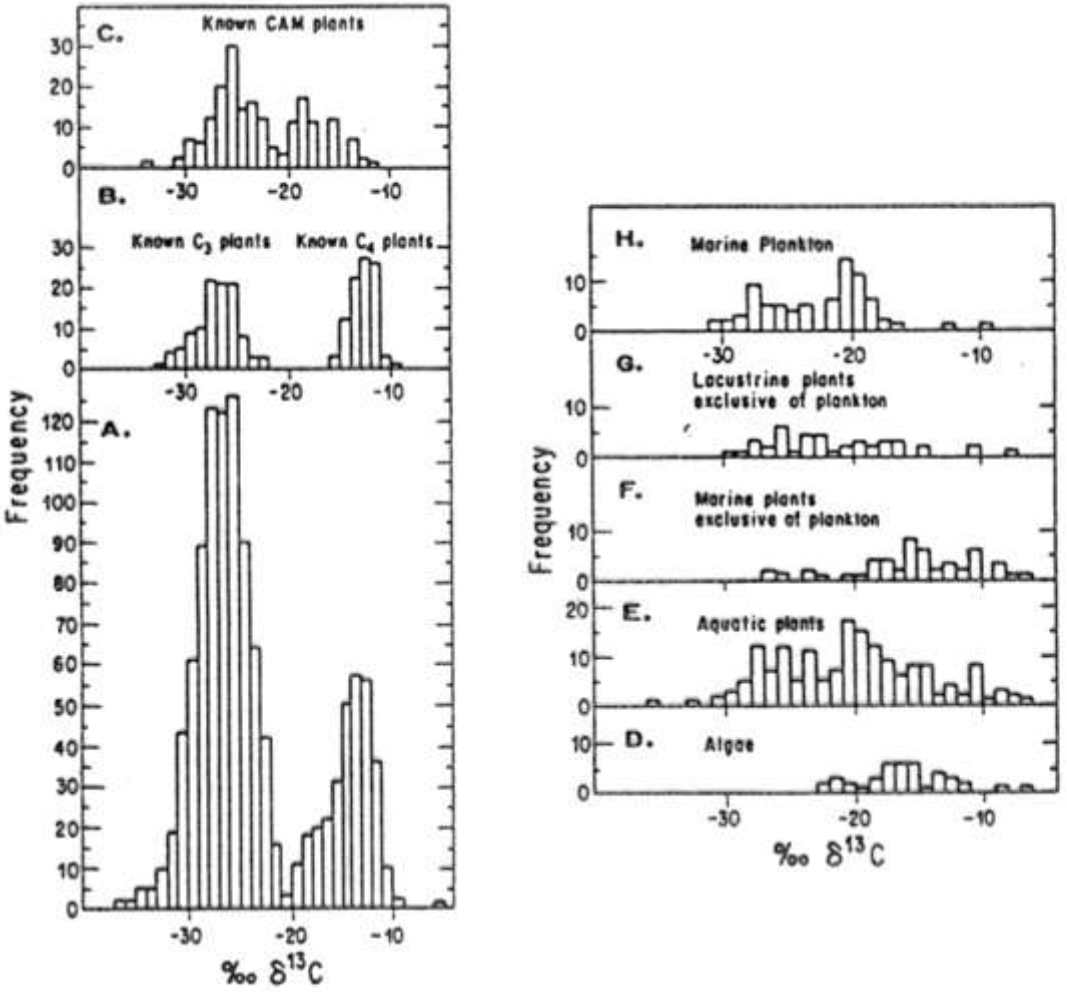

Fig. 9-3. Carbon isotopic composition of photosynthetically fixed carbon A. Terrestrial plants. B. Known C_3 and C_4 plants. C. Known CAM plants. D. Algae. E. Aquatic plants. F. Marine plants exclusive of plankton. G. Lacustrine plants exclusive of plankton. H. Marine plankton. Data from Bender (1968, 1971), Bender et al. (1973), Brown and Smith (1974), Craig (1953a), Deevey and Stuiver (1964), Degens et al. (1968b), Eadie (1972), Lerman et al. (1969), Lowdon and Dyck (1974), Oana and Deevey (1960), Osmond et al. (1975), Parker (1964), Sackett et al. (1965, 1974a), Smith and Brown (1973), Smith and Epstein (1970, 1971), Stahl (1968a), Troughton (1972), Wickman (1952), and Williams and Gordon (1970).

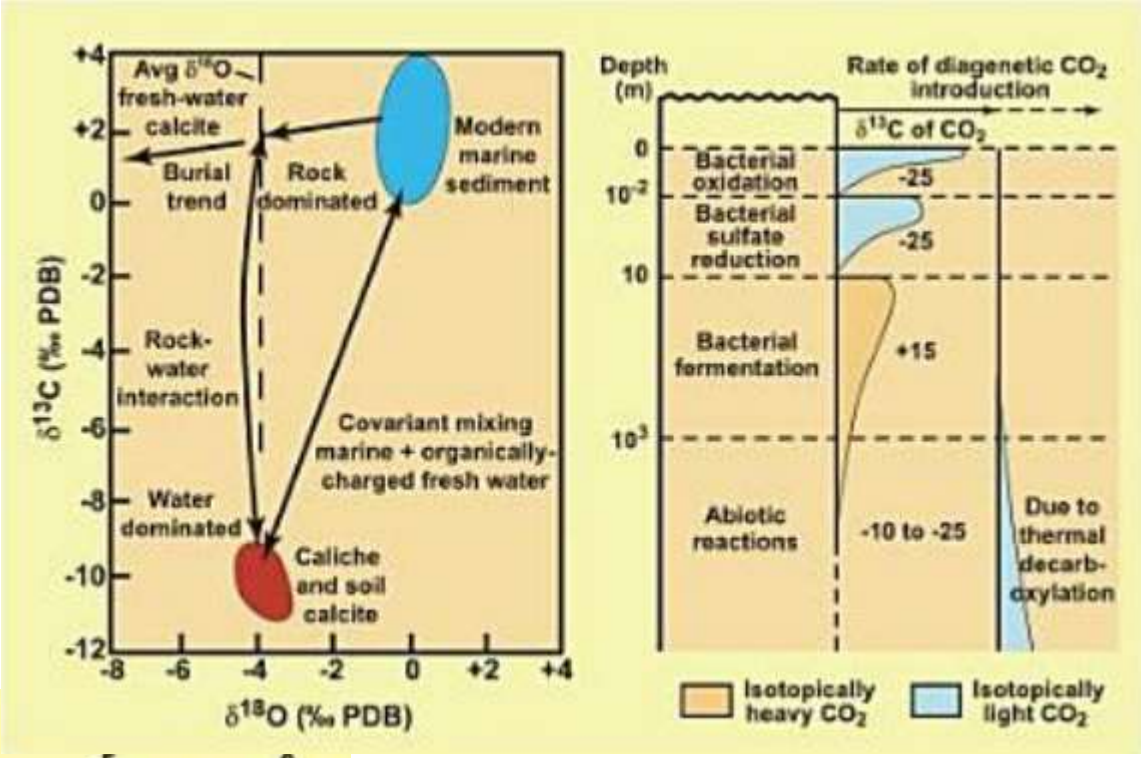

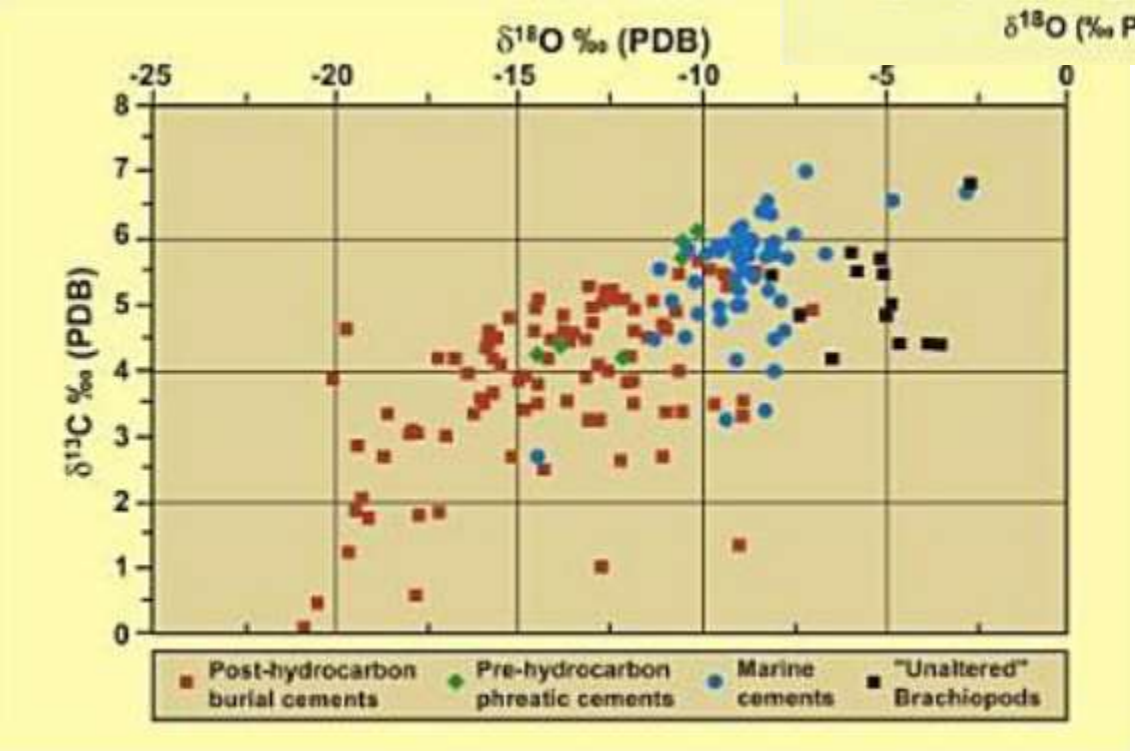

Up. Permian Wegener Halvo Fm., E. Greenland

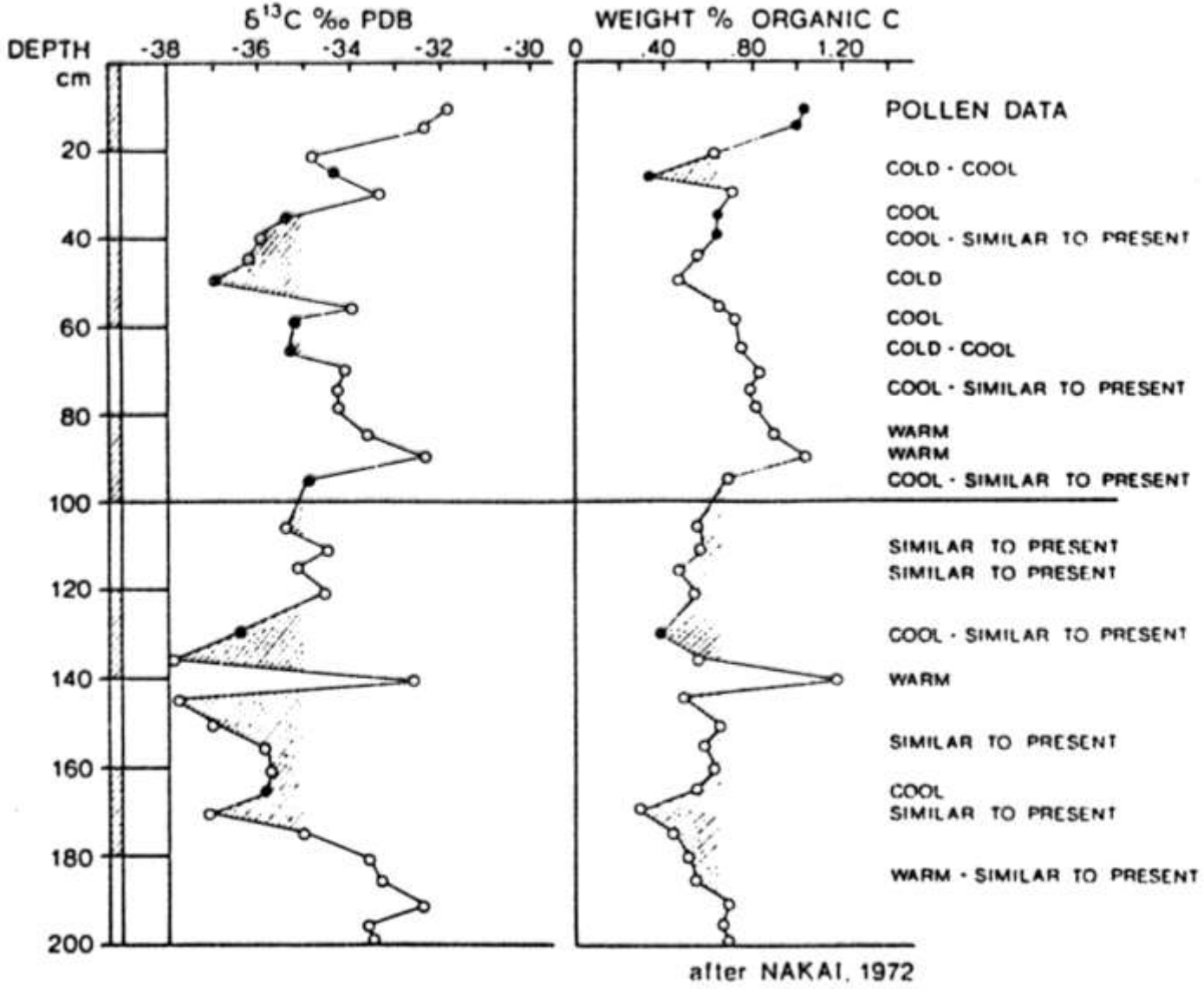

Fig. 12-3. A composition of ^{13}C data with organic carbon contents and pollen data from Lake Biwa (Japan) to document the agreement between paleoclimates and varying $\delta^{13}C$ values (after Nakai, 1972).

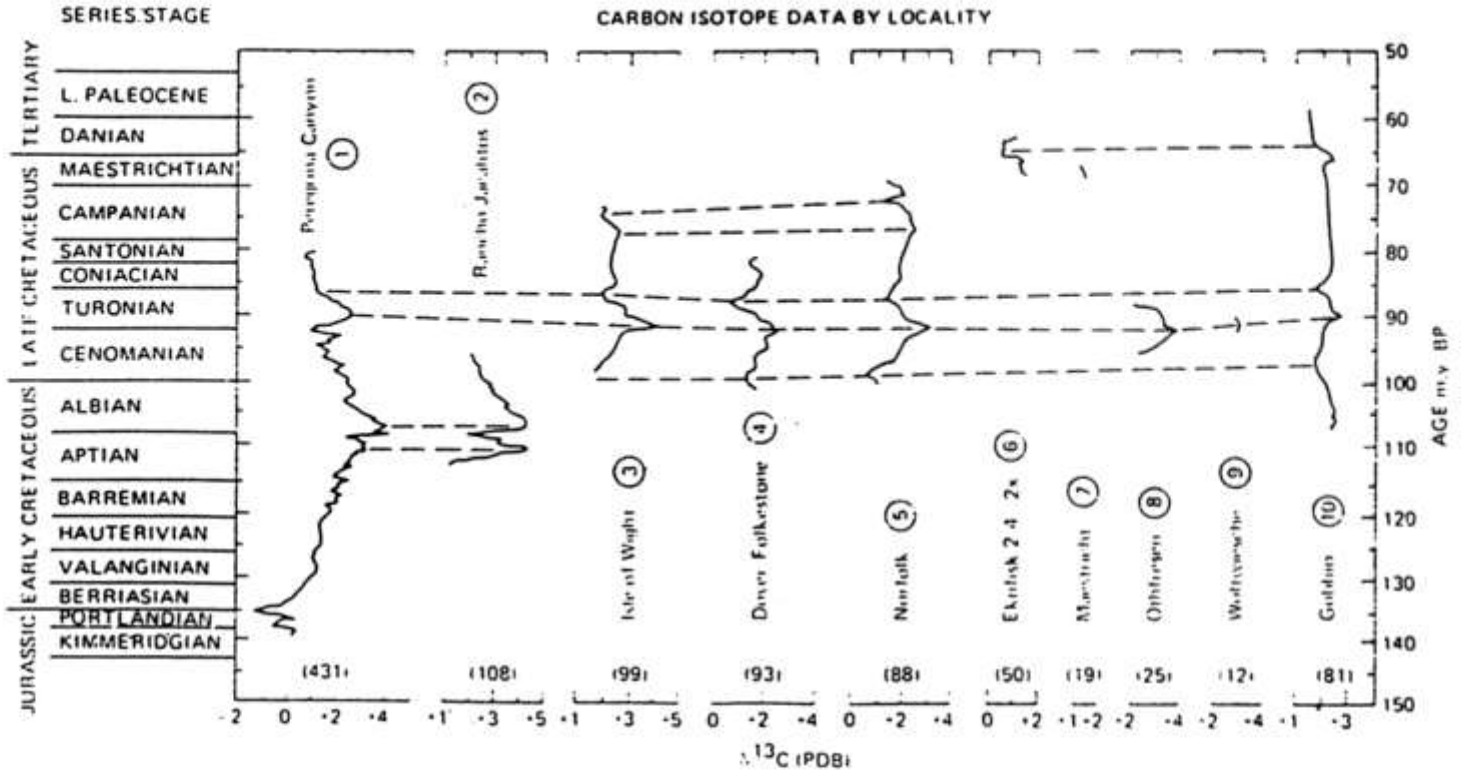

Chemostratigraphy, eventstratigraphy

Figure 1-53. $\delta^{13}C$ stratigraphy of Cretaceous pelagic limestones from different global localities (after Scholle and Arthur, 1980). 1 and 2 - Mexico; 3-5-U.K.; 6 and 7 - North Sea and Netherlands; 8 and 9 - Germany; 10 Central Italy. Many new data have confirmed these patterns.

izotopy stroncia – stratigrafie, paleoprostředí

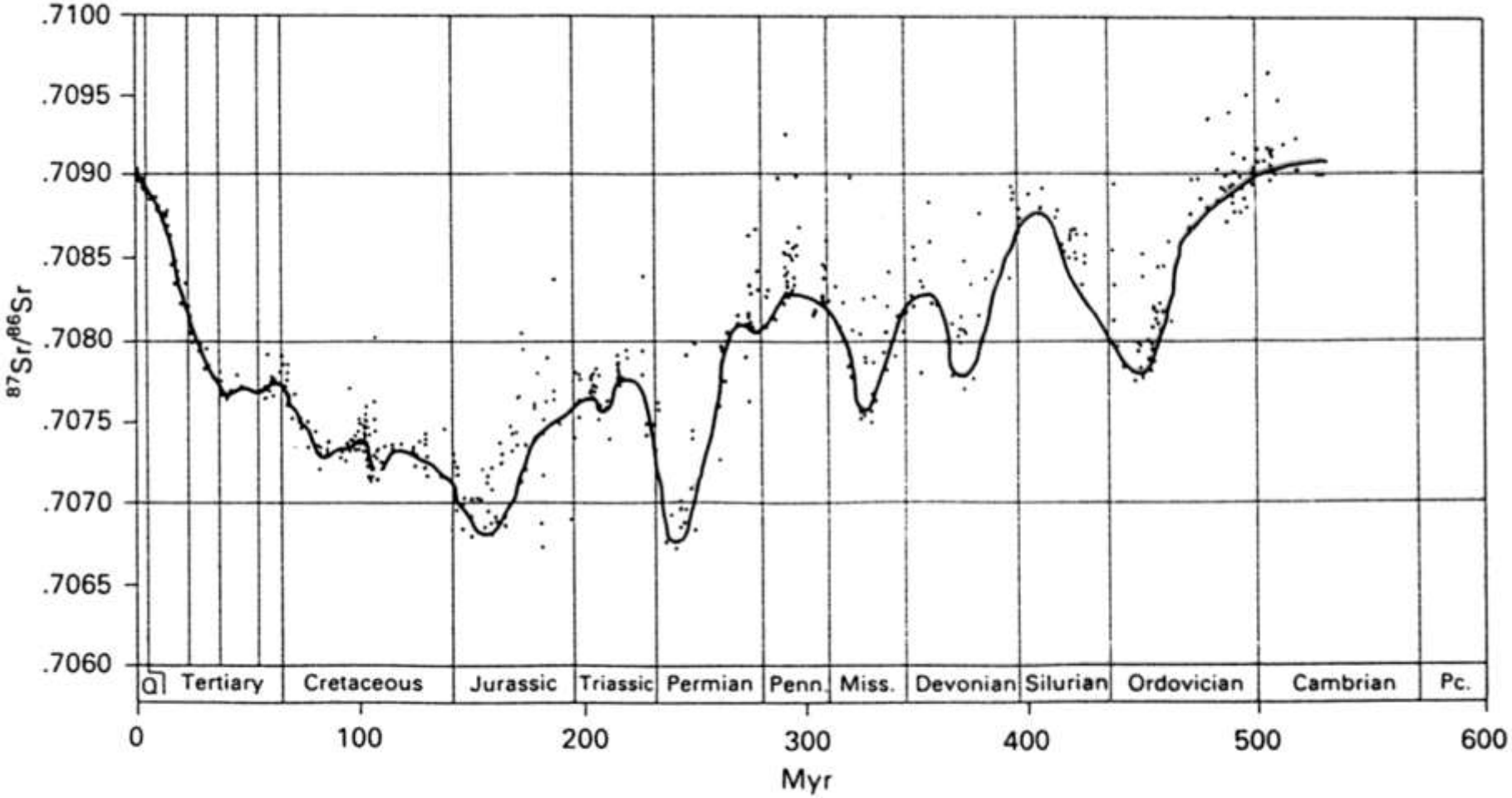

Fig. 9.34. Plot of Sr isotope variation with age of 744 samples of marine carbonates, evaporites and phosphorites (from Burke *et al.*, 1982). Data points scatter above the line because of diagenetic alteration and short-lived positive excursions (e.g. Cretaceous–Tertiary boundary. Hess, Bender & Schilling, 1986).

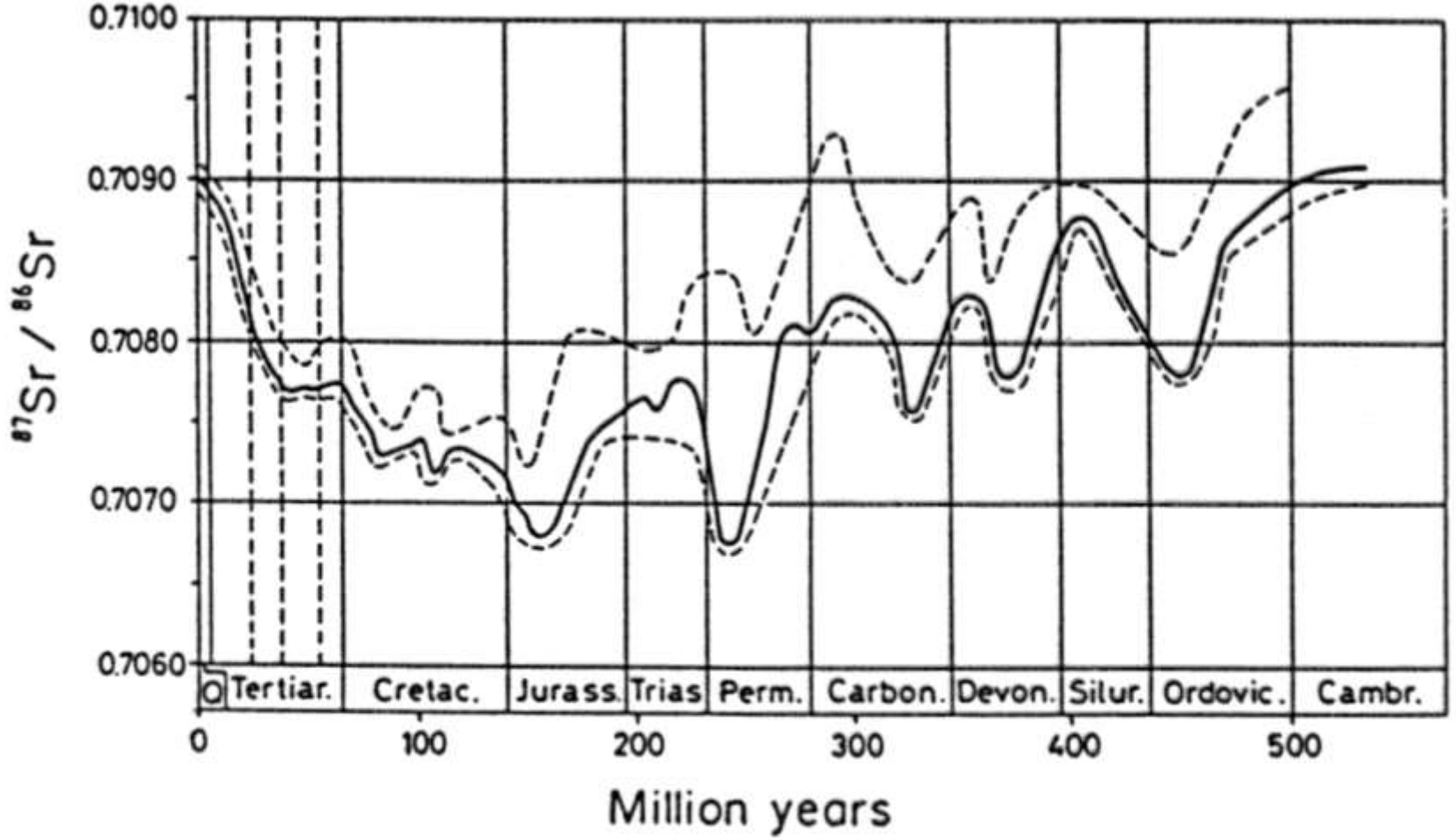

Fig. 5.2. Temporal variations of the Sr isotope ratio in seawater based on 786 isotopic analyses of marine carbonate rocks. The dashed lines show the extent of 95% of the data points. (Burke et al., 1982)

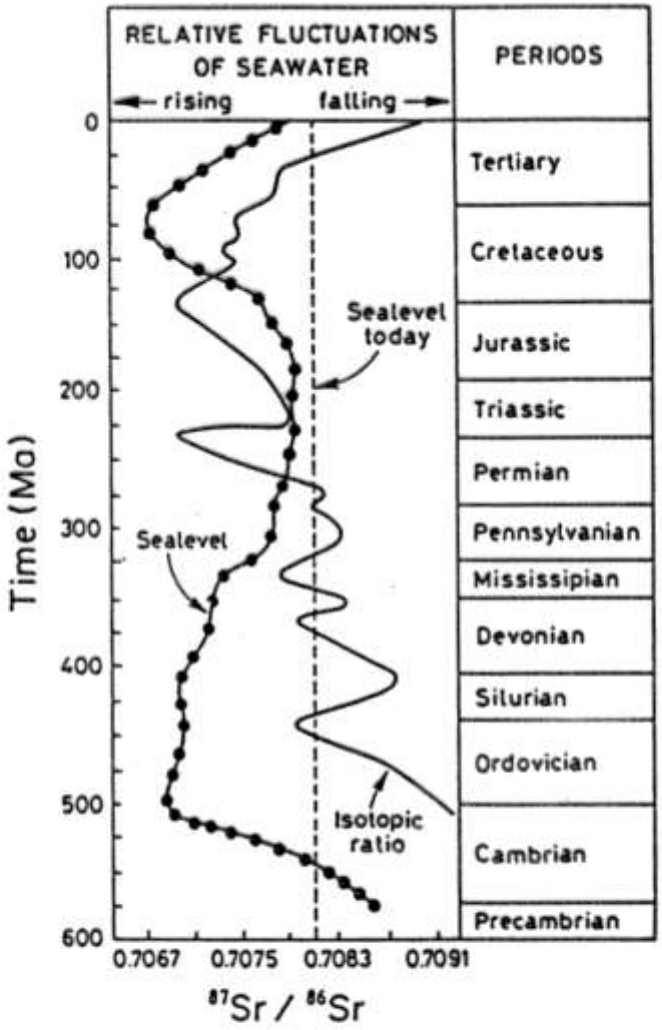

Fig. 5.15. Relationship between Sr isotopic variation in the oceans and sea level fluctuations through geologic time. Chauduri and Clauer (1986) were able to show that sea-level fluctuations and related hydrothermal seawater circulation are not always the majpr influences on the Sr isotopic composition of seawater. The authors postulate an additional source of Sr that supplies the oceans with relatively more radiogenic Sr groundwater.

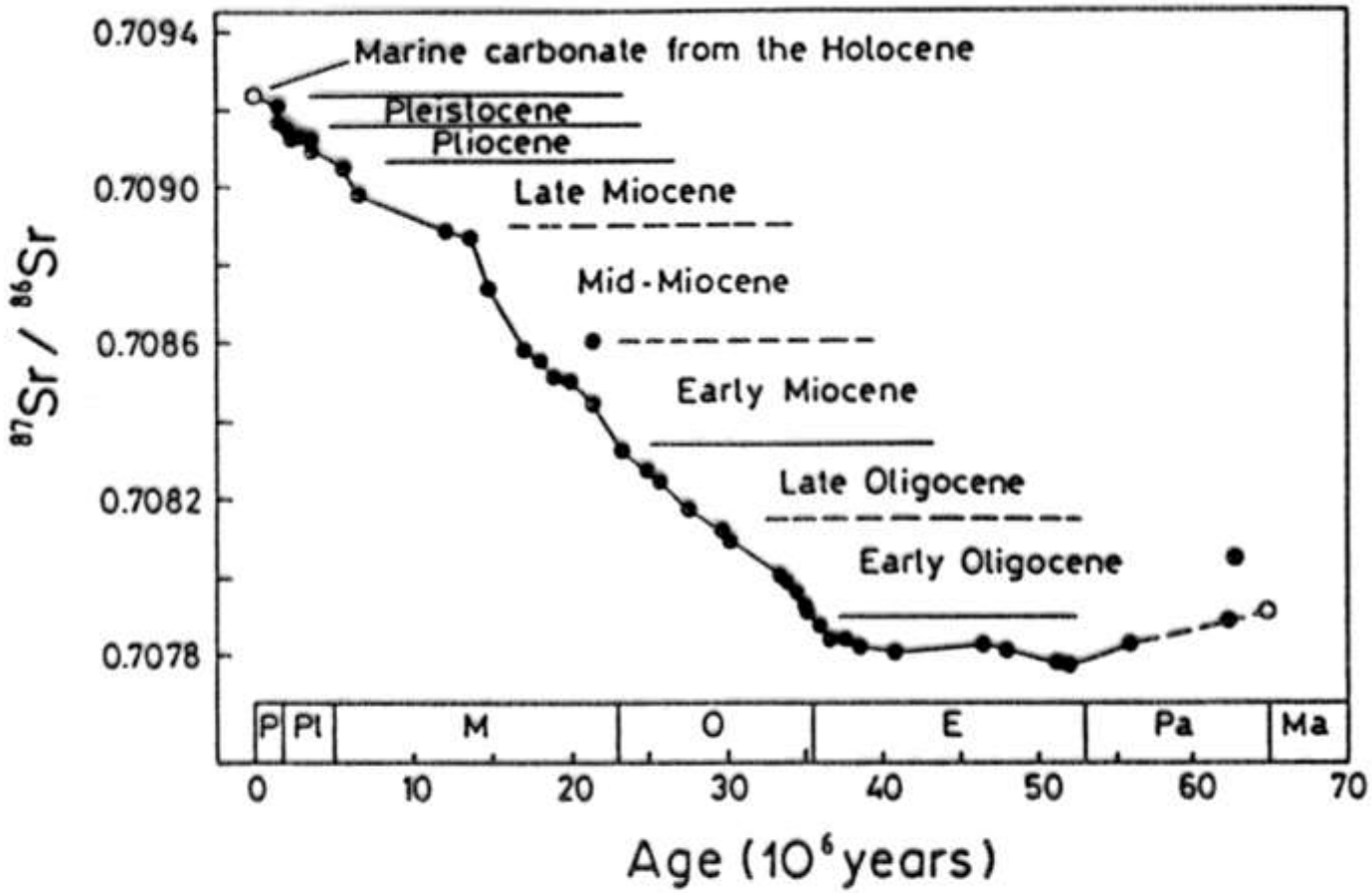

Fig. 5.3. The precise $^{87}Sr/^{86}Sr$ isotopic analyses of DePaolo and Ingram (1985) on stratigraphically well constrained marine carbonates allowed the reconstruction of a single clear trend in Tertiary seawater isotopic variation for the first time.

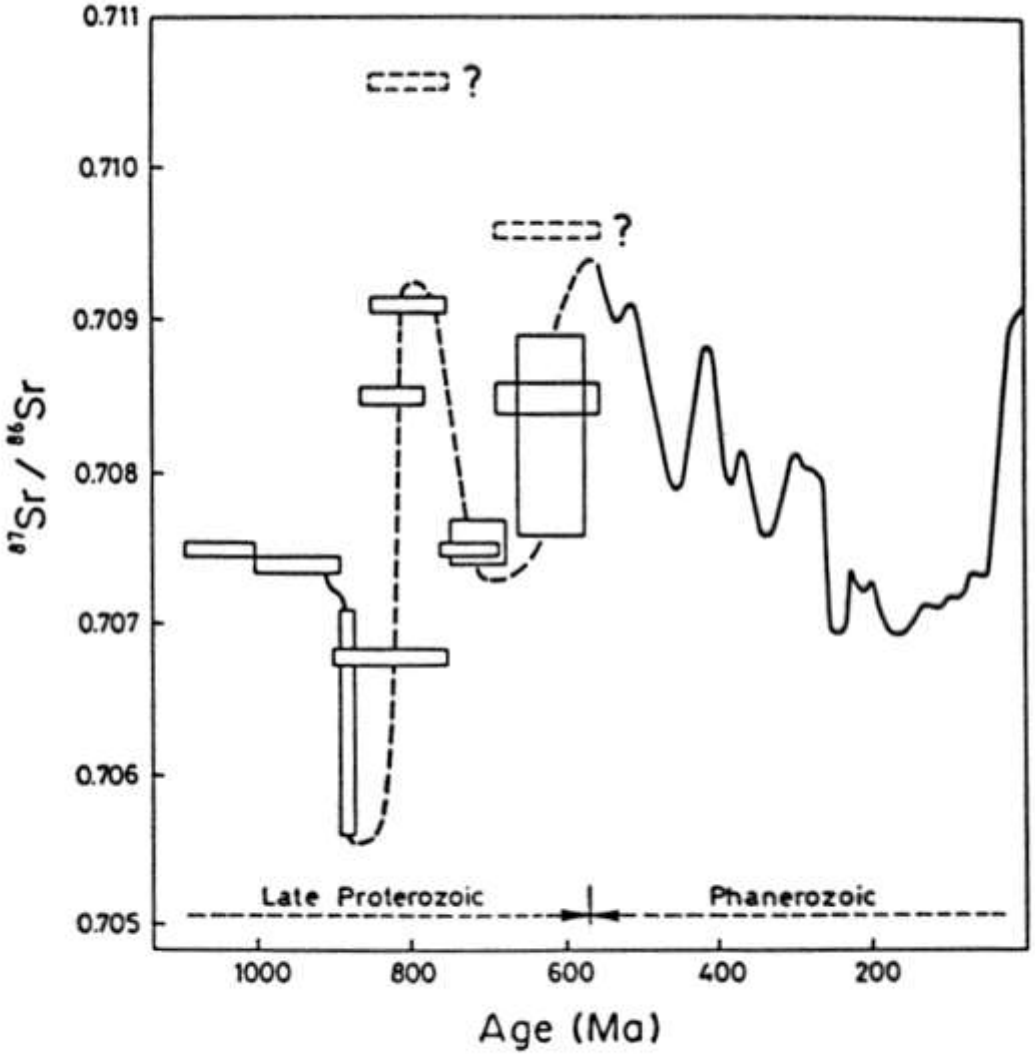

Fig. 5.8. The Sr isotopic composition of late Precambrian seawater. The lateral error bars represent stratigraphic uncertainties. The spread in the data is caused by reasons discussed in the text. (after Veizer and Compston 1974, 1976; Burke et al. 1982)

Chemostratigraphy

sensu lato

- Study of variation in the chemical composition of sedimentary strata
- First common use 1980s
- Stimulated by advances in analytical geochemistry: IR-MS, XRF, ICP-AES, ICP-MS
- Rapid, cost-effective determination of wide range of elements and isotopes in geological samples

Chemostratigraphy
sensu stricto

- Characterisation, correlation and dating of sedimentary units based on variations in geochemistry
  - high-resolution correlation of units
  - geochemical typing of key stratal surfaces for correlation above resolution of conventional biostratigraphy or physical stratigraphy
  - provenance determination

Major and trace elements

B, Ba – Boron or Barium in clay minerals as an paleosalinity indicator

Si, Zr, Ti (Si/Al, Zr/Al, Ti/Al) – proxies for terrestrial input and altered alkaline basic volcanism; Vanadium could be used for discrimination of terrigenous and volcanogenic Ti, V usually correlates with Ti in volcanogenic rocks

Si/Al peaks can correspond to quartz concentrations

High Ti/Al, Zr/Al can indicate heavy minerals (rutile, ilmenite, sphene, zircon) and titanomagnetite inclusions in quartz

Rb – proxy for clay

Ba, Pb – proxy for feldspars

---

* proxy = a measured variable used to infer the value of a variable of interest e.g. in paleoclimate research

- Variations in Mn depositional and diagenetic fluxes are complex but can be related to sea-level change
  - Mn concentation of seawater (redox and hydrothermal supply)
  - Organic, carbonate and detrital fluxes
  - Bulk sedimentation rate
  - TOC content of sediment
- environmental magnetism (MS - magnetic susceptibility)
  - Fe minerals – proxy of terrestrial input, weathering intensity (magnetite, hematite, limonite, sulphides, ... could be distinguished)

katodová luminiscence (CL)

principy; excitace elektronovým proudem, emise záření

Mn^{2+} aktivátor, Fe^{2+} inhibitor luminiscence v karbonátech

studium karbonátových a křemitých tmelů, rekrystalizace → stratigrafie tmelů, historie složení a trajektorií pánevních fluid

provenience klastického materiálu

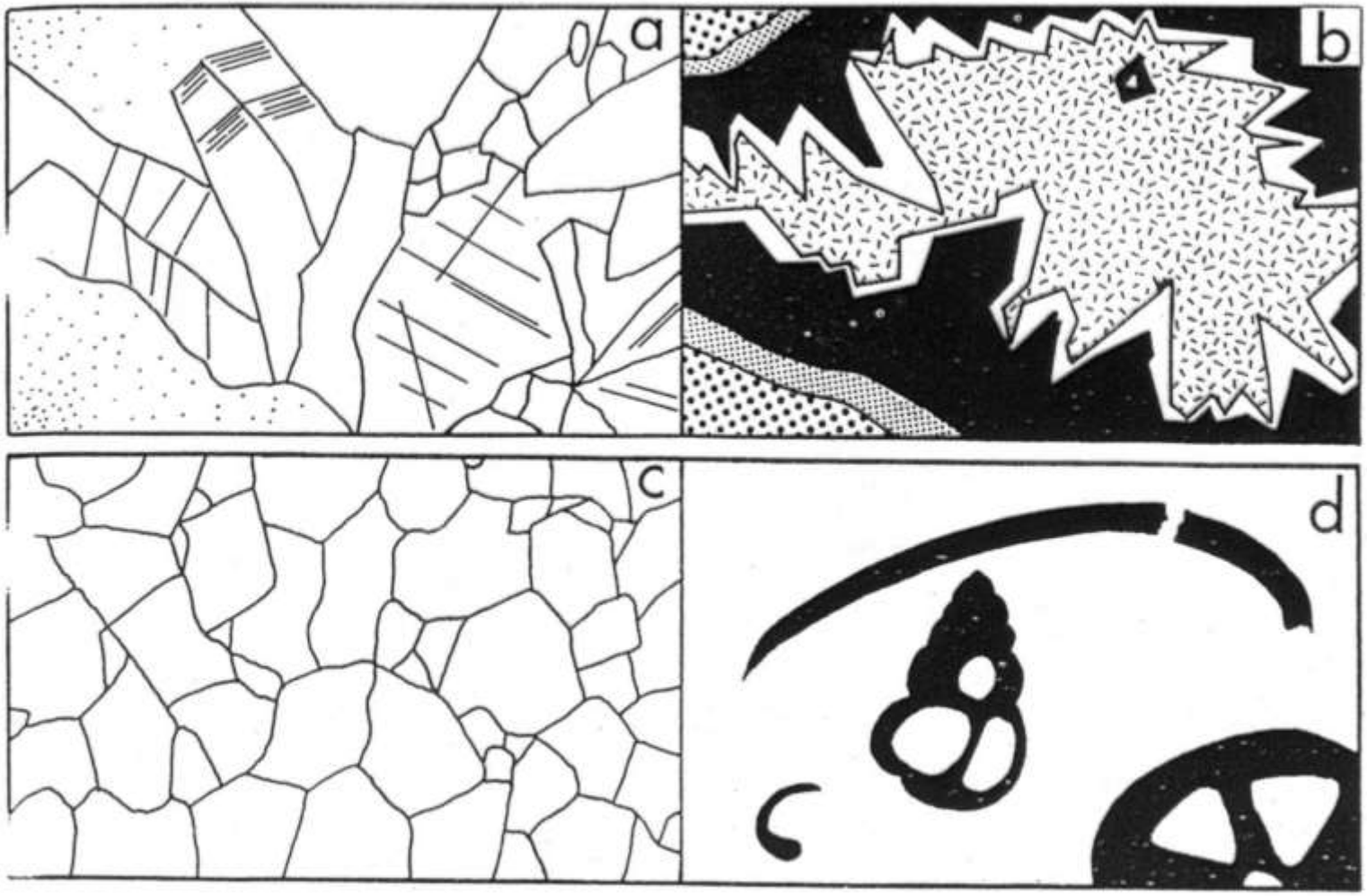

Fig. 6.3. Drawings made from photographs of CL in limestones from the Dinantian (Lower Carboniferous) of Ireland. (a) Coarse sparry calcite mass seen in transmitted light. (b) Same view but with cathodoluminescence, showing a void developed in micrite (coarse stipple), with a cement sequence of radial fibrous spar (light stipple), non-luminescent ferroan calcite (black) and brightly luminescent outer zone (white). The void fill is completed by dolomite (hashures). (c) Medium-grained blocky spar mosaic seen under transmitted light is revealed under cathodoluminescence (d) as a neomorphosed, brightly luminescent biomicrite with gastropods, bivalves and foraminifera which are weakly luminescent.

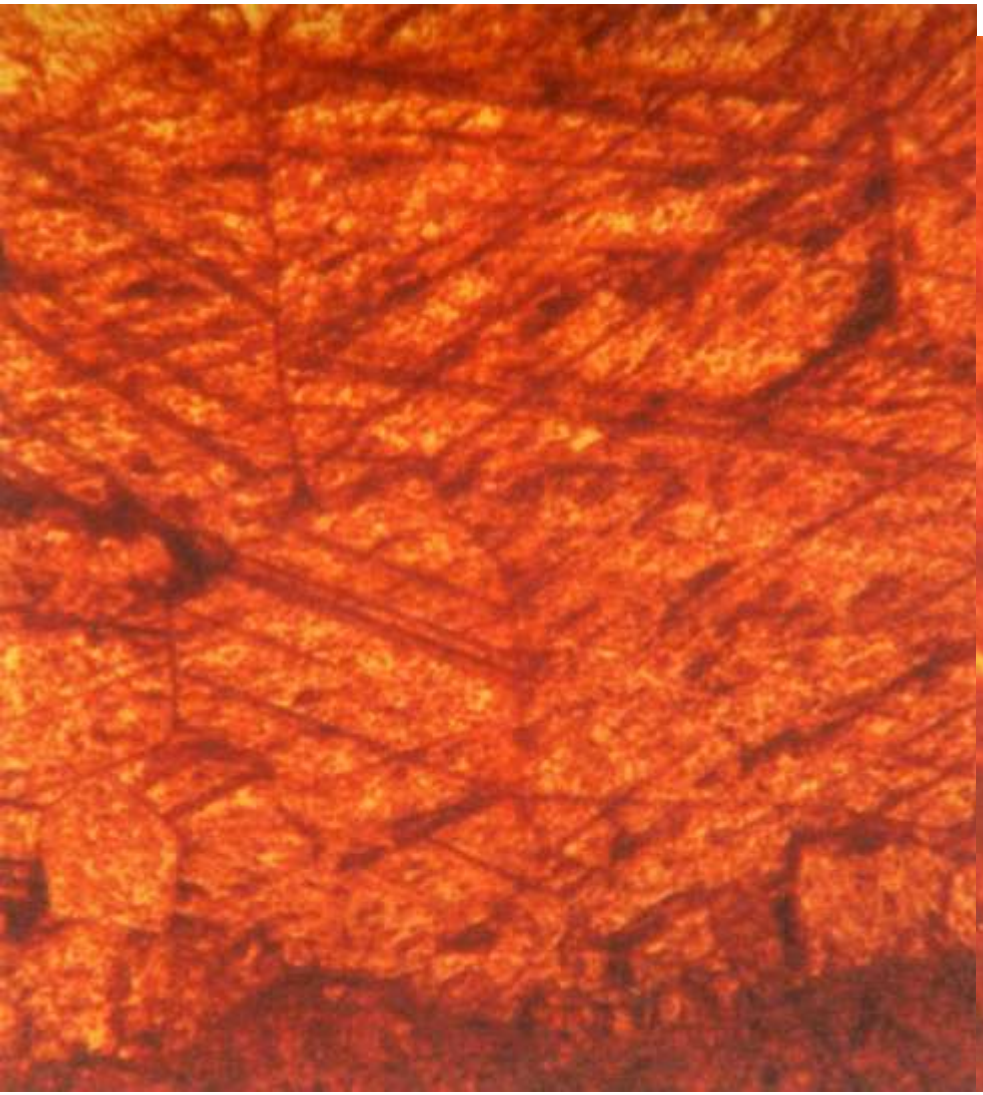

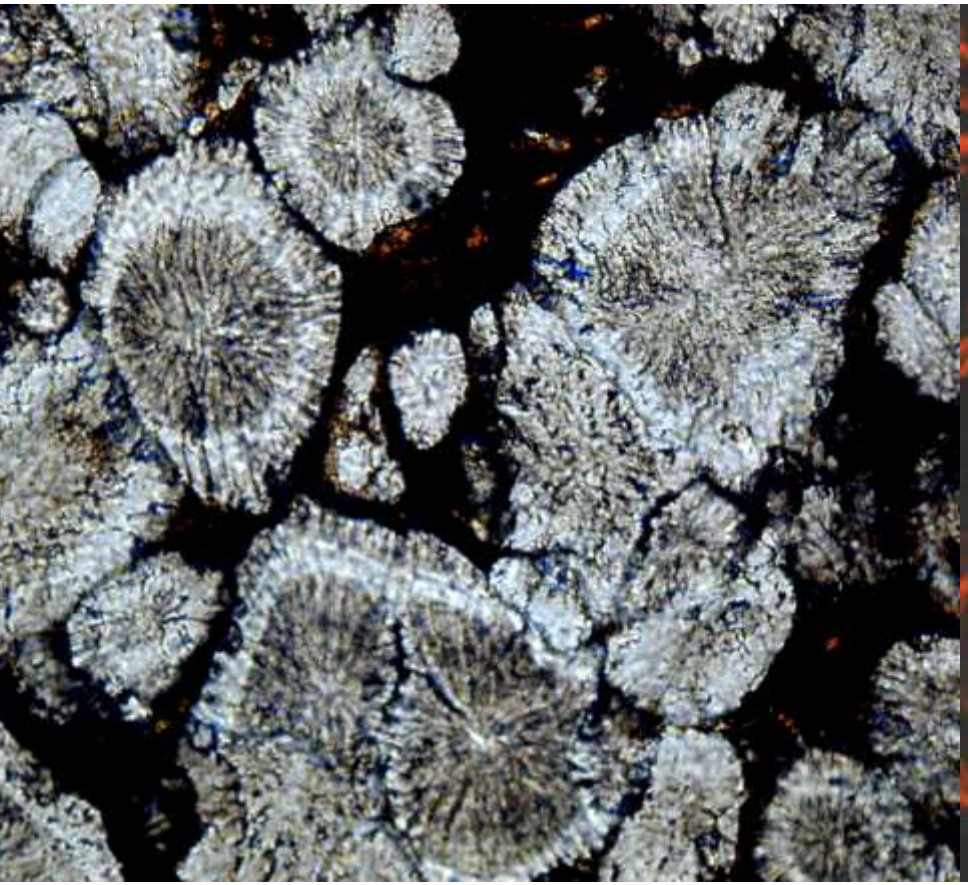

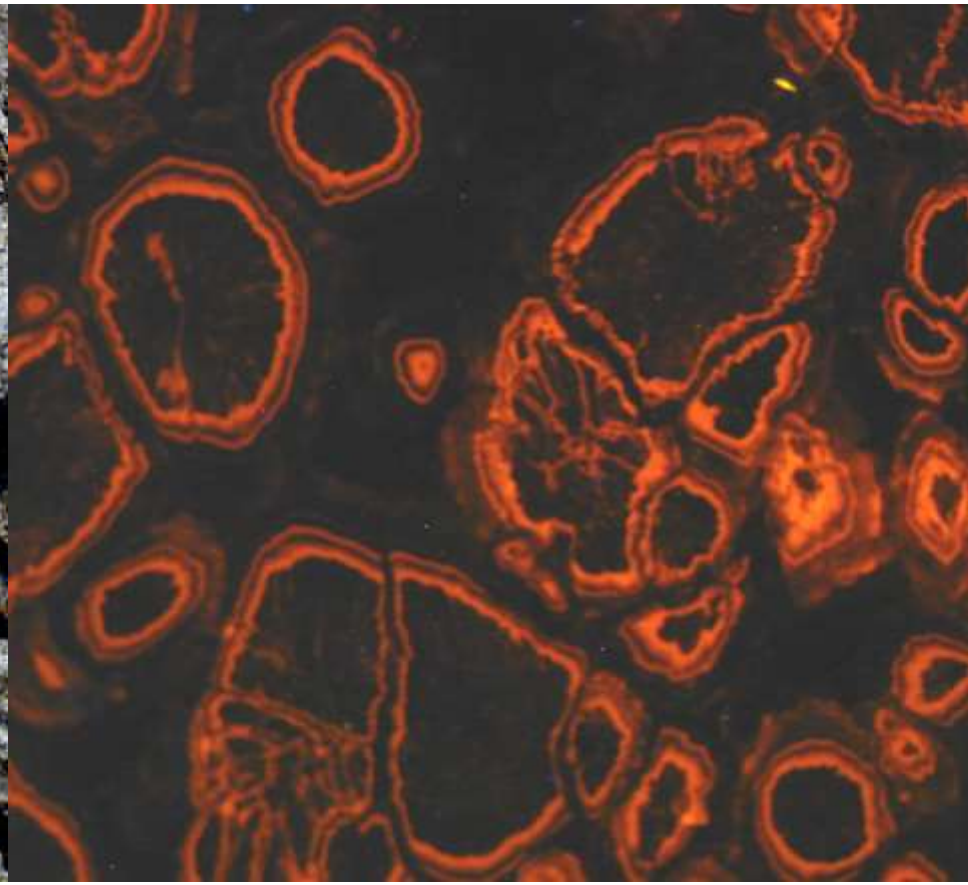

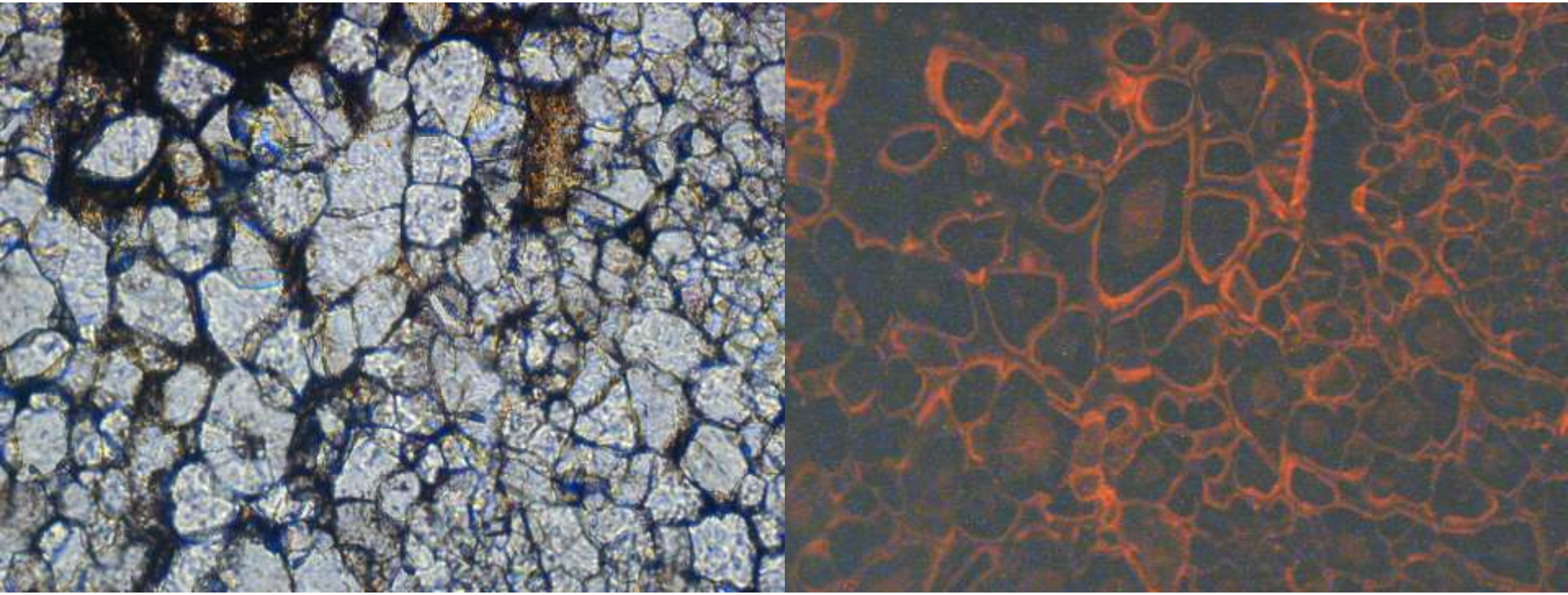

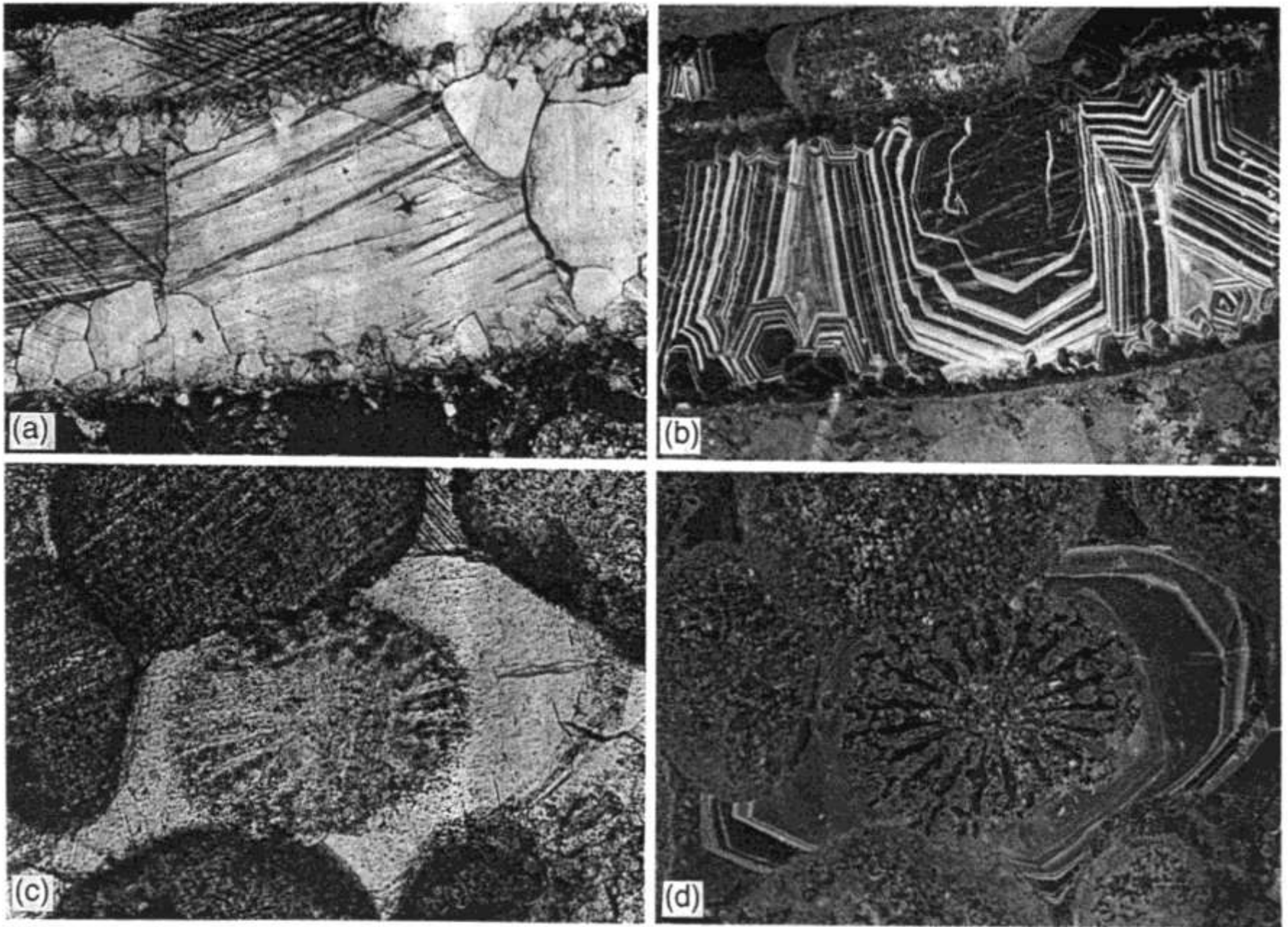
(a)
(b)
(c)
(d)

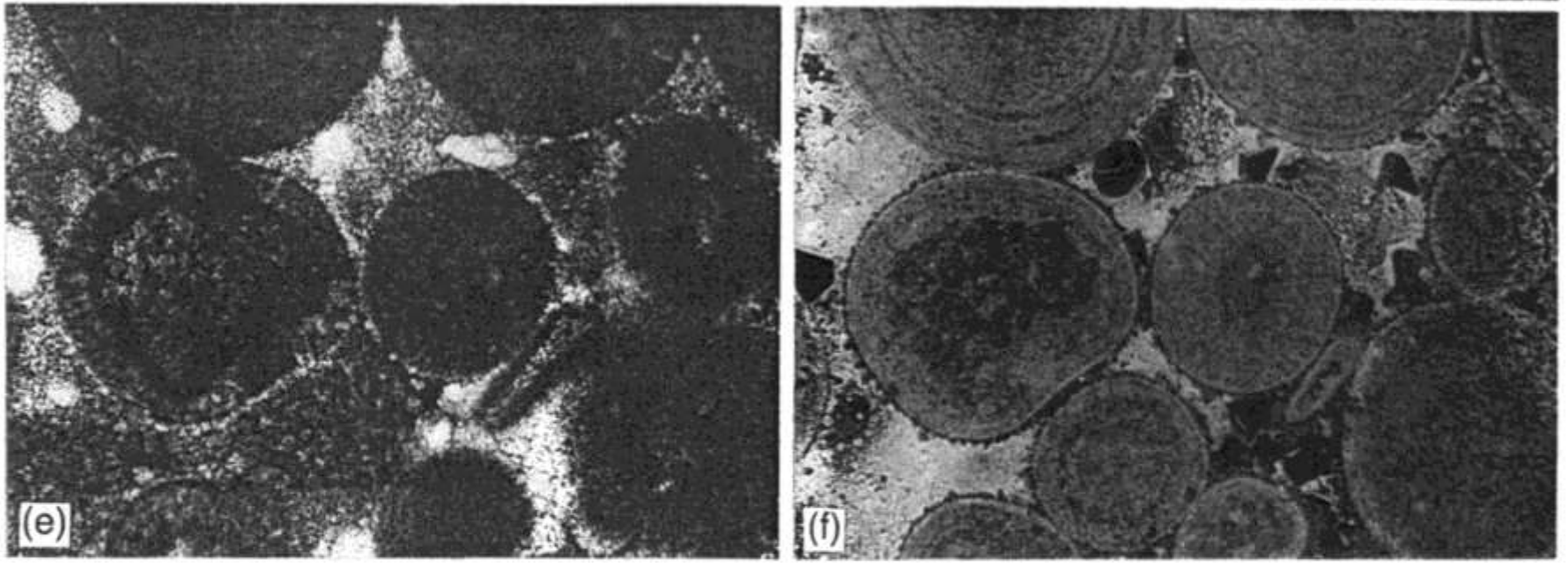

Fig. 6.4. Paired photomicrographs of limestone thin sections, with transmitted light view to the left and cathodoluminescence view to the right. All from the Dinantian (Lower Carboniferous) of South Wales. (a), (b) Pwll-y-Cwm Oolite. Calcite cement fill of bivalve mould, showing details of crystal growth by fine luminescent and non-luminescent growth bands. (c), (d) Blaen Onneu Oolite. Syntaxial calcite overgrowth on an echinoid spine, showing preferential nucleation on the crystallographically suitable substrate. CL reveals detail of the internal structure of the recrystallized spine. Changes in CL intensity in the overgrowth cement are due to varying concentrations of Fe^{2+} quencher. (e), (f) Gilwern Oolite. Details of the internal structure of ooids is better revealed by CL. Thin, non-luminescent calcite cement fringes occur on the ooids, followed by brightly-luminescent microspar associated with calcrete formed during subaerial exposure. Photographs by courtesy of Dr M. Raven.

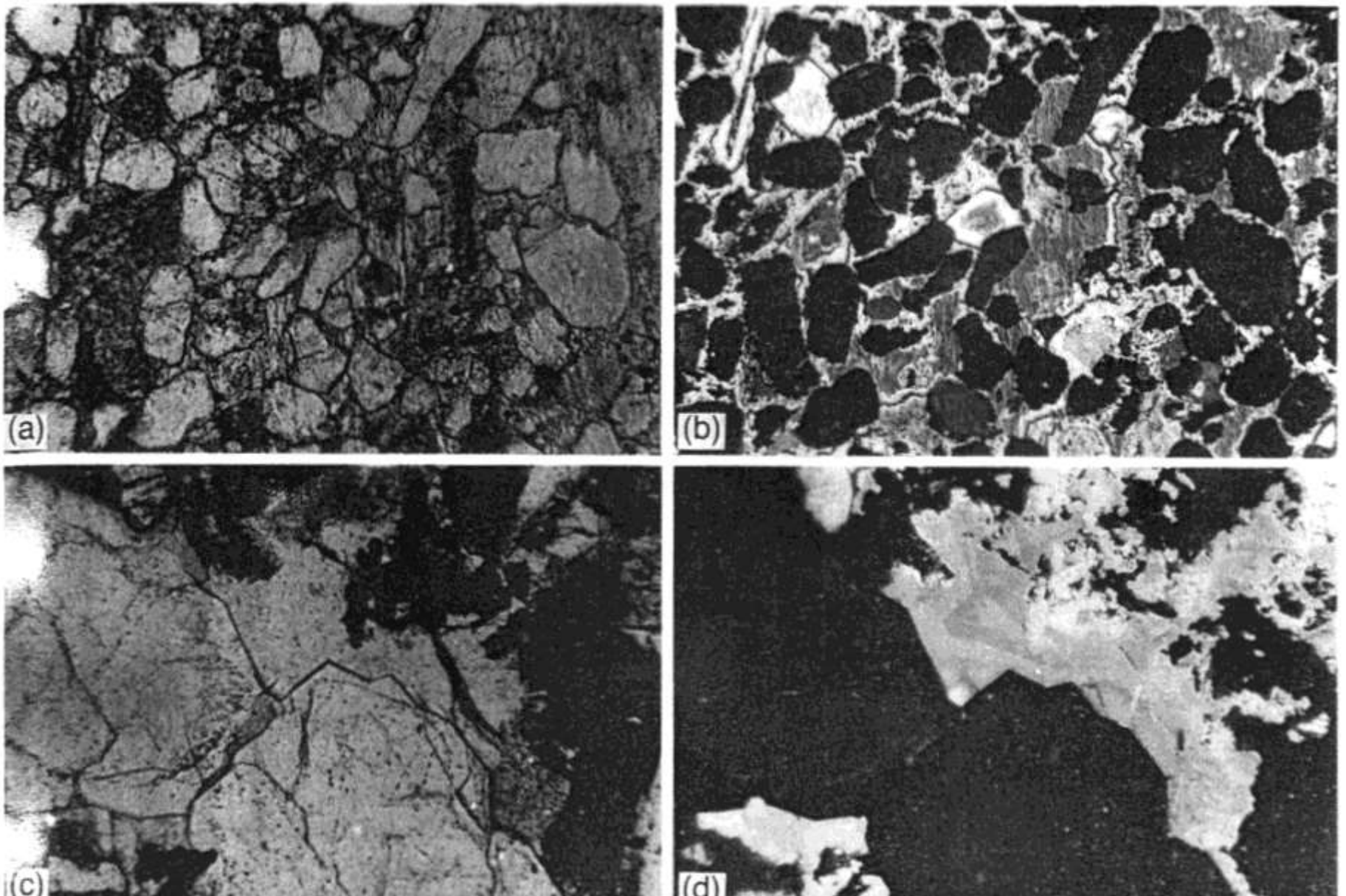
(a)
(b)
(c)
(d)

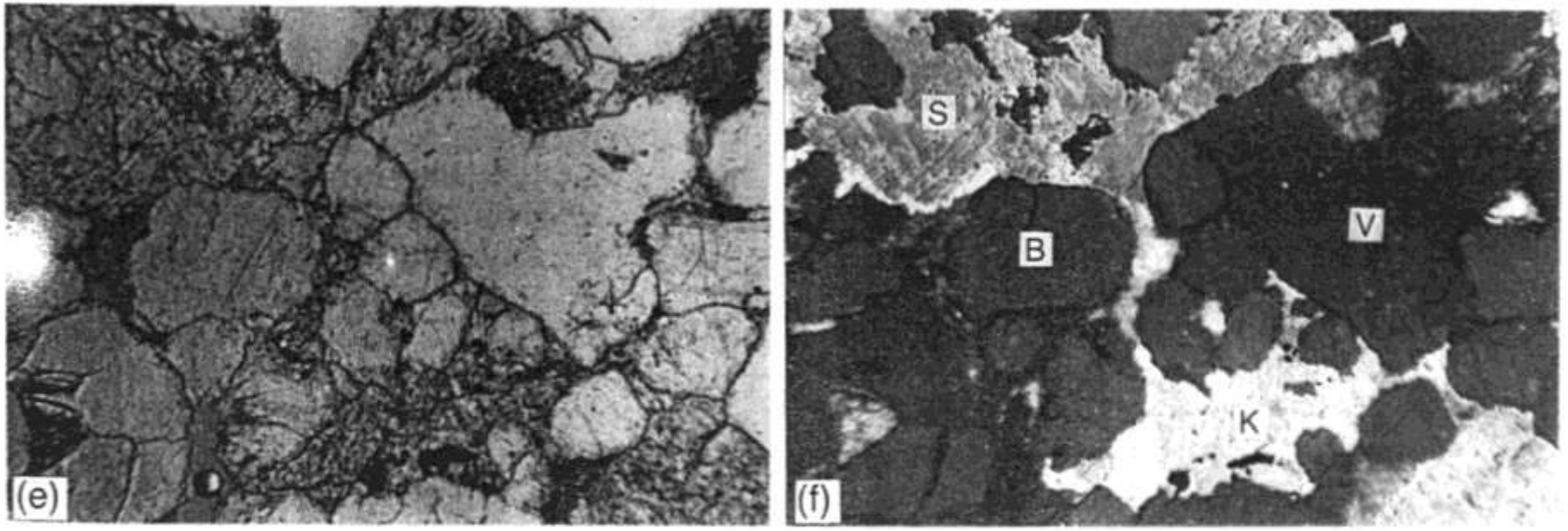

. 6.5. Paired photomicrographs of sandstones from North Sea cores, transmitted light view to the left and CL view to the right. (a), (b) Medium-grained sandstone with a carbonate cement is seen under CL to have a fairly high fossil content, mainly echinoderms: crinoid fragments and an echinoid spine (top left) provide substrates for large, zoned overgrowths which have occluded the primary porosity. (c), (d) Coarse sandstone with non-luminescent authigenic quartz overgrowths on violet-luminescing quartz grains. A subsequent zoned calcite cement is being dissolved by kaolinite (white on picture, royal blue CL). (e), (f) Violet luminescing (V) and brown (B) quartz grains showing a mixture of metamorphic and igneous sources. A sparry calcite cement (S) is suffering dissolution by brightly-luminescing kaolinite (K).

čtení:

J.Miller (1988): Cathodoluminiscence microscopy. In: M.Tucker ed.: Techniques in sedimnetology, Blackwell.
D.J.Marshall (1988): Cathodoluminiscence of geological materials. Unwin Hyman, Boston.
P.Stille a G.Shields (1997): Radiogenic isotope geochemistry of sedimentary and aquatic systems. Lecture notes in Earth sciences 68, Springer.
J.Hladíková (1988): Základy geochemie stabilních izotopů lehkých prvků. skripta PřF UJEP, Brno.
G.Faure (1986): Principles of isotope geology. John Wiley&sons.
P.Fritz a J.Ch.Fontes eds (1980): Handbook of environmental isotope geology. Elsevier.
P.K.Swart et al. eds. (1993): Climate change in continental isotopic records. Geophysical monograph 78, AGU.
L.Pratt et al. : Geochemistry of organic matter in sediments and sedimentary rocks. SEPM short course 27.
J.Parnell et al. (1993): Bitumens in ore deposits. Springer.

Record of palaeoenvironmental changes in a Lower Permian organic-rich lacustrine succession: integrated sedimentological and geochemical study of the Rudník member, Krkonoše Piedmont Basin, Czech Republic

Karel Martínek, Martin Blecha, Vilém Daněk, Jiří Franců, Jana Hladíková, Renata Johnová, David Uličný

Palaeo 3x, 2006

Lower Permian paleogeography

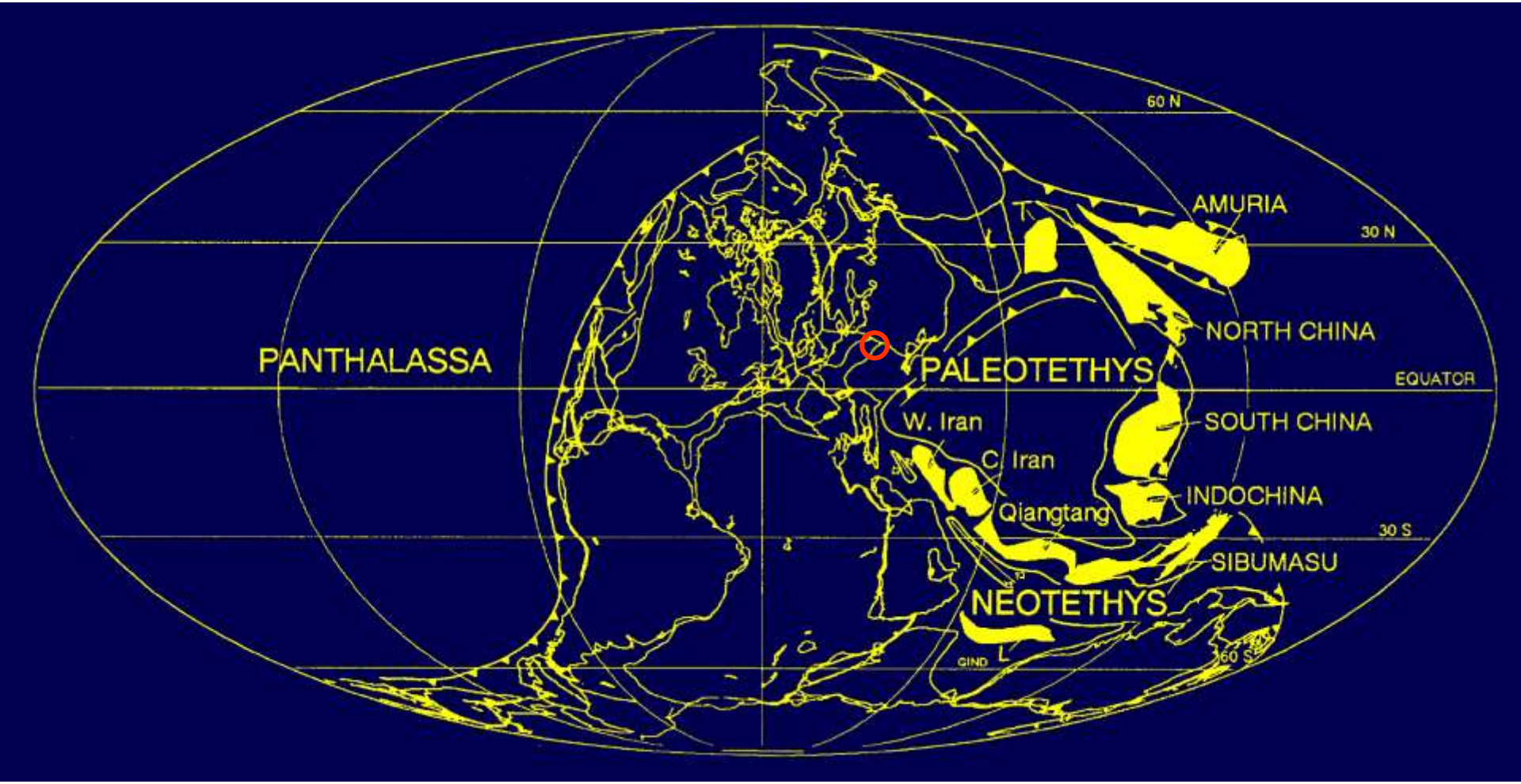

Lower Permian paleoclimate

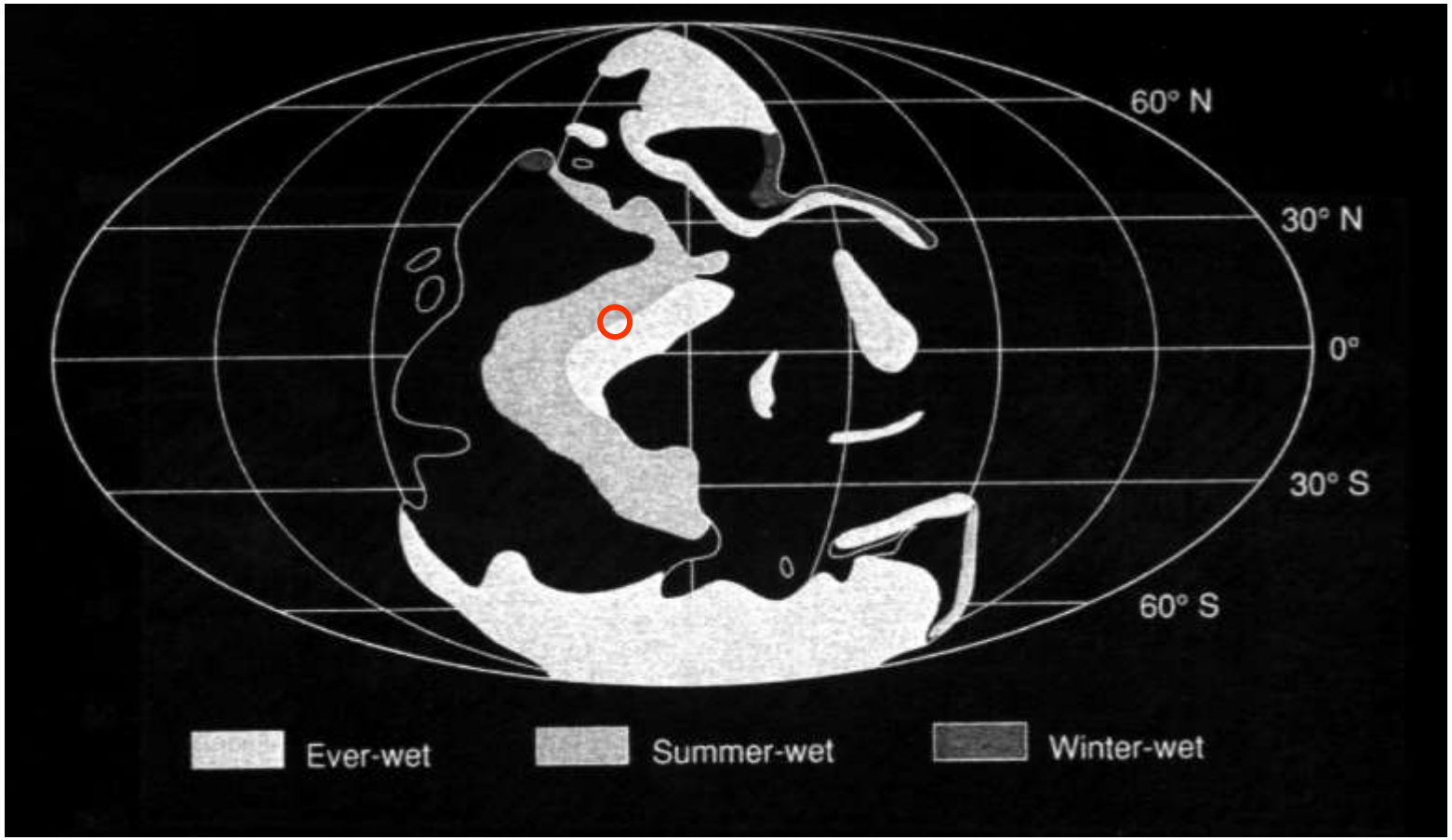

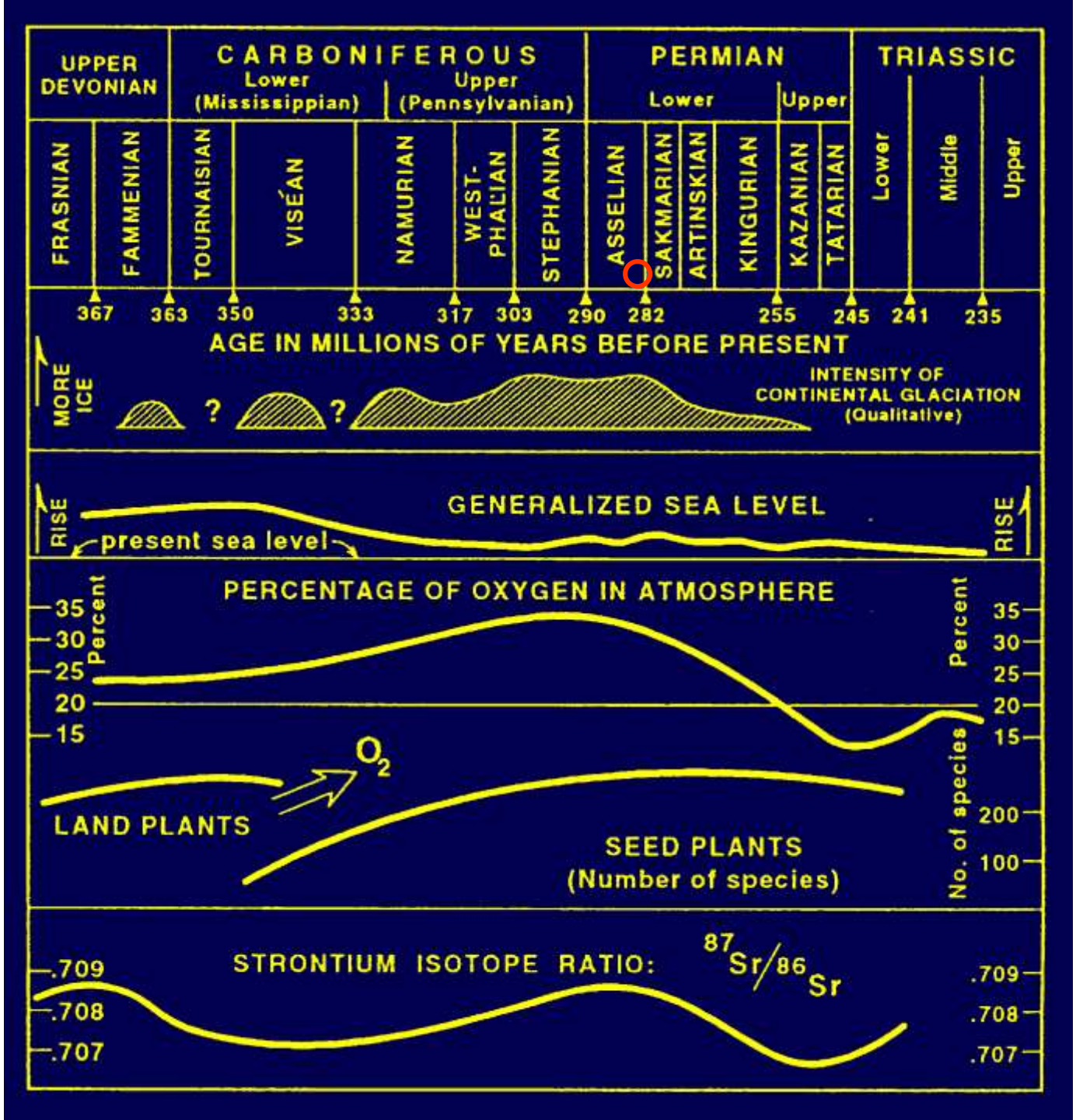
UPPER DEVONIAN
CARBONIFEROUS
Lower (Mississippian)
Upper (Pennsylvanian)
PERMIAN
Lower
Upper
TRIASSIC
FRASNIAN
FAMMENIAN
TOURNAISIAN
VISÉAN
NAMURIAN
WEST-PHALIAN
STEPHANIAN
ASSELIAN
SAKMARIAN
ARTINSKIAN
KINGURIAN
KAZANIAN
TATARIAN
Lower
Middle
Upper
367 363 350 333 317 303 290 282 255 245 241 235
AGE IN MILLIONS OF YEARS BEFORE PRESENT
MORE ICE
INTENSITY OF CONTINENTAL GLACIATION (Qualitative)
RISE
GENERALIZED SEA LEVEL
present sea level
RISE
PERCENTAGE OF OXYGEN IN ATMOSPHERE
35 30 25 20 15
Percent
O_2
LAND PLANTS
SEED PLANTS
(Number of species)
No. of species
200 100
STRONTIUM ISOTOPE RATIO: $^{87}Sr/^{86}Sr$
.709 .708 .707

Krkonoše Piedmont Basin (KP Basin)

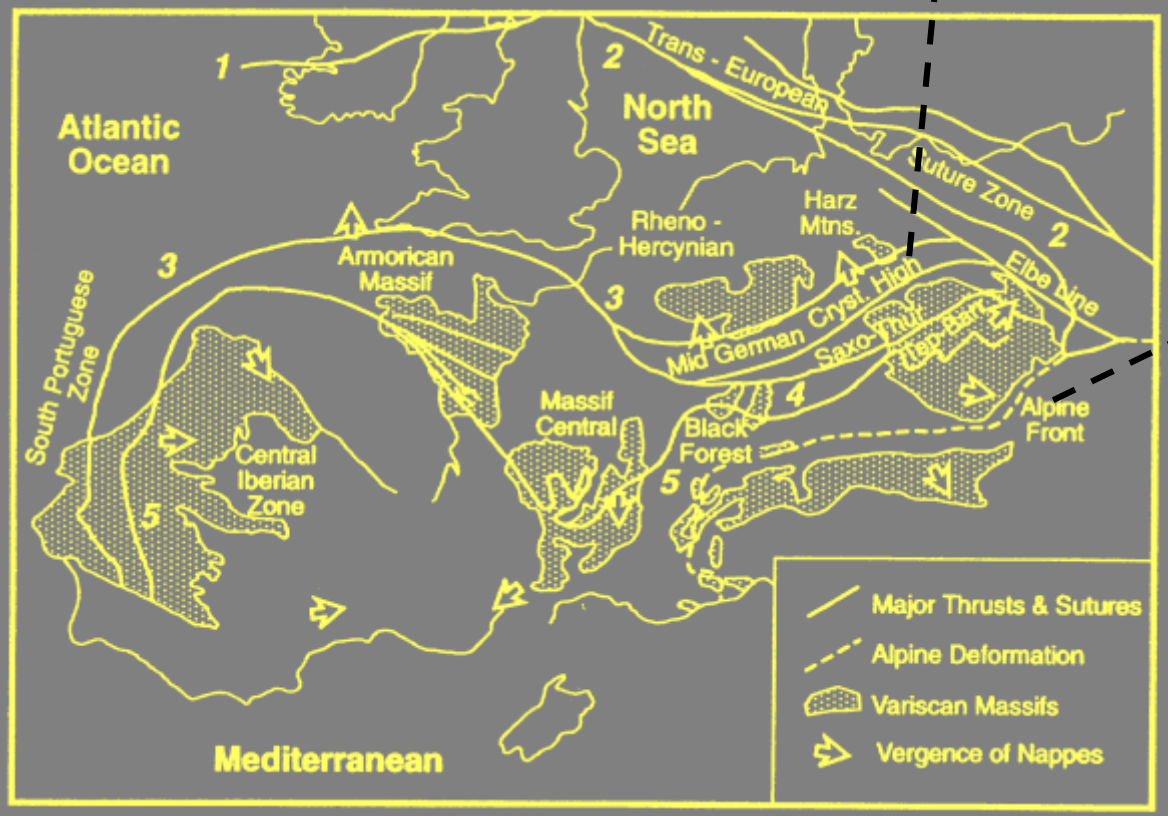

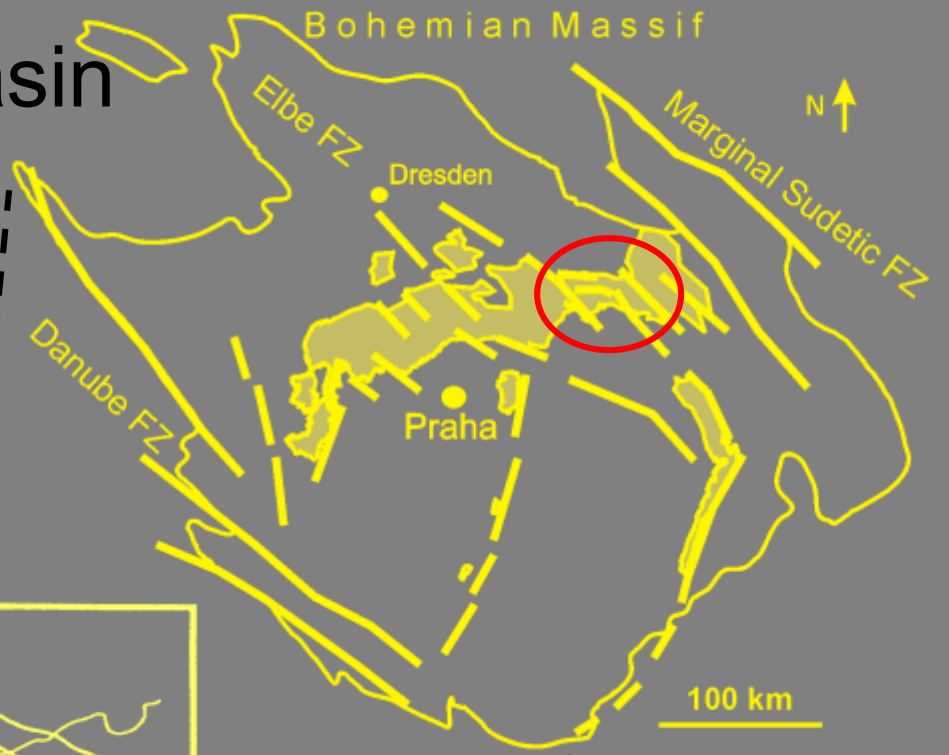

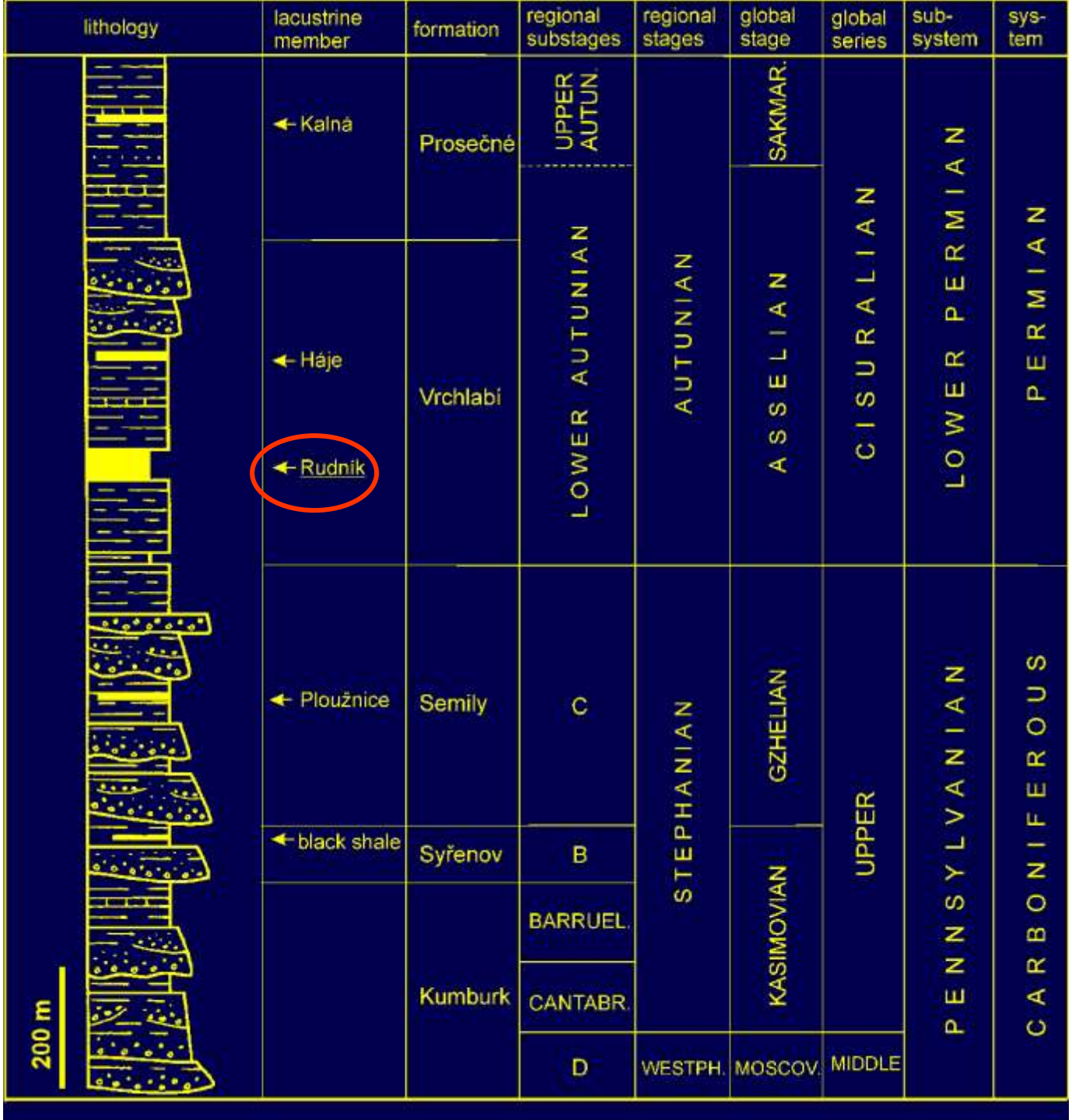
lithology
lacustrine member
formation
regional substages
regional stages
global stage
global series
sub-system
sys-tem
Kalná
Háje
Rudník
Ploužnice
black shale
Prosečné
Vrchlabí
Semily
Syřenov
Kumburk
UPPER AUTUN.
LOWER AUTUNIAN
C
B
BARRUEL.
CANTABR.
D
AUTUNIAN
STEPHANIAN
WESTPH.
SAKMAR.
ASSELIAN
GZHELIAN
KASIMOVIAN
MOSCOV.
CISURALIAN
UPPER
MIDDLE
LOWER PERMIAN
PERMIAN
PENNSYLVANIAN
CARBONIFEROUS
200 m

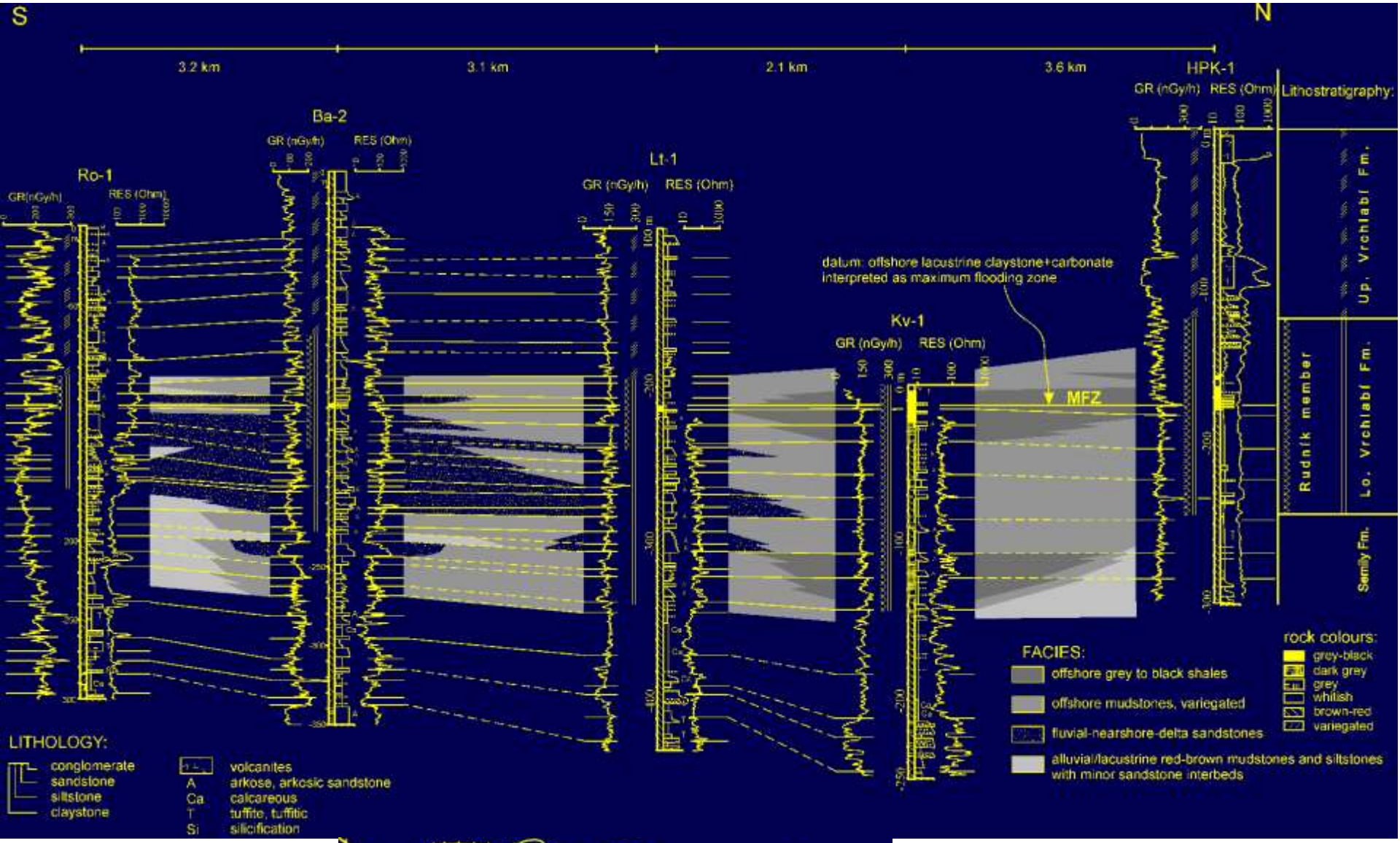
S
N
3.2 km
3.1 km
2.1 km
3.6 km
Ro-1
Ba-2
Lt-1
Kv-1
HPK-1
GR (nGy/h)
RES (Ohm)
Lithostratigraphy:
Up. Vrchlabí Fm.
Rudník member
Lo. Vrchlabí Fm.
Semily Fm.
datum: offshore lacustrine claystone+carbonate interpreted as maximum flooding zone
MFZ
FACIES:
offshore grey to black shales
offshore mudstones, variegated
fluvial-nearshore-delta sandstones
alluvial/lacustrine red-brown mudstones and siltstones with minor sandstone interbeds
rock colours:
grey-black
dark grey
grey
whitish
brown-red
variegated
LITHOLOGY:
conglomerate
sandstone
siltstone
claystone
volcanites
A arkose, arkosic sandstone
Ca calcareous
T tuffite, tuffitic
Si silicification


Vrchlabí
Kunratice
Trutnov
Nová Paka


3 mm

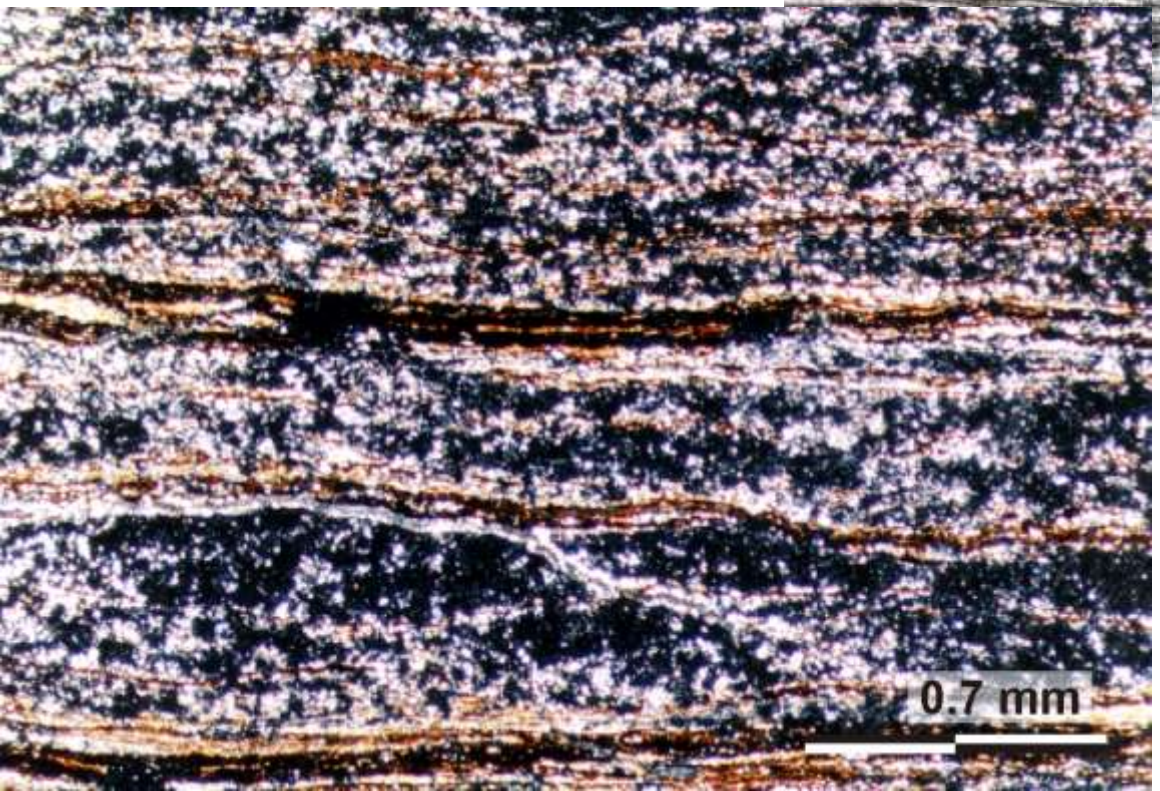
0.7 mm


u
l
u
5 cm
i

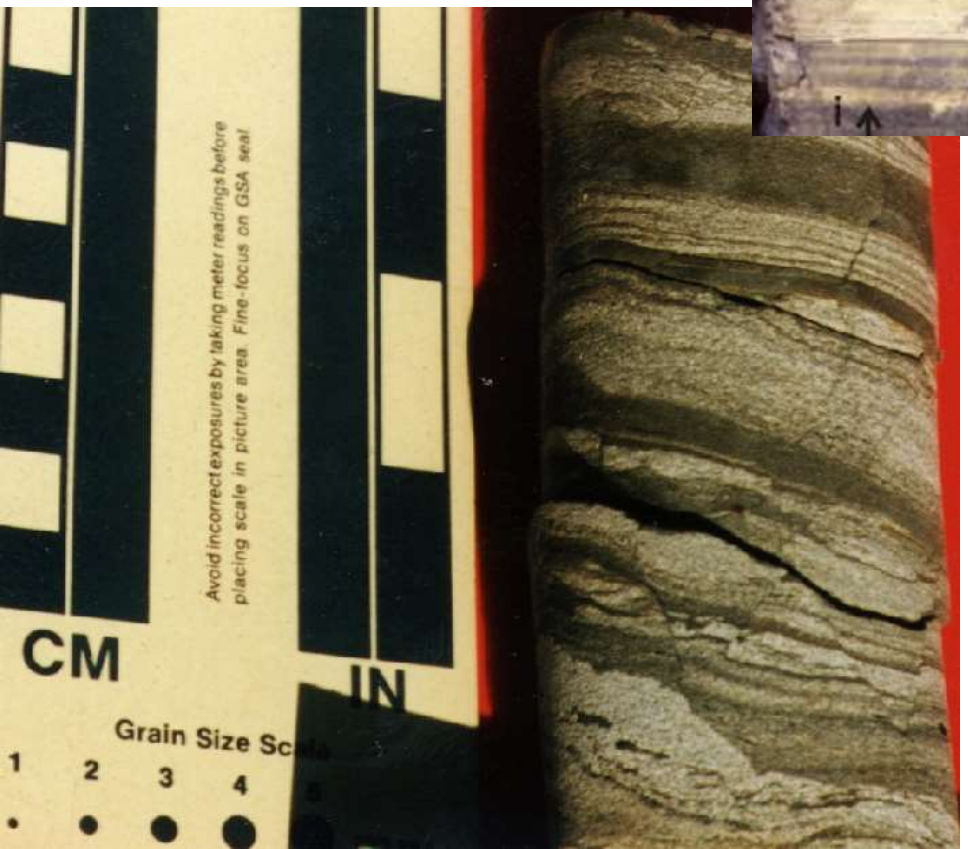
CM
IN
Avoid incorrect exposures by taking meter readings before placing scale in picture area. Fine-focus on GSA seal
Grain Size Sc
1
2
3
4

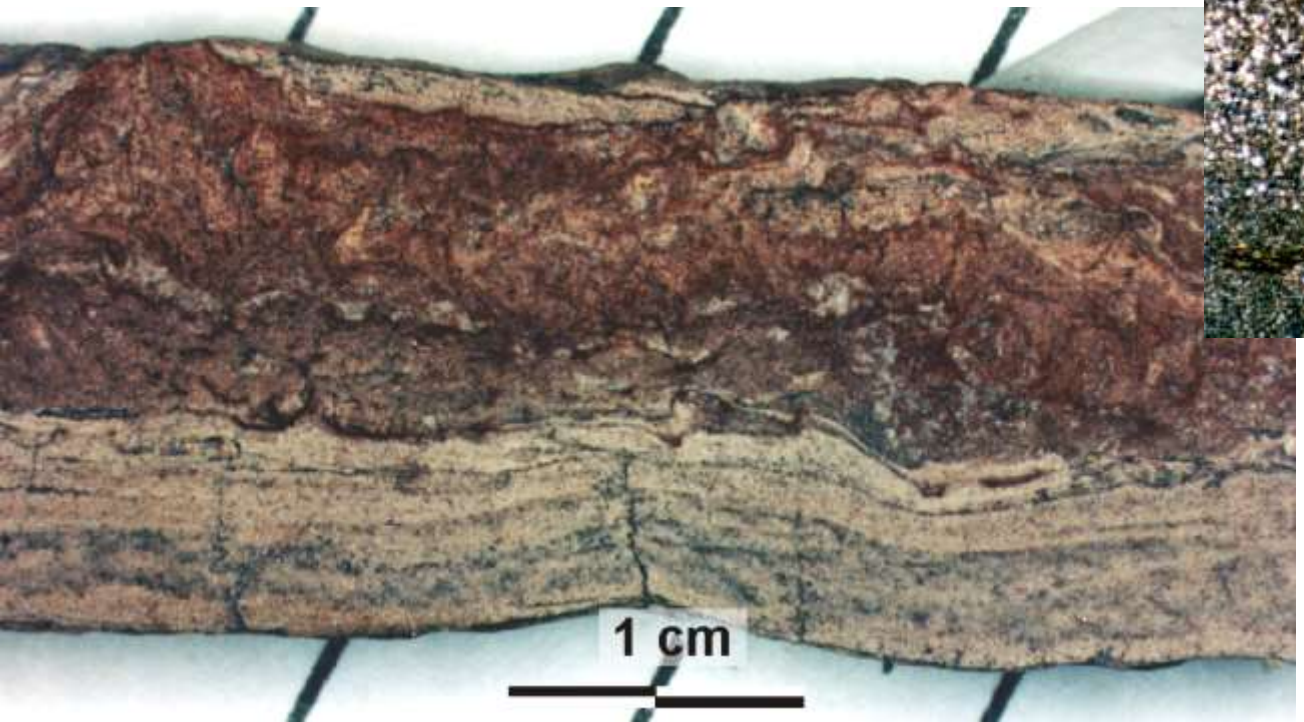
1 cm


0.7 mm

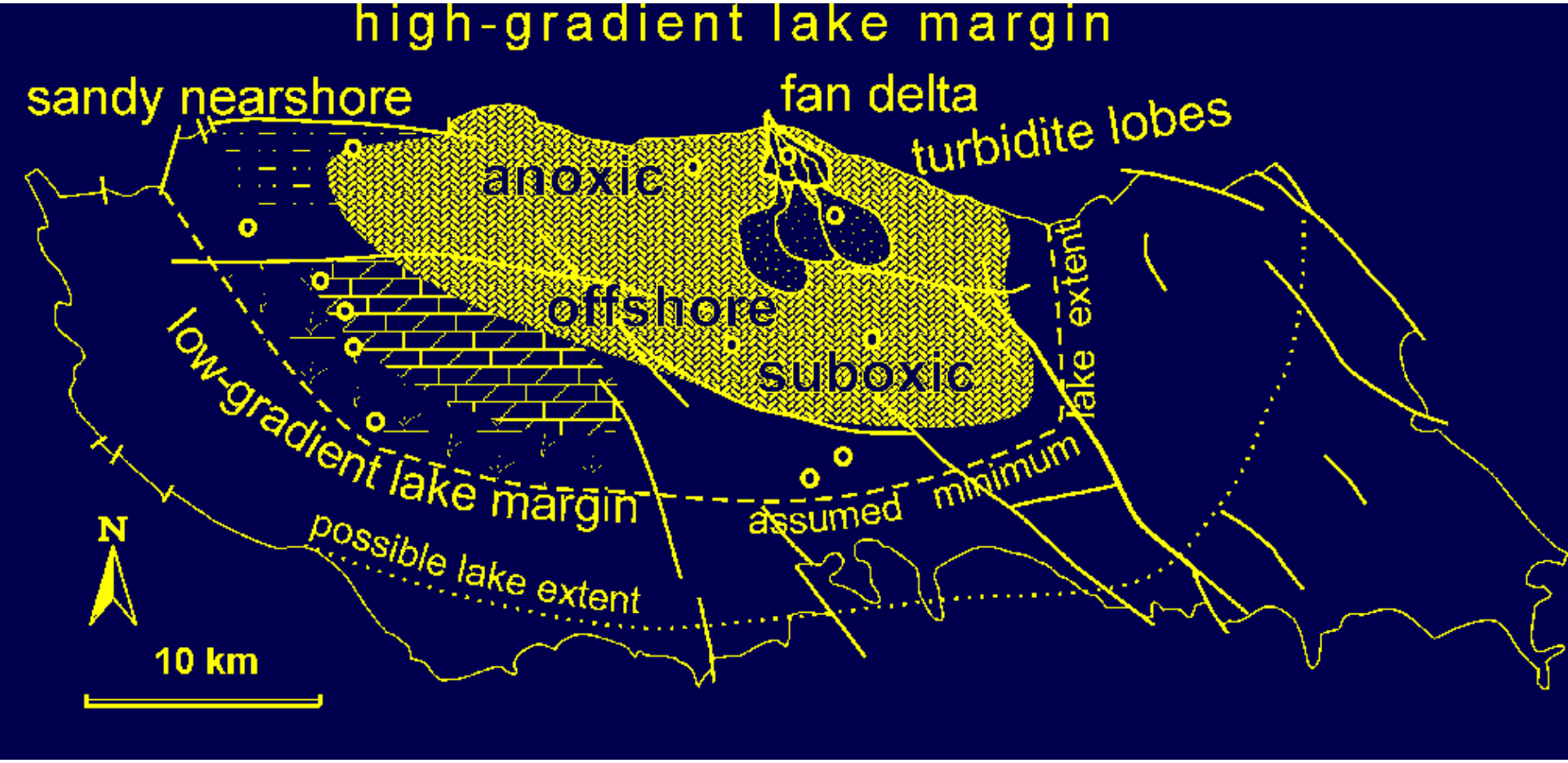
high-gradient lake margin
sandy nearshore
fan delta
turbidite lobes
anoxic
offshore
suboxic
low-gradient lake margin
assumed minimum lake extent
possible lake extent
N
10 km

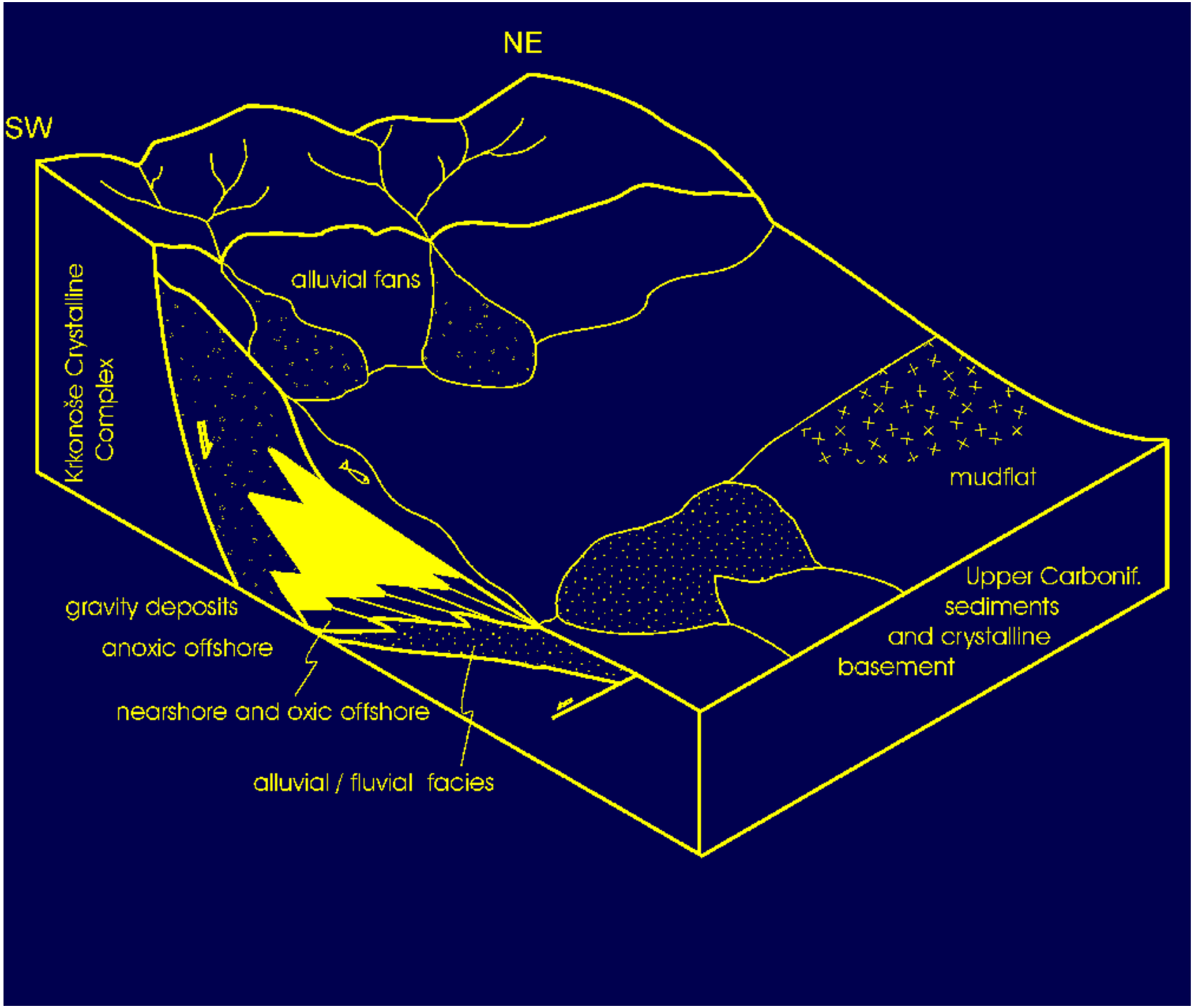
NE
SW
Krkonoše Crystalline Complex
alluvial fans
mudflat
Upper Carbonif. sediments and crystalline basement
gravity deposits
anoxic offshore
nearshore and oxic offshore
alluvial / fluvial facies

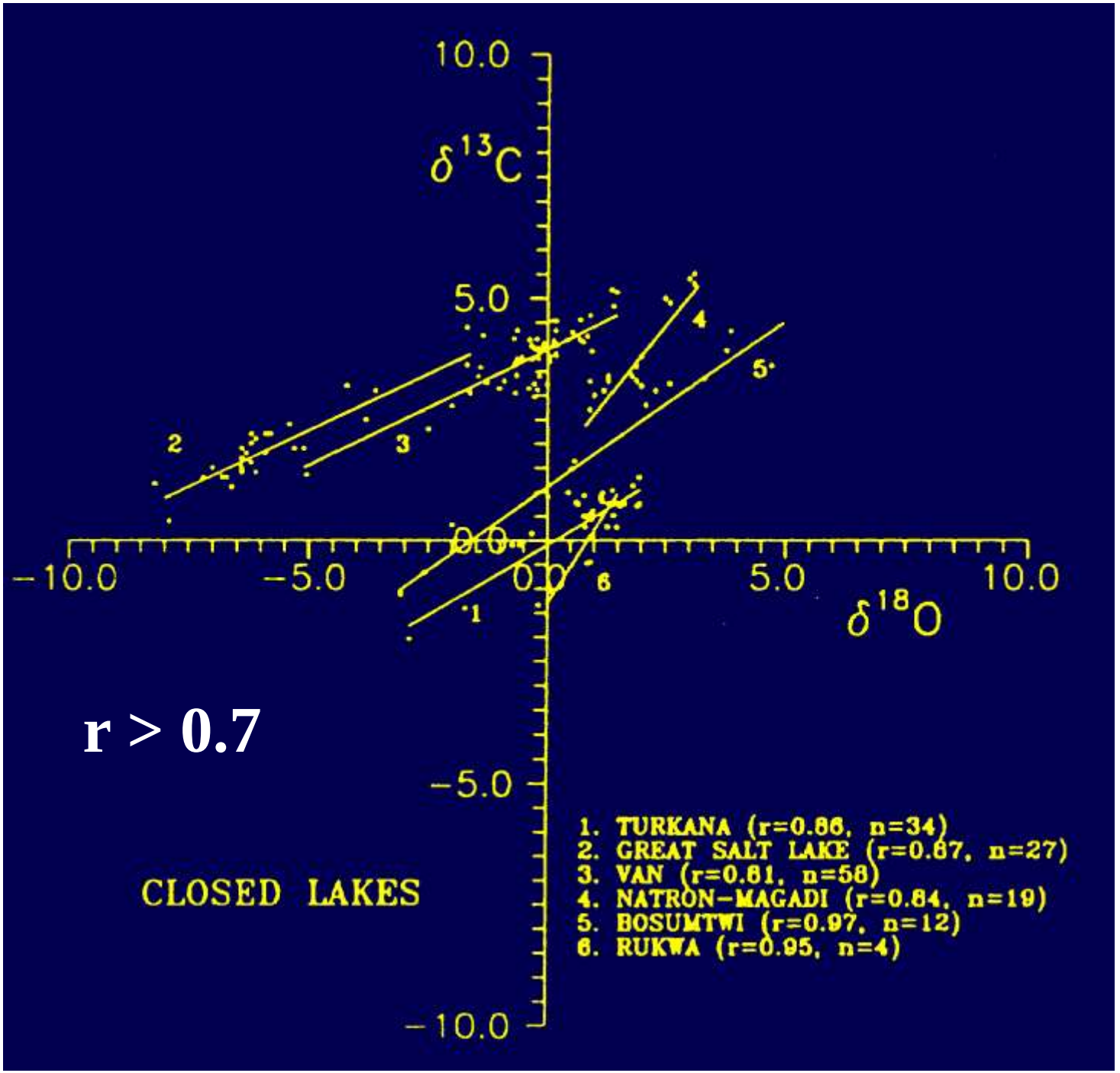
10.0
δ13C
5.0
0.0
−5.0
−10.0
−10.0
−5.0
0.0
5.0
10.0
δ18O
1
2
3
4
5
6
r > 0.7
CLOSED LAKES
1. TURKANA (r=0.86, n=34)
2. GREAT SALT LAKE (r=0.87, n=27)
3. VAN (r=0.81, n=58)
4. NATRON−MAGADI (r=0.84, n=19)
5. BOSUMTWI (r=0.97, n=12)
6. RUKWA (r=0.95, n=4)

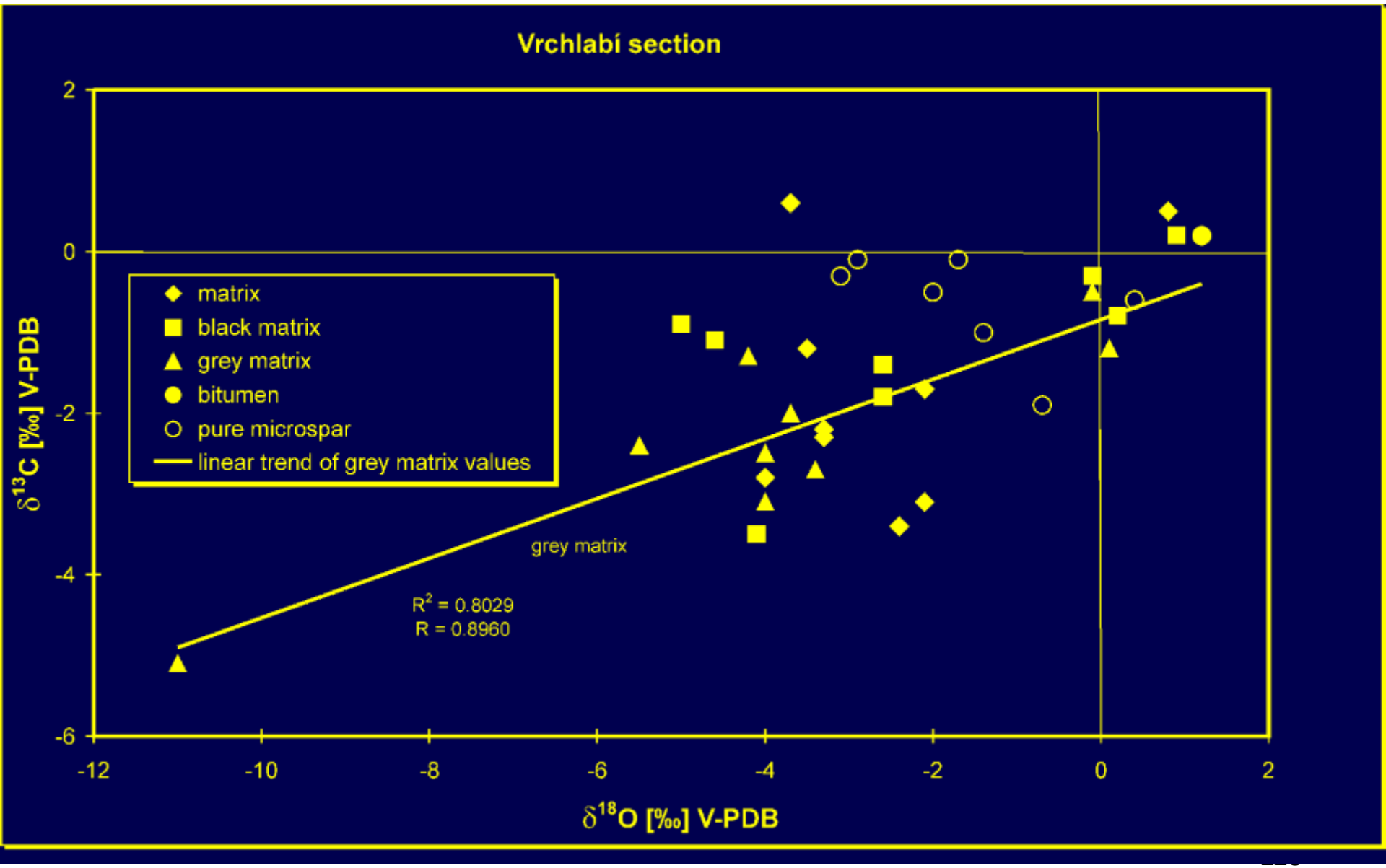
Vrchlabí section
2
0
-2
-4
-6
-12
-10
-8
-6
-4
-2
0
2
δ13C [‰] V-PDB
δ18O [‰] V-PDB
matrix
black matrix
grey matrix
bitumen
pure microspar
linear trend of grey matrix values
grey matrix
R2 = 0.8029
R = 0.8960

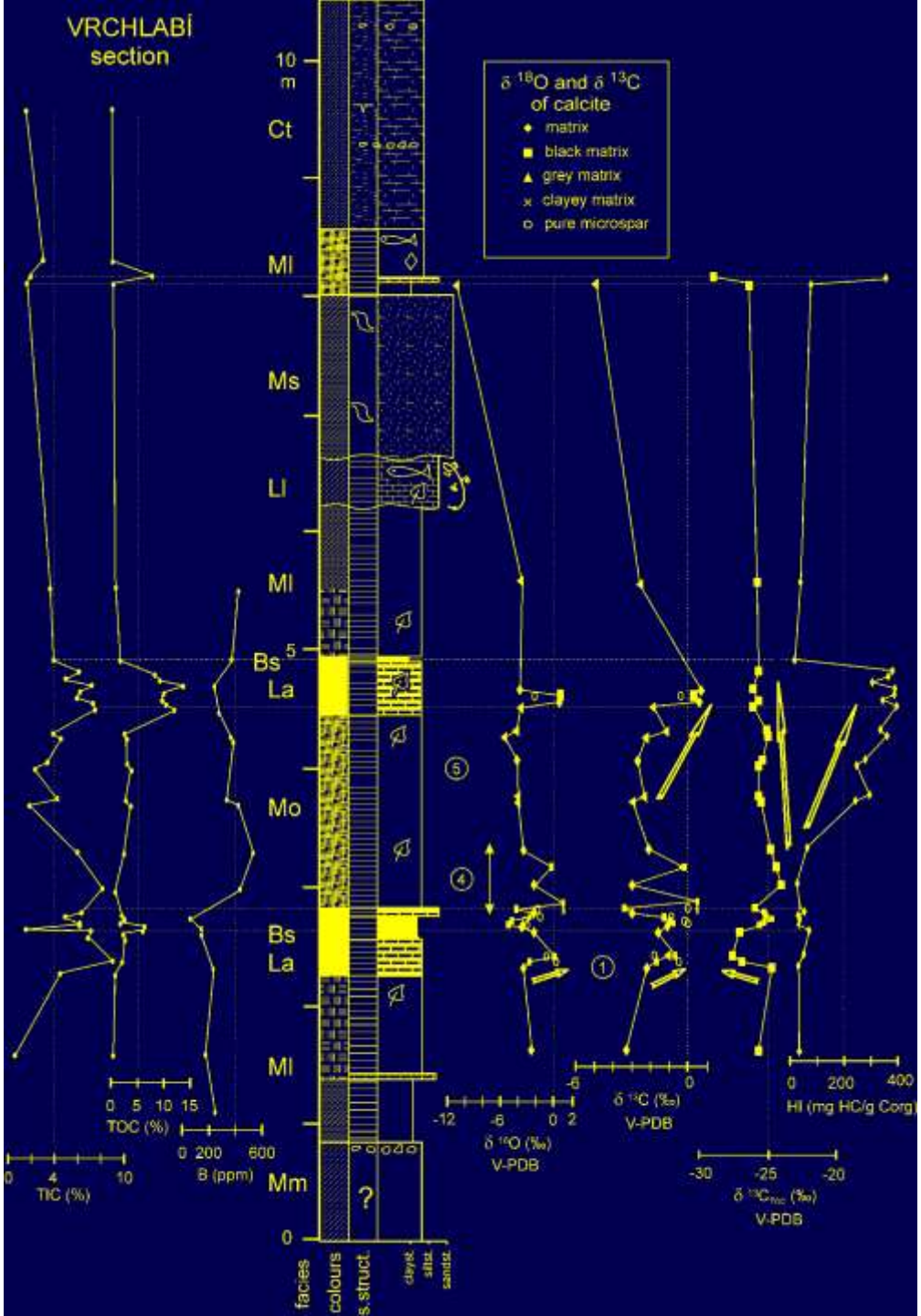
VRCHLABÍ
section
10
m
Ct
Ml
Ms
Li
Ml
5
Bs
La
Mo
Bs
La
Ml
Mm
0
δ 18O and δ 13C
of calcite
matrix
black matrix
grey matrix
clayey matrix
pure microspar
0 5 10 15
TOC (%)
0 200 600
B (ppm)
0 4 10
TIC (%)
-12 -6 0 2
δ 18O (‰)
V-PDB
-5 0
δ 13C (‰)
V-PDB
0 200 400
HI (mg HC/g Corg)
-30 -25 -20
δ 13Corg (‰)
V-PDB
facies
colours
s.struct.
clayst.
siltst.
sandst.

Further reading:

G.Faure and T. M. Mensing (2005): Principles of isotope geology. John Wiley&sons.
Baskaran, Mark Ed. (2012): Handbook of Environmental Isotope Geochemistry, Springer.
P.Stille a G.Shields (1997): Radiogenic isotope geochemistry of sedimentary and aquatic systems. Lecture notes in Earth sciences 68, Springer.
P.Fritz a J.Ch.Fontes eds (1980): Handbook of environmental isotope geology. Elsevier.
P.K.Swart et al. eds. (1993): Climate change in continental isotopic records. Geophysical monograph 78, AGU.
L.Pratt et al. (1991) : Geochemistry of organic matter in sediments and sedimentary rocks. SEPM short course 27.
J.Parnell et al. (1993): Bitumens in ore deposits. Springer.

Questions and Answers